
000
001
002
003
004
005
006
007
008
009
010
011
012
013
014
015
016
017
018
019
020
021
022
023
024
025
026
027
028
029
030
031

INPHYRE DISCOVERS: LARGE MULTIMODAL MODELS STRUGGLE IN INDUCTIVE PHYSICAL REASONING

005 **Anonymous authors**

006 Paper under double-blind review

ABSTRACT

012 Large multimodal models (LMMs) encode universal physical laws observed during
013 training, such as momentum conservation, as *parametric knowledge*. It allows
014 LMMs to answer physical reasoning queries, such as the outcome of a potential
015 collision event from visual input. However, since parametric knowledge includes
016 only the physical laws seen during training, it is insufficient for reasoning when
017 the inference scenario follows physical laws unseen during training. In contrast,
018 humans can adapt their physical reasoning to unseen physical environments with
019 only a few visual examples. This *inductive physical reasoning* ability is indispensable
020 for LMMs if they are to replace human agents in safety-critical applications.
021 Despite its importance, existing visual benchmarks evaluate only the parametric
022 knowledge in LMMs, and not inductive physical reasoning. To this end, we propose
023 INPHYRE, the first visual question answering benchmark to measure inductive
024 physical reasoning in LMMs. INPHYRE evaluates LMMs on their ability to predict
025 the outcome of collision events in algorithmically generated synthetic videos. By
026 inspecting over 13 open-source and proprietary LMMs, INPHYRE informs us that
027 (1) LMMs struggle to apply their limited parametric knowledge about universal
028 physical laws to reasoning, (2) inductive physical reasoning in LMMs is weak when
029 inference scenarios obey physical laws unseen during training, and (3) inductive
030 physical reasoning in LMMs suffers from language bias and largely ignores the
031 visual inputs, questioning the trustworthiness of LMMs regarding visual inputs.

1 INTRODUCTION

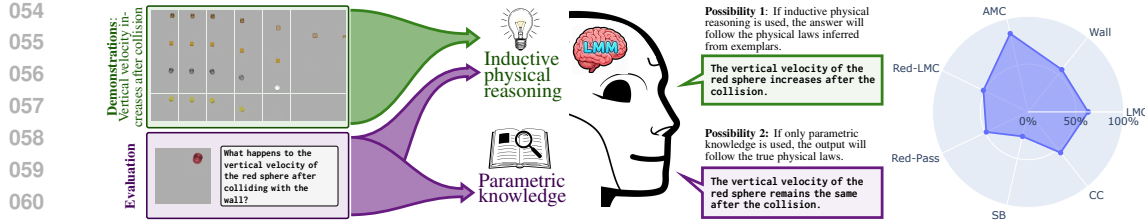
CASE STUDY

035 **Premise:** A large multimodal model (LMM) is used to determine whether a car crash will occur
036 on a snowy road from a video. To ensure the LMM understands that the physical coefficients of
037 the snowy road differ from those of a dry road, a few demonstration videos of snowy roads with
038 and without collisions are provided as context. The LMM predicts that a crash is unlikely.

039 **Question:** Did the LMM account for the unseen physical coefficients using the demonstration
040 videos, or did it use only its parametric physical knowledge to make its prediction?

042 Large multimodal models (LMMs) are known to encode universal physical laws (*e.g.*, momentum
043 conservation) observed during training as *parametric knowledge* to answer physical reasoning
044 queries (*e.g.*, whether a collision occurs or not) from visual input (Chen et al., 2024d; Cherian et al.,
045 2024; Mudur et al., 2025). However, since parametric knowledge includes only the physical laws
046 seen during training, it is insufficient in scenarios that potentially follow unobserved physical laws
047 and conditions, such as the case study of the snowy road. In contrast, humans would easily adapt
048 their physical knowledge about collisions to snowy road conditions with the help of demonstration
049 videos to predict any collision, if presented with the same case study. This crucial skill, that we
050 refer to as *inductive physical reasoning*¹, is a hallmark of intelligence that humans develop at a very
051 young age (Hayes, 2007; Ricco, 2015). Inductive physical reasoning is an indispensable ability that
052 LMMs must possess in addition to parametric knowledge if they are to be deployed in safety-critical
053 applications such as autonomous driving (Zhou et al., 2024; Zhang, 2025) to replace human agents.

¹Inductive physical reasoning is closer to inductive reasoning than general visual reasoning. See § D.



054
055
056
057
058
059
060
061
062
063
064
065
066
067
068
069
Figure 1: (Left) A large multimodal model (LMM) is asked to predict the change in vertical velocity of an object colliding with a vertical wall. The model will output “possibility 2” if it uses its **parametric knowledge** that encodes the universal physical laws (in this case, the momentum conservation principle). However, parametric knowledge would be insufficient if the collision event violated the physical laws encoded in the model. For the model to infer the underlying physical laws, we provide the model with exemplar videos of collisions that violate the momentum conservation principle. The model may now rely on its **inductive physical reasoning** capabilities to generate “possibility 1”. (Right) INPHYRE shows that LMMs struggle with inductive physical reasoning.

070
071
072
073
074
Despite its vital nature, there are no visual benchmarks that quantitatively evaluate inductive physical reasoning in LMMs. Existing benchmarks (Baradel et al., 2020; Chen et al., 2022; Tung et al., 2023; Chow et al., 2025) evaluate only the parametric knowledge of LMMs, particularly about universal physical concepts observable in natural videos, such as friction and gravity, and not the inductive physical reasoning ability. However, creating inductive physical reasoning benchmarks is challenging.

075
076
077
078
079
080
081
082
083
To evaluate inductive physical reasoning separated from parametric knowledge in LMMs, the benchmark must exclude scenarios seen during LMMs’ training. Since we cannot always know which scenarios have been seen by LMMs, we opt to build our benchmark using physically impossible scenarios that violate universal physical laws, as they are less likely to have been seen by LMMs during training. However, it is inherently impossible to find such scenarios in natural videos, and prohibitively expensive to manually edit and repurpose existing benchmarks that measure parametric knowledge. Thus, algorithmically generated synthetic videos become the only viable option. Algorithmic generation of physical event videos violating universal physical laws still requires careful design and manual interventions on environment design, modified physical laws, and object trajectories.

084
085
086
087
088
089
090
091
092
093
094
We propose **INPHYRE** (Inductive Physical Reasoning), the *first* visual question answering benchmark that evaluates how well LMMs can infer the underlying physics from demonstration samples and use it to make physical reasoning predictions. INPHYRE comprises algorithmically generated synthetic videos of collision events. During evaluation, LMMs are given the first frame of a video and asked questions about the outcome of a textually described collision involving the objects in this frame. However, some of these scenarios violate universal physical laws. In these scenarios, where parametric knowledge is ineffective, LMMs must infer the underlying physics from demonstration videos taken from the same scenarios for physical reasoning. INPHYRE quantifies inductive physical reasoning in LMMs as the performance disparity between scenarios that follow the true physical laws and those that do not. INPHYRE’s goal is not to evaluate the utility of LMMs in unrealistic scenarios that violate universal physical laws, but rather to evaluate their adaptability in scenarios with unseen physical laws. This goal also differs from that of “intuitive physics understanding” (see § C).

095
096
097
098
099
Scope of INPHYRE: Since it is difficult to create a benchmark visualizing the violations of every universal physical law exhaustively, we limit our studies to the laws of mechanics, such as momentum and energy conservation principles. Nonetheless, the outcomes of the collision events in INPHYRE violate the most fundamental laws of mechanics. Therefore, we believe that the conclusions from INPHYRE are likely valid for inductive physical reasoning in LMMs about other branches of physics.

100
101
102
103
104
105
106
107
What does INPHYRE find? Our results show that INPHYRE is a formidable benchmark for current LMMs, despite its visual simplicity. Our results indicate that both **open-source and proprietary LMMs struggle to infer and utilize unseen physical laws from demonstration samples** (Fig. 1). From empirical evidence, we conjecture that LMMs do not understand physical laws as transferable mathematical models, but rather as a fixed set of rules that all objects obey. Moreover, we show that LMMs primarily derive their inductive physical reasoning capabilities from their language components and ignore the visual inputs in the demonstration samples. Chain-of-thought prompting and fine-tuning are also futile for conditional physical reasoning tasks in INPHYRE (§§ E.3 and E.4). This means that it is possible that the LMM in our case study did not account for the snowy conditions.

108
109**Contributions and Findings**110
111

- ◆ We introduce INPHYRE, the *first* visual question answering benchmark to evaluate the inductive physical reasoning capabilities of large multimodal models (LMMs).
- ◆ Finding 1: LMMs have only limited parametric knowledge about universal physical laws and struggle to apply these laws even in scenarios that follow these physical laws (§ 4.2).
- ◆ Finding 2: Demonstration samples improve LMMs’ predictions only when the samples agree with the models’ parametric knowledge, resulting in poor inductive physical reasoning on scenarios that violate the true physical laws (§§ 4.3, 4.4 and E.2).
- ◆ Finding 3: Inductive physical reasoning in LMMs suffers from strong language bias. As a result, visual inputs in the exemplars play very little role in the final prediction (§ 4.5).

112
113
114
115
116
117
118
119
120
121
122**2 RELATED WORKS**

Benchmark	What are the physical reasoning tasks	Physical conditions change between training and testing?	Require test-time inference of physical conditions?
CLEVRER [1]	Factual and counterfactual physical reasoning	No ✗	No ✗
ComPhy [2]	Physical reasoning requiring latent property prediction	No ✗	Yes ✓
CoPhy [3]	Counterfactual physical reasoning	No ✗	No ✗
PhysBench [4]	Physical reasoning about object properties and dynamics	No ✗	No ✗
IntPhys [5]	Physical plausibility prediction	Yes ✓	No ✗
Physion [6]	Object contact prediction	No ✗	No ✗
Physion++ [7]	Object contact prediction involving property prediction	No ✗	No ✗
ContPhy [8]	Physical property and dynamics prediction	No ✗	No ✗
INPHYRE	Infer physical laws from demo samples and apply them.	Yes ✓	Yes ✓

133

Table 1: **How does INPHYRE differ from prior physical reasoning benchmarks?** [1] (Yi et al., 2020), [2] (Chen et al., 2022), [3] (Baradel et al., 2020), [4] (Chow et al., 2025), [5] (Riochet et al., 2021; Bordes et al., 2025), [6] (Bear et al., 2021), [7] (Tung et al., 2023), [8] (Zheng et al., 2024)

134

The proliferation of large language models (LLMs) has increased focus on zero-shot commonsense physical reasoning, where the objective is to evaluate the ability of LLMs to reason and provide instructions for everyday tasks such as picking up objects or cutting fruits (Bisk et al., 2020; Aroca-Ouellette et al., 2021; Wang et al., 2023). Other physical reasoning benchmarks focus on the theoretical physics knowledge in LLMs (Pang et al., 2025; Mudur et al., 2025; Yu et al., 2025) and their ability to reason about the latent physical properties (Chen et al., 2024d; Chow et al., 2025), sometimes using interactive simulators (Cherian et al., 2024). Synthetic collision events are also commonly used in physical reasoning benchmarks (Yi et al., 2020; Baradel et al., 2020; Chen et al., 2022). However, **these works only evaluate the parametric knowledge** of LLMs about the tools in the evaluation environment, and do not consider inductive physical reasoning in LMMs at all. **These datasets are also not suitable to evaluate inductive physical reasoning**, as the presence of true physical laws in these datasets may confound the evaluation of inductive physical reasoning. **Example:** Benchmarks that measure counterfactual physical reasoning do not check if the model predicted using its memorized physical laws/conditions, or based on the provided factual scenario. In contrast, by relying on impossible physics, we ensure that LMMs can only answer the queries using the physics dynamics inferred from demonstration samples. **Our work is also in contrast with “intuitive physics understanding”** (Riochet et al., 2021; Garrido et al., 2025), where parametric knowledge of learned models is evaluated through their ability to detect violations of universal physical laws. **The key differences between INPHYRE and some prior physical reasoning benchmarks are shown in Tab. 1.** See § C for more discussion on related works.

135

3 INPHYRE: INDUCTIVE PHYSICAL REASONING BENCHMARK136
137
138
139
140
141
142
143
144
145
146
147
148
149
150
151
152
153
154
155
156
157
158
159
160
161

In this section, we will describe our proposed benchmark, INPHYRE – Inductive Physical Reasoning and how we will utilize it to evaluate the inductive physical reasoning capabilities of large multimodal

models (LMMs). Our benchmark comprises collision event videos that violate real-world physical laws, such as momentum conservation and object continuity. During evaluation, the inputs to the LMM are the first frame from a collision video and a multiple-choice question about the outcome of a described collision event. The model is then evaluated in zero-shot and few-shot settings to quantify its relative strengths of parametric knowledge and inductive physical reasoning.

Visual Inputs	Violation	Task	Visual Inputs	Violation	Task	
LMC	The colliding object continues with its original velocity after collision.	Predict the change in velocity of the colliding object after the collision.	Red-1-MC	Red-colored objects do not preserve their velocity after head-on collision.	Predict the change in velocity of the colliding object after the collision.	
	The object collides horizontally against a wall and increases its vertical velocity.	Predict the change in vertical velocity of the colliding object after the collision.		Red-colored objects can pass through other objects, while others cannot.	Predict the change in velocity of the object, originally at rest, after the collision.	
	Two objects rotate about their center of mass after a head-on collision.	Predict whether one or more objects rotate or not after the collision.		A large object deflects after colliding with a tiny, but heavier, object.	Predict the change in state of the tiny object after the collision.	
AMC	Scenario Legend		SB	An object collides with another object and assumes the shape of the latter object.	Predict the change in shape of the colliding object after the collision.	
	Momentum conservation violation			Inconsistent Physics		
	Miscellaneous					

Figure 2: **INPHYRE** comprises videos (“visual inputs”) of collision events that violate a real-world physical law (“violation”). LMMs must predict state changes in objects due to the collisions, while accounting for the violated physical law (“task”). The videos are grouped into “scenarios”, which are further grouped into three categories based on the nature of physical law they violate. Arrows indicate object motion and are not part of the actual images in the dataset.

Research Question: We will first explain the key prerequisite concepts and then state the research question addressed by **INPHYRE**. As mentioned before, each evaluation sample consists of the first frame of a collision video and a multiple-choice question about the collision’s outcome. The model may answer this question using its implicit knowledge of the physical laws that it obtained during training. We refer to this as physical reasoning using parametric knowledge. However, if the physical reasoning required to correctly answer the question does not follow the physical laws embedded in the model, parametric knowledge is insufficient. To let the model infer the physical laws required to answer the question, we provide demonstration samples² containing videos of similar events governed by the same physical laws required to answer the question. This ability to infer the physical laws from exemplars and answer the question is referred to as inductive physical reasoning.

INPHYRE is designed to answer the following research question about physical reasoning in LMMs:

(RQ) Can LMMs flexibly switch between parametric knowledge and inductive physical reasoning by comparing the physical laws in the exemplars to those encoded in the models’ parameters?

To answer **(RQ)**, **INPHYRE** evaluates LMMs in scenarios that follow the true physical laws and those that do not. An LMM with strong inductive physical reasoning will perform identically in both situations, as parametric knowledge and inductive physical reasoning are not competing qualities.

Task Description: **INPHYRE** is a visual question answering benchmark for physical reasoning. Each evaluation sample includes an image of a scene with one or more objects and a question about the outcome of a described collision event involving the objects in that image. Similar to (Johnson et al., 2017; Yi et al., 2020; Chen et al., 2022), the objects are primitive shapes (cubes, cylinders, and spheres) of various colors and textures lying on a plain surface (Fig. 2). The question is about the change in the state of an object after the collision. *E.g.*, What happens to the velocity of the red cube after colliding with the blue sphere? To answer the question, we provide four options as possible answers to the model. *E.g.*, “A. red cube’s velocity increases, B. red cube’s velocity decreases, C. cannot be determined, D. no change in velocity.” The questions may also contain additional information about the objects or the collision event. *E.g.*, “red cube and yellow cylinder have equal mass” or “blue sphere collides elastically against the wall.” The option chosen by the model is parsed from its generation output. See §§ B.2 and B.3 for more details about prompting and parsing, respectively.

²Henceforth referred to as “exemplars”.

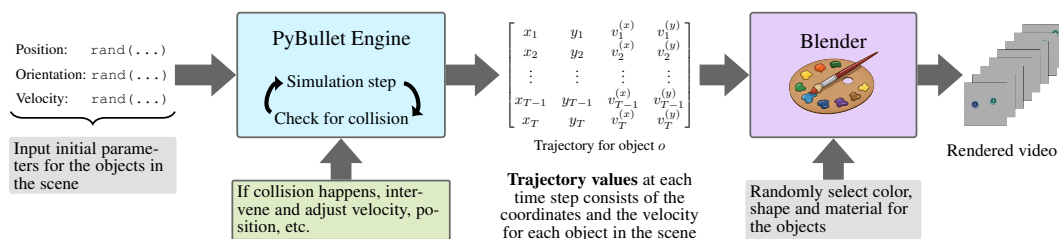
216 **Irregular Scenarios:** The collision event videos in INPHYRE are grouped into “scenarios.” Each
 217 scenario is characterized by the true physical law that it violates. We call them “irregular scenarios”
 218 and denote them with their shorthand notations shown in Fig. 2. The irregular scenarios are further
 219 grouped into three categories based on the nature of the violated physical laws (see Fig. 2):
 220

221 (1) Scenarios in the momentum conservation violation category evaluate the inductive physical
 222 reasoning of LMMs when the principle of momentum conservation is violated. It comprises three
 223 scenarios: linear momentum conservation (**LMC**), angular momentum conservation (**AMC**), and
 224 directional linear momentum conservation (**Wall**). In **LMC**, a moving object collides elastically with
 225 an object of equal mass at rest, and, instead of losing its momentum, continues with the same velocity.
 226 A similar collision event occurs in **AMC**, except the objects rotate about their center of mass, despite
 227 the collision being head-on, violating the principle of angular momentum conservation. In **Wall**,
 228 the vertical velocity of an object increases after colliding with a vertical wall, violating the linear
 229 momentum conservation principle, but only along the vertical direction.
 230

231 (2) In the inconsistent physics category, objects with certain visual properties follow physical laws
 232 different from other objects. In the real world, these visual properties would not have affected the
 233 modified physical laws. The objective is to examine whether LMMs can logically combine parametric
 234 knowledge and inductive physical reasoning based on the object’s visual properties. For this category,
 235 few-shot evaluations will include exemplars with both sets of physical laws. This category includes
 236 two scenarios: (i) **Red-LMC**, where red-colored objects violate linear momentum conservation, and
 237 (ii) **Red-Pass**, where only red-colored objects can physically pass through other objects.
 238

239 (3) INPHYRE also includes some miscellaneous scenarios to evaluate whether LMMs have a visually
 240 biased perception of physical laws. For instance, in size-bias (**SB**), a dimensionally large object
 241 deflects after colliding with a dimensionally small, but much heavier, object. We include information
 242 about mass in the question. **SB** evaluates whether LMMs conflate the concepts of volume and mass.
 243 In color-constancy (**CC**), a moving object collides with an object at rest and assumes the visual
 244 appearance of the latter object. This collision obeys linear momentum conservation. **CC** evaluates the
 245 object permanence of LMMs as it may seem to the model that the colliding object has disappeared.
 246

247 **Regular Scenarios:** For each irregular scenario, there is a corresponding “regular” scenario de-
 248 picting similar collisions while following the true physical laws. Since multiple types of violations
 249 are possible for every universal physical law, regular scenarios are fewer than irregular scenarios.
 250 INPHYRE includes regular versions of **LMC**, **SB**, and **AMC** that act as real-world counterparts of
 251 various irregular scenarios. These regular scenarios are used to evaluate the parametric knowledge of
 252 LMMs. INPHYRE uses both regular and irregular scenarios jointly to answer (RQ).
 253



254
 255
 256
 257
 258 Figure 3: We initialize the object states in PyBullet. When a collision occurs during the simulation,
 259 we intervene and manually adjust the objects’ states such that the resulting trajectory violates some
 260 real-world physical law. The object trajectories are then used by Blender to render the final video.
 261

262 **Video generation details:** We modify the video generation pipeline from (Yi et al., 2020) to generate
 263 synthetic videos using PyBullet (Coumans & Bai, 2016–2021) and Blender (Community, 2025). First,
 264 we define objects and their properties such as mass and lateral friction. Then we randomly initialize
 265 their state variables, such as position and velocity, in a PyBullet environment. The trajectories are
 266 obtained by running the simulation. However, unlike in (Yi et al., 2020), our trajectories are governed
 267 by custom physical laws that differ from real-world physical laws. To simulate these custom physical
 268 laws, we intervene when collisions occur during simulation and manually adjust states of objects
 269 such as linear/angular velocity and direction. These trajectories are then used by Blender to render
 the final video. Visual object properties such as color and texture are randomly chosen. See Fig. 3.

270 **Question generation details:** Each scenario comprises around 2000 samples, of which 10 randomly
271 chosen samples are set aside as exemplars. Question-answer pairs are generated for each sample
272 from pre-defined templates. Since each scenario concerns a particular query (e.g., change in the
273 vertical velocity in **Wall**), we use multiple templates for the questions and the answer options to avoid
274 lexical repetition. For instance, in **Wall**, the templates for the question are {“What happens to the
275 vertical velocity of **<obj>** when it collides with wall?”, “What is the outcome of **<obj>** colliding with
276 wall?”, “What occurs to the vertical velocity of **<obj>** when **<obj>** and wall collide?”}. A similar
277 multi-template approach is used to generate answers. The answer options are also shuffled for each
278 sample so that the model may not simply repeat the answer options from the exemplars.
279

280 **4 WHAT DOES INPHYRE DISCOVER ABOUT PHYSICAL REASONING IN**
281 **LMMs?**
282

283 Before we examine the physical reasoning abilities of LMMs, we will describe the evaluation setup
284 and codify the procedure to answer specific queries about physical reasoning using INPHYRE.
285

286 **4.1 EVALUATION SETUP**
287

288 **Evaluated LMMs:** We use INPHYRE to evaluate the quality of physical reasoning (both parametric
289 and inductive) in a diverse cohort of LMMs. To represent the variety of choices in model design
290 and training datasets, we include **13 open-source LMMs**: LLaVA-NeXT-Video (Zhang et al., 2024),
291 LLaVA-OneVision (Li et al., 2024a), LLaVA-NeXT-Interleave (Li et al., 2024c), Gemma 3 (Kamath
292 et al., 2025) herd, Aria (Li et al., 2024b), VideoLLaMA3 (Zhang et al., 2025) herd, InternVL3 (Zhu
293 et al., 2025) herd, Qwen2-VL (Wang et al., 2024a), and Qwen2.5-Omni (Xu et al., 2025). The chosen
294 models use different vision encoders and language models, and cover an extensive parameter count
295 range (from 1B to nearly 25B). The image encoders in the chosen LMMs are pre-trained and then
296 fine-tuned. The majority of the chosen LMMs fine-tune separately trained LLMs, while Gemma and
297 Aria train their language models from scratch. Aria uses a mixture-of-experts (MoE) architecture.
298 More details are listed in Tab. 3. **Results on closed models** such as GPT-4 and Gemini are in § E.2.

299 **Evaluation tools:** INPHYRE contains regular scenarios that follow real-world physical laws and
300 irregular scenarios that violate one or more real-world physical laws. For each LMM, we conduct
301 zero-shot evaluation in regular scenarios and few-shot evaluations in both regular and irregular
302 scenarios. The few-shot setting is further categorized into two sub-settings: (i) “visual-text”, where
303 the exemplars contain collision videos along with a question-answer pair, and (ii) “visual-only”,
304 where the exemplars include only videos. In all settings, the evaluation metric is the model’s accuracy
305 in choosing the correct option for the multiple-choice question. Below, we enunciate our specific
306 questions about physical reasoning in LMMs and how to quantitatively answer them using INPHYRE:
307

308 § 4.2 *How much parametric knowledge do LMMs have about universal physical laws?* We answer
309 this using the zero-shot predictive accuracy of the model in regular scenarios that follow
310 universal physical laws.

311 § 4.3 *Can LMMs augment their parametric knowledge with exemplars?* To answer this question,
312 we compare the few-shot performance of the model in regular scenarios with the zero-shot
313 accuracy. Here, exemplars are taken from the evaluated regular scenario.

314 § 4.4 *How strong is inductive physical reasoning in LMMs?* Inductive physical reasoning in LMMs
315 is evaluated by comparing their few-shot performances in regular and irregular scenarios.

316 § 4.5 *How much of this inductive physical reasoning is aided by language?* We answer this
317 question by computing the difference between the few-shot performances of the model in
318 irregular scenarios under “video-text” and “video-only” settings.

319 **4.2 HOW MUCH PARAMETRIC KNOWLEDGE DO LMMs HAVE ABOUT UNIVERSAL PHYSICS?**
320

321 INPHYRE includes regular versions of **LMC**, **SB**, and **Wall** that obey universal physical laws of
322 mechanics, such as principles of momentum and energy conservation. We measure the parametric
323 knowledge about these universal laws in LMMs as their zero-shot accuracy in these regular scenarios.

LMM	LMC (Regular)			SB (Regular)			Wall (Regular)			Average	
	Zero-shot	3-shot	Zero-shot	3-shot	Zero-shot	3-shot	Zero-shot	3-shot	Zero-shot	3-shot	Zero-shot
InternVL3-1B (Zhu et al., 2025)	71.46	33.27 (-38.19)	87.42	47.54 (-39.88)	5.68	9.30 (+3.62)	54.85	30.03 (-24.82)			
VideoLLaMA3-2B (Zhang et al., 2025)	56.13	62.96 (+6.83)	51.70	63.93 (+12.23)	3.72	37.69 (+33.97)	37.18	54.86 (+17.68)			
InternVL3-2B (Zhu et al., 2025)	77.89	90.00 (+12.11)	66.87	76.92 (+10.05)	29.90	91.61 (+61.71)	58.22	86.17 (+27.95)			
Gemma 3-4B (Kamath et al., 2025)	20.35	52.46 (+32.11)	58.35	69.51 (+11.16)	77.69	74.42 (- 3.27)	52.13	65.46 (+13.34)			
LLaVA-NeXT-Vid (Zhang et al., 2024)	50.10	56.18 (+ 6.08)	16.44	35.06 (+18.62)	2.46	7.59 (+ 5.13)	23.00	32.94 (+ 9.94)			
InternVL3-8B (Zhu et al., 2025)	60.60	99.65 (+39.05)	94.47	99.85 (+ 5.38)	57.19	98.74 (+41.56)	70.75	99.41 (+28.66)			
LLaVA-OneVision (Li et al., 2024a)	75.83	99.10 (+23.27)	83.97	99.29 (+15.32)	4.57	99.75 (+95.18)	54.79	99.38 (+44.59)			
VideoLLaMA3-7B (Zhang et al., 2025)	78.69	98.04 (+19.35)	69.10	93.46 (+24.35)	7.44	51.76 (+44.32)	51.74	81.08 (+29.34)			
LLaVA-NeXT-IL (Li et al., 2024c)	83.42	97.14 (+13.72)	65.20	63.72 (- 1.47)	0.55	78.84 (+78.29)	49.72	79.90 (+30.18)			
Qwen2-VL (Wang et al., 2024a)	66.83	98.14 (+31.31)	73.57	98.73 (+25.16)	7.09	99.25 (+92.16)	49.16	98.71 (+49.54)			
Qwen2.5-Omni (Xu et al., 2025)	57.99	45.83 (-12.16)	94.52	86.66 (- 7.86)	3.72	44.27 (+40.55)	52.08	58.92 (+ 6.84)			
Gemma 3-12B (Kamath et al., 2025)	35.68	85.33 (+49.65)	86.71	76.51 (-10.20)	68.84	60.75 (- 8.09)	63.74	74.20 (+10.45)			
Aria (Li et al., 2024b)	39.70	53.12 (+13.42)	77.32	92.29 (+14.97)	36.03	65.88 (+29.85)	51.02	70.43 (+19.41)			

Table 2: Zero-shot and 3-shot evaluation results on regular scenarios.

Tab. 2 shows the zero-shot accuracy of LMMs in regular scenarios. In each scenario, the task was to predict the change in velocity of an object after colliding with another object at rest from the initial image frame of the collision video. Surprisingly, **many LMMs struggle to answer even these simple questions using the momentum conservation principle**, and the models achieve above 80% accuracy in only 6 out of 39 scenarios, mainly in **SB** (Reg.). The performances of LMMs also vary greatly between scenarios, despite these scenarios following the same physical laws, *e.g.*, most models performed poorly in **Wall** (Reg.) compared to other scenarios. Qualitative inspection of their outputs in § E.6 reveals that LMMs can state universal physical laws (*e.g.*, “kinetic energy is conserved in an elastic collision”) but struggle to apply them for physical reasoning. They also hallucinate irrelevant assumptions (*e.g.*, about material) and incorrect physical laws that further hurt their reasoning. We conclude that LMMs memorize the laws of mechanics and can recollect them as factual information, but fail to apply this knowledge for physical reasoning. A similar conclusion was made in (Yu et al., 2025), but for abstract physical reasoning.

CONCLUSION

LMMs have limited parametric knowledge about the laws of mechanics. Although LMMs can state these universal laws, they often struggle to apply them for physical reasoning.

4.3 CAN LMMs AUGMENT THEIR PARAMETRIC KNOWLEDGE WITH EXEMPLARS?

Before evaluating the inductive physical reasoning of LMMs in irregular scenarios, we must verify that exemplars can improve physical reasoning in LMMs. Therefore, we evaluate LMMs in regular scenarios in the few-shot setting with exemplars that do not contradict any universal physical laws encoded in the models’ parameters. Specifically, we consider the “visual-text” setting, where question-answer pairs accompany videos in exemplars. Then we compare the few-shot performance of LMMs in regular scenarios with their corresponding zero-shot performance.

Tab. 2 compares the 3-shot performance of LMMs in regular scenarios with their corresponding zero-shot performance. **All LMMs significantly improved their performance when provided with exemplars in at least one scenario.** On average, we observe that all models except InternVL3-1B improved their performance with exemplars. Among the LMMs evaluated, Qwen2-VL achieved the highest average increase in performance with exemplars. LLaVA-Onevision, Qwen2-VL, and InternVL3-8B also achieved nearly 100% average accuracy over all scenarios. These results clearly demonstrate that LMMs can use exemplars to improve their prediction accuracy.

CONCLUSION

Exemplars that obeyed universal physical laws support parametric knowledge in LMMs successfully. With only three exemplars, several LMMs achieve nearly 100% prediction accuracy.

4.4 HOW STRONG IS INDUCTIVE PHYSICAL REASONING IN LMMs?

We established that exemplars that obey universal physical laws improve the performance of LMMs in regular scenarios. We will now evaluate whether LMMs can leverage exemplars that do not follow the true physical laws to reason in irregular scenarios. Following the previous experiments, the task is to predict the outcome of a potential collision event from an image with the help of exemplar videos

378 from the same scenario. Exemplars also include question-answer pairs. However, these collision
 379 events (and the provided exemplars) violate the true physical laws. Therefore, to correctly answer the
 380 questions, LMMs must infer the underlying physical laws from exemplars through inductive physical
 381 reasoning.

382 Fig. 4 compares 3-shot accuracy of each
 383 combination of model and irregular scenario against that model’s best performance
 384 among zero-shot and few-shot evaluations in the corresponding regular scenario that depicts similar events while following universal physical laws. For **SB**
 385 and **Wall**, the corresponding regular scenarios are **SB** (Reg.) and **Wall** (Reg.), respectively. For all other irregular scenarios, **LMC** (Reg.) is the corresponding regular scenario. A negative value means poor inductive physical reasoning in that scenario. In Fig. 4, we observe that
 386 **most models show a drop in accuracy compared to regular scenarios, indicating weak inductive physical reasoning**.
 387 However, the drop in accuracy varies with the models. InternVL3-2B and Gemma3-4B show the highest and the lowest average drop in accuracy, respectively. Performance deterioration also varies with the scenario. Almost all models suffer a considerable drop in accuracy in **SB**, indicating that LMMs struggle to differentiate between volume and mass. Surprisingly, several LMMs performed better in **AMC** than **LMC** (Reg.). However, as we show in § E.7, this apparent inductive physical reasoning is due to LMMs possessing the wrong parametric knowledge about angular momentum conservation, thus inadvertently performing well in irregular scenarios. The absolute accuracy values are given in § B.4.

CONCLUSION

408 LMMs demonstrate only weak inductive physical reasoning when exemplars violate parametric
 409 knowledge. Almost all LMMs showed significant deterioration in performance.

4.5 HOW MUCH OF THIS INDUCTIVE PHYSICAL REASONING IS AIDED BY LANGUAGE?

412 In our previous experiments, exemplars
 413 included both videos and question-answer
 414 pairs. However, multimodal models are
 415 well known to exploit their language
 416 bias in visual question answering (VQA)
 417 tasks (Goyal et al., 2017). This raises
 418 the possibility that the observed inductive
 419 physical reasoning, limited as it may
 420 be, originated primarily from the language
 421 component of LMMs. The existence of
 422 language bias can undermine the trustworthiness
 423 of LMMs on visual inputs. To detect the
 424 presence of language bias, we repeat our
 425 few-shot experiments from § 4.4 but with
 426 exemplars that contain *only* the
 427 collision videos. This setup entirely
 428 restricts LMMs to their visual inductive
 429 physical reasoning capabilities. Following
 430 (Min et al., 2022), we include randomly
 431 chosen options in the exemplars to entice the
 432 model to choose an option instead of providing
 433 open-ended reasoning (see § B.2).

434 Fig. 5 shows the difference between performances under video-only and video-text settings. We find
 435 that the **inductive physical reasoning in LMMs, unfortunately, arises largely from the language**

	LMC	Wall	AMC	Red-LMC	Red-Pass	SB	CC	Average over scenarios
InternVL3-1B	-23.22	9.20	11.76	-13.01	-15.47	-76.97	-23.52	-18.75
VideoLLaMA3-2B	-25.83	-15.33	-3.62	-27.28	-13.49	-55.84	-16.93	-22.62
InternVL3-2B	-74.92	-91.36	9.05	-64.94	-68.90	-76.81	-80.65	-64.08
Gemma 3-4B	33.92	-21.56	7.24	28.19	9.64	-44.88	-15.38	-0.40
LLaVA-NeXT-Vid	-39.50	27.69	-10.60	-48.56	-44.40	-16.62	-24.57	-22.37
InternVL3-8B	-5.33	-0.20	0.35	-27.87	-52.38	-53.87	-30.70	-24.29
LLaVA-OneVision	-0.90	-2.56	0.30	-24.16	-31.38	-67.88	-33.32	-22.84
VideoLLaMA3-7B	-14.42	29.65	-0.30	-48.97	-44.01	-29.28	-21.76	-18.44
LLaVA-NeXT-IL	-3.42	15.33	-4.97	-34.63	-37.29	-21.48	0.95	-12.21
Qwen2-VL	-2.11	0.75	-2.81	1.01	-1.45	-84.96	-7.79	-13.91
Qwen2.5-Omni	5.83	-4.97	32.11	-4.36	5.62	-38.29	-13.72	-2.54
Gemma 3-12B	-28.04	23.52	6.18	-57.66	-63.92	-68.62	1.81	-26.68
Aria	-25.88	-65.18	27.24	-24.54	-33.17	-85.35	-45.63	-36.07
Average over LMMs	-15.68	-7.31	5.53	-26.67	-30.04	-55.45	-23.94	

Figure 4: Difference in 3-shot accuracy of LMMs between irregular and regular scenarios when exemplars contain both videos and QA pairs.

	LMC	Wall	AMC	Red-LMC	Red-Pass	SB	CC	Average over scenarios
InternVL3-1B	-25.08	-10.75	-51.41	-32.33	-27.42	6.53	1.56	-19.84
VideoLLaMA3-2B	-23.97	-9.10	-26.13	-21.50	-31.28	18.04	-32.86	-18.11
InternVL3-2B	-9.35	-0.25	-36.33	-16.74	-12.38	7.84	-9.20	-10.92
LLaVA-NeXT-Vid	-1.01	7.19	-2.36	9.22	4.36	10.80	9.85	5.44
InternVL3-8B	-76.13	-41.11	-41.66	-55.09	-26.32	-31.86	-59.15	-47.33
LLaVA-OneVision	-94.97	-71.56	-42.66	-72.13	-64.51	-17.64	-65.73	-61.31
VideoLLaMA3-7B	-79.50	-61.31	-52.66	-40.05	-43.61	-34.27	-67.24	-54.09
LLaVA-NeXT-IL	-93.32	-77.64	-42.76	-62.11	-59.45	-23.72	-65.78	-60.68
Qwen2-VL	-92.21	-54.32	-28.49	-94.54	-93.48	-6.03	-44.82	-59.13
Qwen2.5-Omni	-63.67	-17.29	-30.95	-51.83	-61.35	-37.84	-2.76	-37.96
Gemma 3-12B	-46.93	-91.91	-24.37	-22.51	-6.37	-13.07	-87.14	-41.76
Aria	-26.33	2.71	-51.01	-27.27	-18.65	6.08	-7.29	-17.39
Average over LMMs	-52.71	-35.44	-35.90	-40.57	-36.70	-9.59	-35.88	

Figure 5: Difference in 3-shot accuracy in irregular scenarios between video-only and video-text settings.

Following (Min et al., 2022), we include randomly chosen options in the exemplars to entice the model to choose an option instead of providing open-ended reasoning (see § B.2).

432 **components** of LMMs. When the exemplars contained only videos, almost all LMMs showed a
 433 significant drop in accuracy compared to their performance when the exemplars contained both
 434 videos and question-answer pairs. In certain scenarios, LMMs could achieve only near-zero accuracy,
 435 *e.g.*, Qwen2.5-Omni in LMC and LLaVA-Next-Interleave in Red-LMC and Red-Pass. The accuracy
 436 drop was higher for larger models. Our findings echo the concurrent evidence of language bias in
 437 LMMs reported by (Baldassini et al., 2024; Chen et al., 2025), although their findings were not about
 438 physical reasoning in LMMs.

439 CONCLUSION

440 Inductive physical reasoning in the evaluated LMMs show strong language bias, relying primarily
 441 on the textual content of the exemplars to answer the question. The presence of language bias
 442 questions the trustworthiness of LMMs in scenarios with unseen physical laws.

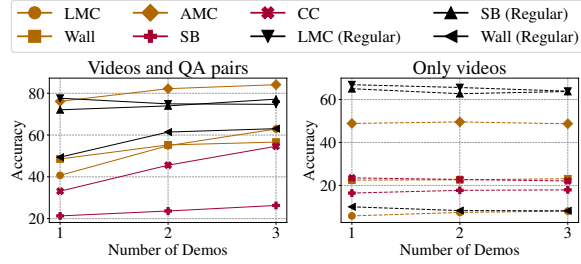
444 5 FURTHER DISCUSSION

445 We investigate the effect of the exemplar retrieval method and the number of retrieved exemplars in
 446 this section. Refer to § E for experiments on quantized models, a visually more complex version of
 447 INPHYRE, evaluation with all evaluation sample frames included, effects of prompt perturbations,
 448 and qualitative results on INPHYRE.

449 **Effect of number of exemplars:** The
 450 number of exemplars in an evaluation sample is limited by the context length in
 451 which the models were trained/fine-tuned.
 452 Our few-shot experiments in § 4 used
 453 three exemplars per evaluation sample. In
 454 this section, we will examine if the
 455 number of exemplars significantly affects
 456 performance on INPHYRE. We vary the
 457 number of exemplars from 1 to 3 and average
 458 the prediction accuracy over the evaluated
 459 LMMs for each scenario. We evaluate on both “video-text” and “video-only” settings to investigate
 460 potential language bias. Fig. 6 (left) shows the change in prediction accuracy with the number of
 461 exemplars when the exemplars contain both videos and question-answer pairs. Across all scenarios,
 462 we observe a clear improvement in predictive performance. In particular, LMC and CC show signifi-
 463 cant improvements in accuracy. However, similar improvement is not present in Fig. 6 (right), where
 464 exemplars contained only videos. Performance even deteriorated in LMC (Reg.) as the number of
 465 exemplars increased, although the remaining scenarios were unaffected. These results reaffirm our
 466 observation about the language bias in LMMs.
 467

468 **We evaluate human performance on INPHYRE** using ten human subjects. Each subject was
 469 provided with one demonstration sample from each scenario, without the accompanying question-
 470 answer pair. For Red-LMC and Red-Pass, they were provided four demonstration samples since they
 471 were required to infer conditional reasoning rules. Then, they were asked to answer one evaluation
 472 query from the same scenario. We asked them to answer only one query since all queries in a scenario
 473 shared the underlying physical logic. Despite being provided only demonstration samples without
 474 textual information, the subjects scored above 90% accuracy in many scenarios. They struggled
 475 relatively more in Red-LMC, Red-Pass, and CC. Detailed subject-wise results are provided in § E.9.

476 **Effect of CoT prompting and fine-tuning:** Chain-of-thought (CoT) prompting (Wei et al., 2022) and
 477 fine-tuning (FT) have been shown to improve reasoning in LMMs (Buschoff et al., 2025). However,
 478 the underlying physical law and the samples themselves must be available in advance for CoT
 479 prompting and fine-tuning, respectively. Therefore, these paradigms are not suitable for the premise
 480 of inductive physical reasoning, which posits that we have access to only visual samples from unseen
 481 scenarios immediately before inference. Nonetheless, we still evaluate the effects of CoT and FT
 482 on INPHYRE to obtain a “soft upper bound” on the LMMs’ performance. The results with CoT
 483 prompting and FT are shown in Tabs. 8 and 9, respectively. We find that both CoT and FT can
 484 generally improve performance in most scenarios, except Red-Pass and Red-LMC, which, unlike
 485 other scenarios, require conditional physical reasoning, signaling the utility limits of CoT prompting
 486 and FT. As a reminder, in these scenarios, only red-colored objects violate the true physical laws.



477 Figure 6: Effect of number of exemplars on the accuracy.

486 **Causes of poor performance in irregular scenarios:** We provide a preliminary analysis of the
 487 causes of poor performance in irregular scenarios in § F. To this end, we use linear probes on the
 488 hidden states from pre-trained and fine-tuned InternVL3-1B, and visualize attention values over
 489 the tokens in the last layer of Gemma3-12B. We find that the hidden states of both pre-trained and
 490 fine-tuned models carry sufficient information to classify the underlying scenario (Fig. 25). Moreover,
 491 after fine-tuning, the hidden states adaptively include attribute information from demonstration and
 492 evaluation samples depending on the underlying scenario (Figs. 26 and 27). Visualization of attention
 493 values from the last layer of Gemma3-12B shows that the model spends an order of magnitude less
 494 attention over image tokens compared to text tokens (Fig. 24). We believe that these findings will
 495 assist in developing methods to explicitly improve inductive physical reasoning.

496 **Effect of exemplar retrieval method:** The choice of re-
 497 tried samples could affect the performance of LLMs (Liu
 498 et al., 2022; Peng et al., 2024). We now verify if this prop-
 499 osition holds for visual inductive physical reasoning. By
 500 adapting the textual exemplar retriever from (Liu et al.,
 501 2022) for vision, we design a “nearest-neighbor exem-
 502 plar retriever” (NNER) that finds the top- k video samples
 503 closest to the initial frame of the evaluation sample ac-
 504 cording to their cosine distance in the feature space of
 505 CLIP-L (Radford et al., 2021). To evaluate the effect of
 506 retrievers on visual inductive physical reasoning, we in-
 507 clude only videos in exemplars. We do not evaluate on
 508 **Red-LMC** and **Red-Pass** since NNER does not guarantee
 509 that the retrieved samples include videos with and without red-colored objects. In Fig. 7, we observe
 510 either an insignificant or no change in performance between a random retriever and NNER, agreeing
 511 with our observation that LMMs rely primarily on language for inductive physical reasoning.

511 6 CONCLUSION

513 When inference scenarios violate the physical laws encoded in the model parameters, LMMs must
 514 ideally derive their physical reasoning from demonstration samples. Therefore, to ensure their
 515 trustworthiness, it is critical to evaluate how well LMMs can infer physical laws from these exemplars.
 516 To this end, we introduced **INPHYRE**, the *first* visual question answering benchmark to quantify
 517 parametric knowledge and inductive physical reasoning in LMMs. **INPHYRE** evaluates LMMs in
 518 collision scenarios that violate universal physical laws such as momentum conservation. Through
 519 zero-shot and few-shot experiments in these scenarios, we found that LMMs have limited parametric
 520 knowledge of universal physical laws and struggle to apply these laws during physical reasoning.
 521 LMMs demonstrate only weak inductive physical reasoning when exemplars violate universal physical
 522 laws. The observed inductive physical reasoning also suffered from language bias and relied little on
 523 visual input in exemplars, shedding doubt on the trustworthiness of LMMs on visual input.

524 **Limitations:** Although **INPHYRE** proved to be a formidable benchmark for LMMs in terms of
 525 physical laws, its simple synthetic scene could not have posed visual challenges to the models.
 526 Inductive physical reasoning of LMMs could be worse in a more crowded and realistic visual scene.
 527 However, since real-world videos cannot violate true physical laws, the closest alternative to evaluate
 528 inductive physical reasoning in LMMs is a hyperrealistic video benchmark generated using advanced
 529 video generation models (OpenAI, 2024; Kondratyuk et al., 2024; Chen et al., 2024b). However,
 530 such endeavors can be fruitful only with absolute control over physical realism, which is lacking in
 531 current video generation models (Cho et al., 2024; Motamed et al., 2025).

532 REFERENCES

534 Josh Achiam, Steven Adler, Sandhini Agarwal, Lama Ahmad, Ilge Akkaya, Florencia Leoni Aleman,
 535 Diogo Almeida, Janko Altenschmidt, Sam Altman, Shyamal Anadkat, et al. GPT-4 Technical
 536 Report. *arXiv preprint arXiv:2303.08774*, 2023.

537 Stéphane Aroca-Ouellette, Cory Paik, Alessandro Roncone, and Katharina Kann. PROST: Physical
 538 Reasoning about Objects through Space and Time. In *Annual Meeting of the Association for
 539 Computational Linguistics*, 2021.

	InternVL3-1B	0.019	0.054	-0.040	-0.013	0.013
VideoLLaMA3-2B	-0.024	-0.004	0.020	-0.006	-0.004	
InternVL3-2B	-0.005	0.000	0.071	0.023	-0.001	
LLaVA-NeXT-Vid	0.005	-0.002	0.011	0.001	-0.007	
InternVL3-8B	0.003	0.008	-0.010	0.017	0.012	
LLaVA-OneVision	-0.006	0.013	-0.011	0.002	0.000	
VideoLLaMA3-7B	0.016	0.013	-0.022	-0.004	0.015	
LLaVA-NeXT-IL	-0.001	-0.003	0.002	-0.003	-0.006	
Qwen2-VL	-0.026	0.007	0.010	-0.012	0.009	
Qwen2.5-Omni	-0.001	-0.010	-0.054	0.020	0.052	
Gemma 3-12B	-0.003	-0.004	-0.003	0.000	0.000	
Aria	0.005	-0.002	0.005	0.001	-0.001	
	LMC	Wall	AMC	SB	CC	

512 Figure 7: Change in accuracy when
 NNER is used to find exemplars.

540 Tayfun Ates, M Ateşoğlu, Çağatay Yiğit, İlker Keser, Mert Kobas, Erkut Erdem, Aykut Erdem,
541 Tilbe Goksun, and Deniz Yuret. CRAFT: A Benchmark for Causal Reasoning About Forces and
542 inTeractions. In *Annual Meeting of the Association for Computational Linguistics*, 2022.

543

544 Jinze Bai, Shuai Bai, Shusheng Yang, Shijie Wang, Sinan Tan, Peng Wang, Junyang Lin, Chang Zhou,
545 and Jingren Zhou. Qwen-VL: A Versatile Vision-Language Model for Understanding, Localization,
546 Text Reading, and Beyond. *arXiv preprint arXiv:2308.12966*, 2023a.

547 Shuai Bai, Keqin Chen, Xuejing Liu, Jialin Wang, Wenbin Ge, Sibo Song, Kai Dang, Peng Wang,
548 Shijie Wang, Jun Tang, et al. Qwen2.5-VL Technical Report. *arXiv preprint arXiv:2502.13923*,
549 2025.

550

551 Yu Bai, Fan Chen, Huan Wang, Caiming Xiong, and Song Mei. Transformers as Statisticians:
552 Provable In-Context Learning with In-Context Algorithm Selection. In *Advances in Neural
553 Information Processing Systems*, 2023b.

554 Anton Bakhtin, Laurens van der Maaten, Justin Johnson, Laura Gustafson, and Ross Girshick.
555 PHYRE: A New Benchmark for Physical Reasoning. In *Advances in Neural Information Processing
556 Systems*, 2019.

557

558 Folco Bertini Baldassini, Mustafa Shukor, Matthieu Cord, Laure Soulier, and Benjamin Piwowarski.
559 What Makes Multimodal In-Context Learning Work? In *IEEE/CVF Conference on Computer
560 Vision and Pattern Recognition Workshop*, 2024.

561 Fabien Baradel, Natalia Neverova, Julien Mille, Greg Mori, and Christian Wolf. CoPhy: Counterfac-
562 tual Learning of Physical Dynamics. In *International Conference on Learning Representations*,
563 2020.

564 Daniel Bear, Elias Wang, Damian Mrowca, Felix Jedidja Binder, Hsiao-Yu Tung, RT Pramod,
565 Cameron Holdaway, Sirui Tao, Kevin A Smith, Fan-Yun Sun, et al. Physion: Evaluating physical
566 prediction from vision in humans and machines. In *Advances in Neural Information Processing
567 Systems*, 2021.

568

569 Yonatan Bisk, Rowan Zellers, Jianfeng Gao, Yejin Choi, et al. PIQA: Reasoning about Physical
570 Commonsense in Natural Language. In *AAAI Conference on Artificial Intelligence*, 2020.

571 Florian Bordes, Quentin Garrido, Justine T Kao, Adina Williams, Michael Rabbat, and Emmanuel
572 Dupoux. IntPhys 2: Benchmarking Intuitive Physics Understanding In Complex Synthetic Envi-
573 ronments. *arXiv preprint arXiv:2506.09849*, 2025.

574

575 Chen Bowen, Rune Sætre, and Yusuke Miyao. A Comprehensive Evaluation of Inductive Reasoning
576 Capabilities and Problem Solving in Large Language Models. In *Conference of the European
577 Chapter of the Association for Computational Linguistics*, 2024.

578 Luca M Schulze Buschoff, Konstantinos Voudouris, Elif Akata, Matthias Bethge, Joshua B Tenen-
579 baum, and Eric Schulz. Testing the Limits of Fine-Tuning for Improving Visual Cognition in
580 Vision Language Models. *arXiv preprint arXiv:2502.15678*, 2025.

581

582 Zhipeng Cai, Ching-Feng Yeh, Hu Xu, Zhuang Liu, Gregory Meyer, Xinjie Lei, Changsheng Zhao,
583 Shang-Wen Li, Vikas Chandra, and Yangyang Shi. DepthLM: Metric Depth From Vision Language
584 Models. *arXiv preprint arXiv:2509.25413*, 2025.

585

586 Meng Cao, Haoran Tang, Haoze Zhao, Hangyu Guo, Jiaheng Liu, Ge Zhang, Ruyang Liu, Qiang
587 Sun, Ian Reid, and Xiaodan Liang. PhysGame: Uncovering Physical Commonsense Violations in
588 Gameplay Videos. *arXiv preprint arXiv:2412.01800*, 2024.

589

590 Liang Chen, Haozhe Zhao, Tianyu Liu, Shuai Bai, Junyang Lin, Chang Zhou, and Baobao Chang.
591 An Image is Worth 1/2 Tokens After Layer 2: Plug-and-Play Inference Acceleration for Large
592 Vision-Language Models. In *European Conference on Computer Vision*, 2024a.

593

594 Lin Chen, Xilin Wei, Jinsong Li, Xiaoyi Dong, Pan Zhang, Yuhang Zang, Zehui Chen, Haodong
595 Duan, Zhenyu Tang, Li Yuan, et al. ShareGPT4Video: Improving Video Understanding and
596 Generation with Better Captions. In *Advances in Neural Information Processing Systems*, 2024b.

594 Shuo Chen, Zhen Han, Bailan He, Jianzhe Liu, Mark Buckley, Yao Qin, Philip Torr, Volker Tresp,
595 and Jindong Gu. Can Multimodal Large Language Models Truly Perform Multimodal In-Context
596 Learning? In *Winter Conference on Applications of Computer Vision*, 2025.

597

598 Zhe Chen, Jiannan Wu, Wenhui Wang, Weijie Su, Guo Chen, Sen Xing, Muyan Zhong, Qinglong
599 Zhang, Xizhou Zhu, Lewei Lu, et al. InternVL: Scaling up Vision Foundation Models and Aligning
600 for Generic Visual-Linguistic Tasks. In *IEEE/CVF Conference on Computer Vision and Pattern
Recognition*, 2024c.

601

602 Zhenfang Chen, Kexin Yi, Yunzhu Li, Mingyu Ding, Antonio Torralba, Joshua B Tenenbaum, and
603 Chuang Gan. ComPhy: Compositional Physical Reasoning of Objects and Events from Videos. In
604 *International Conference on Learning Representations*, 2022.

605

606 Zhenfang Chen, Shilong Dong, Kexin Yi, Yunzhu Li, Mingyu Ding, Antonio Torralba, Joshua B
607 Tenenbaum, and Chuang Gan. Compositional Physical Reasoning of Objects and Events from
608 Videos. *arXiv preprint arXiv:2408.02687*, 2024d.

609

610 Kewei Cheng, Jingfeng Yang, Haoming Jiang, Zhengyang Wang, Binxuan Huang, Ruirui Li, Shiyang
611 Li, Zheng Li, Yifan Gao, Xian Li, et al. Inductive or deductive? Rethinking the fundamental
612 reasoning abilities of LLMs. In *ACL Workshop on Natural Language Reasoning and Structure
Explanations*, 2024.

613

614 Anoop Cherian, Radu Corcodel, Siddarth Jain, and Diego Romero. LLMPhy: Complex Physical
615 Reasoning Using Large Language Models and World Models. *arXiv preprint arXiv:2411.08027*,
616 2024.

617

618 Joseph Cho, Fachrina Dewi Puspitasari, Sheng Zheng, Jingyao Zheng, Lik-Hang Lee, Tae-Ho Kim,
619 Choong Seon Hong, and Chaoning Zhang. Sora as an AGI World Model? A Complete Survey on
620 Text-to-Video Generation. *arXiv preprint arXiv:2403.05131*, 2024.

621

622 François Chollet. On the Measure of Intelligence. *arXiv preprint arXiv:1911.01547*, 2019.

623

624 Wei Chow, Jiageng Mao, Boyi Li, Daniel Seita, Vitor Campagnolo Guizilini, and Yue Wang. Phys-
625 Bench: Benchmarking and Enhancing Vision-Language Models for Physical World Understanding.
626 In *International Conference on Learning Representations*, 2025.

627

628 Gheorghe Comanici, Eric Bieber, Mike Schaeckermann, Ice Pasupat, Noveen Sachdeva, Inderjit
629 Dhillon, Marcel Blistein, Ori Ram, Dan Zhang, Evan Rosen, et al. Gemini 2.5: Pushing the
630 Frontier with Advanced Reasoning, Multimodality, Long Context, and Next Generation Agentic
631 Capabilities. *arXiv preprint arXiv:2507.06261*, 2025.

632

633 The Blender Community. Blender 4.4. <https://docs.blender.org/manual/en/4.4/index.html>,
634 2025.

635

636 Erwin Coumans and Yunfei Bai. PyBullet, a Python module for physics simulation for games,
637 robotics and machine learning. <http://pybullet.org>, 2016–2021.

638

639 Stephanie Denison and Fei Xu. Integrating physical constraints in statistical inference by 11-month-
old infants. *Cognitive science*, 34(5):885–908, 2010.

640

641 Yuhao Dong, Zuyan Liu, Hai-Long Sun, Jingkang Yang, Winston Hu, Yongming Rao, and Ziwei Liu.
642 Insight-V: Exploring Long-Chain Visual Reasoning with Multimodal Large Language Models.
643 *arXiv preprint arXiv:2411.14432*, 2024.

644

645 Dave Epstein, Boyuan Chen, and Carl Vondrick. Oops! Predicting Unintentional Action in Video. In
646 *IEEE/CVF Conference on Computer Vision and Pattern Recognition*, 2020.

647

648 Laura Faßbender, Johannes Falck, Francisco M López, Yee Lee Shing, Jochen Triesch, and Gudrun
649 Schwarzer. A comparison of force adaptation in toddlers and adults during a drawer opening task.
650 *Scientific Reports*, 15(1):3699, 2025.

651

652 Shivam Garg, Dimitris Tsipras, Percy S Liang, and Gregory Valiant. What Can Transformers Learn
653 In-Context? A Case Study of Simple Function Classes. In *Advances in Neural Information
654 Processing Systems*, 2022.

648 Quentin Garrido, Nicolas Ballas, Mahmoud Assran, Adrien Bardes, Laurent Najman, Michael
649 Rabbat, Emmanuel Dupoux, and Yann LeCun. Intuitive physics understanding emerges from
650 self-supervised pretraining on natural videos. *arXiv preprint arXiv:2502.11831*, 2025.
651

652 Gaël Gendron, Qiming Bao, Michael Witbrock, and Gillian Dobbie. Large Language Models Are
653 Not Strong Abstract Reasoners. In *International Joint Conference on Artificial Intelligence*, 2024.
654

655 Yash Goyal, Tejas Khot, Douglas Summers-Stay, Dhruv Batra, and Devi Parikh. Making the V
656 in VQA Matter: Elevating the Role of Image Understanding in Visual Question Answering. In
657 *IEEE/CVF Conference on Computer Vision and Pattern Recognition*, 2017.
658

659 Brett K Hayes. The Development of Inductive Reasoning. *Inductive Reasoning Experimental,*
660 *Developmental, and Computational Approaches*, pp. 25–54, 2007.
661

662 Kaiyu He, Mian Zhang, Shuo Yan, Peilin Wu, and Zhiyu Zoey Chen. IDEA: Enhancing the Rule
663 Learning Ability of Large Language Model Agent through Induction, Deduction, and Abduction.
664 *arXiv preprint arXiv:2408.10455*, 2024.
665

666 Edward J Hu, Yelong Shen, Phillip Wallis, Zeyuan Allen-Zhu, Yuanzhi Li, Shean Wang, Lu Wang,
667 and Weizhu Chen. LoRA: Low-Rank Adaptation of Large Language Models. In *International*
668 *Conference on Learning Representations*, 2022.
669

670 Benoit Jacob, Skirmantas Kligys, Bo Chen, Menglong Zhu, Matthew Tang, Andrew Howard, Hartwig
671 Adam, and Dmitry Kalenichenko. Quantization and Training of Neural Networks for Efficient
672 Integer-Arithmetic-Only Inference. In *IEEE/CVF Conference on Computer Vision and Pattern*
673 *Recognition*, 2018.
674

675 Serwan Jassim, Mario Holubar, Annika Richter, Cornelius Wolff, Xenia Ohmer, and Elia Bruni.
676 GRASP: A Novel Benchmark for Evaluating Language GRounding and Situated Physics Un-
677 derstanding in Multimodal Language Models. In *International Joint Conference on Artificial*
678 *Intelligence*, 2024.
679

680 Justin Johnson, Bharath Hariharan, Laurens Van Der Maaten, Li Fei-Fei, C Lawrence Zitnick, and
681 Ross Girshick. CLEVR: A Diagnostic Dataset for Compositional Language and Elementary Visual
682 Reasoning. In *IEEE/CVF Conference on Computer Vision and Pattern Recognition*, 2017.
683

684 Aishwarya Kamath, Johan Ferret, Shreya Pathak, Nino Vieillard, Ramona Merhej, Sarah Perrin,
685 Tatiana Matejovicova, Alexandre Ramé, Morgane Rivière, et al. Gemma 3 Technical Report. *arXiv*
686 *preprint arXiv:2503.19786*, 2025.
687

688 Dan Kondratyuk, Lijun Yu, Xiuye Gu, Jose Lezama, Jonathan Huang, Grant Schindler, Rachel
689 Hornung, Vighnesh Birodkar, Jimmy Yan, Ming-Chang Chiu, et al. VideoPoet: A Large Language
690 Model for Zero-Shot Video Generation. In *International Conference on Machine Learning*, 2024.
691

692 Laura Kotovsky and Renée Baillargeon. The development of calibration-based reasoning about
693 collision events in young infants. *Cognition*, 67(3):311–351, 1998.
694

695 Adam Lerer, Sam Gross, and Rob Fergus. Learning Physical Intuition of Block Towers by Example.
696 In *International Conference on Machine Learning*, 2016.
697

698 Bo Li, Yuanhan Zhang, Dong Guo, Renrui Zhang, Feng Li, Hao Zhang, Kaichen Zhang, Peiyuan
699 Zhang, Yanwei Li, Ziwei Liu, et al. LLaVA-OneVision: Easy Visual Task Transfer. *arXiv preprint*
700 *arXiv:2408.03326*, 2024a.
701

702 Dongxu Li, Yudong Liu, Haoning Wu, Yue Wang, Zhiqi Shen, Bowen Qu, Xinyao Niu, Fan Zhou,
703 Chengen Huang, Yanpeng Li, et al. ARIA: An Open Multimodal Native Mixture-of-Experts Model.
704 *arXiv preprint arXiv:2410.05993*, 2024b.
705

706 Feng Li, Renrui Zhang, Hao Zhang, Yuanhan Zhang, Bo Li, Wei Li, Zejun Ma, and Chunyuan Li.
707 LLaVA-NeXT-Interleave: Tackling Multi-image, Video, and 3D in Large Multimodal Models.
708 *arXiv preprint arXiv:2407.07895*, 2024c.
709

702 Jiachun Li, Pengfei Cao, Zhuoran Jin, Yubo Chen, Kang Liu, and Jun Zhao. MIRAGE: Evaluating
703 and Explaining Inductive Reasoning Process in Language Models. In *International Conference on*
704 *Learning Representations*, 2025.

705 Jiaoda Li, Yifan Hou, Mrinmaya Sachan, and Ryan Cotterell. What Do Language Models Learn in
706 Context? The Structured Task Hypothesis. In *Annual Meeting of the Association for Computational*
707 *Linguistics*, 2024d.

708 Jiachang Liu, Dinghan Shen, Yizhe Zhang, William B Dolan, Lawrence Carin, and Weizhu Chen.
709 What Makes Good In-Context Examples for GPT-3? In *Deep Learning Inside Out (DeeLIO): The*
710 *3rd Workshop on Knowledge Extraction and Integration for Deep Learning Architectures*, 2022.

711 Francesco Margoni, Luca Surian, and Renée Baillargeon. The Violation-of-Expectation Paradigm: A
712 Conceptual Overview. *Psychological Review*, 131(3):716, 2024.

713 Francesco Margoni, Luca Surian, and Renée Baillargeon. The Violation-of-Expectation Paradigm: A
714 Conceptual Overview. *Psychological Review*, 131(3):716, 2024.

715 Sewon Min, Xinxi Lyu, Ari Holtzman, Mikel Artetxe, Mike Lewis, Hannaneh Hajishirzi, and Luke
716 Zettlemoyer. Rethinking the Role of Demonstrations: What Makes In-Context Learning Work? In
717 *Conference on Empirical Methods in Natural Language Processing*, 2022.

718 Suvir Mirchandani, Fei Xia, Pete Florence, Brian Ichter, Danny Driess, Montserrat Gonzalez Arenas,
719 Kanishka Rao, Dorsa Sadigh, and Andy Zeng. Large Language Models as General Pattern
720 Machines. In *Conference on Robot Learning*, 2023.

721 Saman Motamed, Laura Culp, Kevin Swersky, Priyank Jaini, and Robert Geirhos. Do generative
722 video models understand physical principles? *arXiv preprint arXiv:2501.09038*, 2025.

723 Roozbeh Mottaghi, Hessam Bagherinezhad, Mohammad Rastegari, and Ali Farhadi. Newtonian
724 Image Understanding: Unfolding the Dynamics of Objects in Static Images. In *IEEE/CVF*
725 *Conference on Computer Vision and Pattern Recognition*, 2016.

726 Nayantara Mudur, Hao Cui, Subhashini Venugopalan, Paul Raccuglia, Michael P Brenner, and Peter
727 Norgaard. FEA Bench: Evaluating Language Models on Multiphysics Reasoning Ability. *arXiv*
728 *preprint arXiv:2504.06260*, 2025.

729 Nayantara Mudur, Hao Cui, Subhashini Venugopalan, Paul Raccuglia, Michael P Brenner, and Peter
730 Norgaard. FEA Bench: Evaluating Language Models on Multiphysics Reasoning Ability. *arXiv*
731 *preprint arXiv:2504.06260*, 2025.

732 Aliakbar Nafar, Kristen Brent Venable, and Parisa Kordjamshidi. Learning vs Retrieval: The Role
733 of In-Context Examples in Regression with LLMs. In *Annual Conference of the North American*
734 *Chapter of the Association for Computational Linguistics*, 2025.

735 OpenAI. Sora – Creating video from text. <https://openai.com/index/sora/>, 2024.

736 Xinyu Pang, Ruixin Hong, Zhanke Zhou, Fangrui Lv, Xinwei Yang, Zhilong Liang, Bo Han, and
737 Changshui Zhang. Physics Reasoner: Knowledge-Augmented Reasoning for Solving Physics
738 Problems with Large Language Models. In *International Conference on Computational Linguistics*,
739 2025.

740 Keqin Peng, Liang Ding, Yancheng Yuan, Xuebo Liu, Min Zhang, Yuanxin Ouyang, and Dacheng
741 Tao. Revisiting Demonstration Selection Strategies in In-Context Learning. In *Annual Meeting of*
742 *the Association for Computational Linguistics*, 2024.

743 Alec Radford, Jong Wook Kim, Chris Hallacy, Aditya Ramesh, Gabriel Goh, Sandhini Agarwal,
744 Girish Sastry, Amanda Askell, Pamela Mishkin, Jack Clark, et al. Learning Transferable Visual
745 Models From Natural Language Supervision. In *International Conference on Machine Learning*,
746 2021.

747 Robert B Ricco. The Development of Reasoning. *Handbook of Child Psychology and Developmental*
748 *Science*, pp. 1–52, 2015.

749 Ronan Riochet, Mario Ynocente Castro, Mathieu Bernard, Adam Lerer, Rob Fergus, Véronique Izard,
750 and Emmanuel Dupoux. IntPhys 2019: A Benchmark for Visual Intuitive Physics Understanding.
751 *IEEE Transactions on Pattern Analysis and Machine Intelligence*, 44(9):5016–5025, 2021.

752 Ronan Riochet, Mario Ynocente Castro, Mathieu Bernard, Adam Lerer, Rob Fergus, Véronique Izard,
753 and Emmanuel Dupoux. IntPhys 2019: A Benchmark for Visual Intuitive Physics Understanding.
754 *IEEE Transactions on Pattern Analysis and Machine Intelligence*, 44(9):5016–5025, 2021.

755 Mohammad Reza Taesiri, Finlay Macklon, and Cor-Paul Bezemer. CLIP meets GamePhysics:
756 Towards bug identification in gameplay videos using zero-shot transfer learning. In *International*
757 *Conference on Mining Software Repositories*, 2022a.

756 Mohammad Reza Taesiri, Finlay Macklon, Yihe Wang, Hengshuo Shen, and Cor-Paul Bezemer.
757 Large Language Models are Pretty Good Zero-Shot Video Game Bug Detectors. *arXiv preprint*
758 *arXiv:2210.02506*, 2022b.

759 Mohammad Reza Taesiri, Tianjun Feng, Cor-Paul Bezemer, and Anh Nguyen. Glitchbench: Can
760 large multimodal models detect video game glitches? In *IEEE/CVF Conference on Computer*
761 *Vision and Pattern Recognition*, 2024.

762 Huajie Tan, Yuheng Ji, Xiaoshuai Hao, Minglan Lin, Pengwei Wang, Zhongyuan Wang, and Shang-
763 hang Zhang. Reason-RFT: Reinforcement Fine-Tuning for Visual Reasoning of Vision Language
764 Models. In *Advances in Neural Information Processing Systems*, 2025.

765 Hsiao-Yu Tung, Mingyu Ding, Zhenfang Chen, Daniel Bear, Chuang Gan, Josh Tenenbaum, Dan
766 Yamins, Judith Fan, and Kevin Smith. Physion++: Evaluating Physical Scene Understanding that
767 Requires Online Inference of Different Physical Properties. In *Advances in Neural Information*
768 *Processing Systems*, 2023.

769 Robert Vacareanu, Vlad-Andrei Negru, Vasile Suciu, and Mihai Surdeanu. From Words to Numbers:
770 Your Large Language Model Is Secretly A Capable Regressor When Given In-Context Examples.
771 In *Conference on Language Modeling*, 2024.

772 Peng Wang, Shuai Bai, Sinan Tan, Shijie Wang, Zhihao Fan, Jinze Bai, Keqin Chen, Xuejing Liu,
773 Jialin Wang, Wenbin Ge, Yang Fan, Kai Dang, Mengfei Du, Xuancheng Ren, Rui Men, Dayiheng
774 Liu, Chang Zhou, Jingren Zhou, and Junyang Lin. Qwen2-VL: Enhancing Vision-Language
775 Model's Perception of the World at Any Resolution. *arXiv preprint arXiv:2409.12191*, 2024a.

776 Qixun Wang, Yifei Wang, Yisen Wang, and Xianghua Ying. Can In-context Learning Really
777 Generalize to Out-of-distribution Tasks? *arXiv preprint arXiv:2410.09695*, 2024b.

778 Ruocheng Wang, Eric Zelikman, Gabriel Poesia, Yewen Pu, Nick Haber, and Noah Goodman.
779 Hypothesis Search: Inductive Reasoning with Language Models. In *International Conference on*
780 *Learning Representations*, 2024c.

781 Yi Ru Wang, Jiafei Duan, Dieter Fox, and Siddhartha S Srinivasa. NEWTON: Are Large Language
782 Models Capable of Physical Reasoning? In *Conference on Empirical Methods in Natural Language*
783 *Processing*, 2023.

784 Jason Wei, Xuezhi Wang, Dale Schuurmans, Maarten Bosma, Fei Xia, Ed Chi, Quoc V Le, Denny
785 Zhou, et al. Chain-of-Thought Prompting Elicits Reasoning in Large Language Models. In
786 *Advances in Neural Information Processing Systems*, 2022.

787 Luca Weihs, Amanda Yuile, Renée Baillargeon, Cynthia Fisher, Gary Marcus, Roozbeh Mottaghi,
788 and Aniruddha Kembhavi. Benchmarking Progress to Infant-Level Physical Reasoning in AI.
789 *Transactions in Machine Learning Research*, 2022.

790 Jin Xu, Zhifang Guo, Jinzheng He, Hangrui Hu, Ting He, Shuai Bai, Keqin Chen, Jialin Wang, Yang
791 Fan, Kai Dang, Bin Zhang, Xiong Wang, Yunfei Chu, and Junyang Lin. Qwen2.5-Omni Technical
792 Report. *arXiv preprint arXiv:2503.20215*, 2025.

793 Kai Yan, Zhan Ling, Kang Liu, Yifan Yang, Ting-Han Fan, Lingfeng Shen, Zhengyin Du, and Jiecao
794 Chen. MIR-Bench: Benchmarking LLM's Long-Context Intelligence via Many-Shot In-Context
795 Inductive Reasoning. *arXiv preprint arXiv:2502.09933*, 2025.

796 An Yang, Baosong Yang, Binyuan Hui, Bo Zheng, Bowen Yu, Chang Zhou, Chengpeng Li,
797 Chengyuan Li, Dayiheng Liu, Fei Huang, et al. Qwen2 Technical Report. *arXiv preprint*
798 *arXiv:2407.10671*, 2024a.

799 An Yang, Baosong Yang, Beichen Zhang, Binyuan Hui, Bo Zheng, Bowen Yu, Chengyuan Li,
800 Dayiheng Liu, Fei Huang, Haoran Wei, et al. Qwen2.5 Technical Report. *arXiv preprint*
801 *arXiv:2412.15115*, 2024b.

802 Kexin Yi, Chuang Gan, Yunzhu Li, Pushmeet Kohli, Jiajun Wu, Antonio Torralba, and Joshua B
803 Tenenbaum. CLEVRER: CoLlision Events for Video REpresentation and Reasoning. In *International*
804 *Conference on Learning Representations*, 2020.

810 Mo Yu, Lemao Liu, Junjie Wu, Tsz Ting Chung, Shunchi Zhang, Jiangnan Li, Dit-Yan Yeung, and Jie
811 Zhou. The Stochastic Parrot on LLM’s Shoulder: A Summative Assessment of Physical Concept
812 Understanding. In *Annual Conference of the North American Chapter of the Association for*
813 *Computational Linguistics*, 2025.

814 Simon Zhai, Hao Bai, Zipeng Lin, Jiayi Pan, Peter Tong, Yifei Zhou, Alane Suhr, Saining Xie, Yann
815 LeCun, Yi Ma, et al. Fine-Tuning Large Vision-Language Models as Decision-Making Agents via
816 Reinforcement Learning. In *Advances in Neural Information Processing Systems*, 2024.

817 Xiaohua Zhai, Basil Mustafa, Alexander Kolesnikov, and Lucas Beyer. Sigmoid Loss for Language
818 Image Pre-Training. In *IEEE/CVF International Conference on Computer Vision*, 2023.

819 Boqiang Zhang, Kehan Li, Zesen Cheng, Zhiqiang Hu, Yuqian Yuan, Guanzheng Chen, Sicong Leng,
820 Yuming Jiang, Hang Zhang, Xin Li, Peng Jin, Wenqi Zhang, Fan Wang, Lidong Bing, and Deli Zhao.
821 VideoLLaMA 3: Frontier Multimodal Foundation Models for Image and Video Understanding.
822 *arXiv preprint arXiv:2501.13106*, 2025. URL <https://arxiv.org/abs/2501.13106>.

823 Xingjian Zhang. How Vision Language Models Will Shape The Future Of Self-Driving Cars,
824 March 2025. URL <https://www.forbes.com/councils/forbestechcouncil/2025/03/18/how-vision-language-models-will-shape-the-future-of-self-driving-cars/>.

825 Yuanhan Zhang, Bo Li, Haotian Liu, Yong Jae Lee, Liangke Gui, Di Fu, Jiashi Feng, Ziwei Liu, and
826 Chunyuan Li. LLaVA-NeXT: A Strong Zero-shot Video Understanding Model, April 2024. URL
827 <https://llava-vl.github.io/blog/2024-04-30-llava-next-video/>.

828 Lianmin Zheng, Wei-Lin Chiang, Ying Sheng, Siyuan Zhuang, Zhanghao Wu, Yonghao Zhuang,
829 Zi Lin, Zhuohan Li, Dacheng Li, Eric. P Xing, Hao Zhang, Joseph E. Gonzalez, and Ion Stoica.
830 Judging LLM-as-a-judge with MT-Bench and Chatbot Arena. *arXiv preprint arXiv:2306.05685*,
831 2023.

832 Zhicheng Zheng, Xin Yan, Zhenfang Chen, Jingzhou Wang, Qin Zhi Eddie Lim, Joshua B Tenenbaum,
833 and Chuang Gan. ContPhy: Continuum Physical Concept Learning and Reasoning from Videos.
834 In *International Conference on Machine Learning*, 2024.

835 Xingcheng Zhou, Mingyu Liu, Ekim Yurtsever, Bare Luka Zagar, Walter Zimmer, Hu Cao, and
836 Alois C Knoll. Vision Language Models in Autonomous Driving: A Survey and Outlook. *IEEE*
837 *Transactions on Intelligent Vehicles*, 2024.

838 Jinguo Zhu, Weiyun Wang, Zhe Chen, Zhaoyang Liu, Shenglong Ye, Lixin Gu, Yuchen Duan, Hao
839 Tian, Weijie Su, Jie Shao, et al. InternVL3: Exploring Advanced Training and Test-Time Recipes
840 for Open-Source Multimodal Models. *arXiv preprint arXiv:2504.10479*, 2025.

841

842

843

844

845

846

847

848

849

850

851

852

853

854

855

856

857

858

859

860

861

862

863

864

865

866

867

868

869

870

Appendix

Table of Contents

871

A	Data-generation Details	17
A.1	Rendering the Videos	17
B	Details of Experimental Setup and Evaluation	19
B.1	Evaluated LMMs	19
B.2	Prompting Methods	19
B.3	Parsing the Chosen Option from Generated Output	21
B.4	Absolute Few-shot Accuracy of LMMs in Irregular Scenarios	21
B.5	Other Details	21
C	Other Related Works	22
D	Various Types of Reasoning	24
E	Additional Experimental Evaluation	25
E.1	Effect of weight quantization on inductive physical reasoning	25
E.2	Evaluation of Proprietary Models	25
E.3	Can Chain-of-Thought Prompting Improve Inductive Physical Reasoning?	26
E.4	Effect of Fine-tuning on Inductive Physical Reasoning	26
E.5	Do the Results from CoT Prompting and Fine-Tuning Experiments Invalidate Inductive Physical Reasoning?	27
E.6	Qualitative Inspection of Generated Outputs	27
E.7	Explaining the apparent inductive physical reasoning in AMC	37
E.8	Do the findings hold for more complex scenes?	41
E.9	Human Evaluation for INPHYRE	42
E.10	Does using all evaluation frames improve performance?	43
E.11	Effect of Structural Perturbations to Prompts	44
F	Why Do LMMs Perform Poorly in Irregular Scenarios	45
F.1	Analysis of Attention Maps in Gemma3-12B	45
F.2	Analysis of Hidden States in InternVL3-1B	46
G	Use of LLMs and Generative AI	49

903

904

905

906

907

A DATA-GENERATION DETAILS

908

A.1 RENDERING THE VIDEOS

910

911

912

913

914

915

916

917

We use Blender’s Python wrapper³ (v4.4.0) to render the video from the trajectories. We modified the image rendering code⁴ from (Johnson et al., 2017). We first designed a base scene with lamp and camera positions suitable for capturing entire object trajectories in INPHYRE. The object textures were taken from (Johnson et al., 2017), but more hues were added. Each video consists of 240 frames from which 8 frames are uniformly sampled to form the video tokens by the corresponding video processors of the LMMs.

³<https://pypi.org/project/bpy/>

⁴<https://github.com/facebookresearch/clevr-dataset-gen>

918 A sample video from each scenario is shown below: regular scenarios in Figs. 8 to 10, momentum
 919 conservation violation scenarios in Figs. 11 to 13, inconsistency physics scenarios in Figs. 16 and 17,
 920 and miscellaneous irregular scenarios in Figs. 14 and 15.

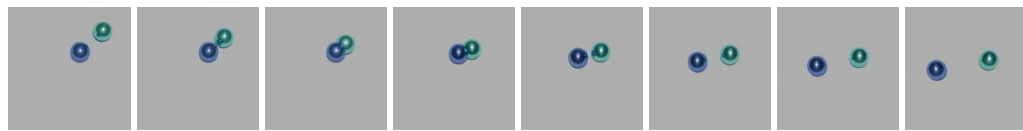


Figure 8: Regular scenario where linear momentum conservation is followed – LMC (Regular)

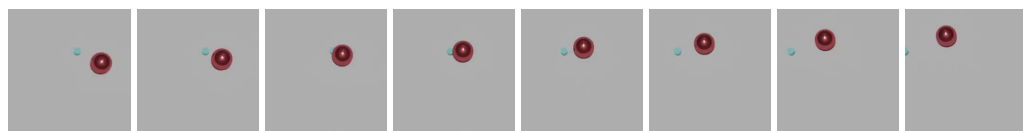


Figure 9: Regular scenario where the larger object has more mass – SB (Regular)

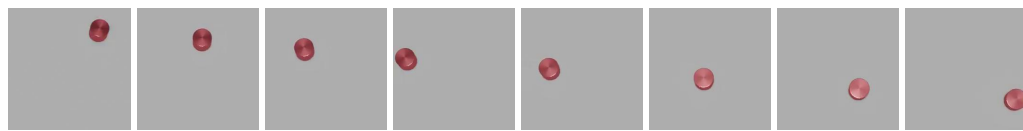


Figure 10: Regular scenario where linear momentum is conserved along the vertical direction – Wall (Regular)



Figure 11: Irregular scenario where linear momentum conservation is violated – LMC



Figure 12: Irregular scenario where angular momentum conservation is violated – AMC

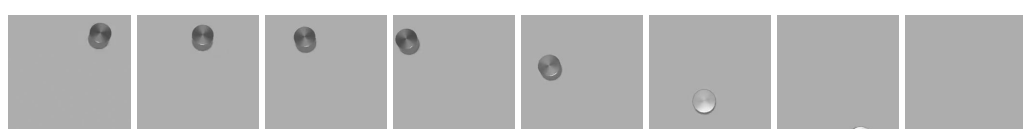


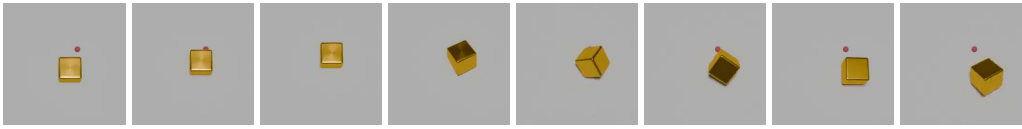
Figure 13: Irregular scenario where linear momentum conservation is violated along the vertical direction – **Wall**



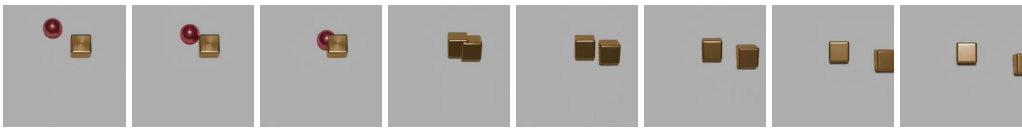
972
973
974
975
976
977 Figure 14: Irregular scenario where only red-colored objects violate linear momentum conservation –
978 Red-LMC



979
980
981
982
983
984 Figure 15: Irregular scenario where red-colored objects can pass through other objects – Red-Pass
985



986
987
988
989
990
991 Figure 16: Irregular scenario where a large object deflects after colliding with a tiny, much heavier,
992 object – SB



993
994
995
996
997
998 Figure 17: Irregular scenario where the colliding object assumes the hue and the shape of the other
999 object after collision – CC

1001 B DETAILS OF EXPERIMENTAL SETUP AND EVALUATION

1002 B.1 EVALUATED LMMs

1003 We evaluate a diverse collection of LMMs trained on both public and proprietary datasets with
1004 different architectural design choices. The model weights were taken from Huggingface⁵. The
1005 models are listed in Tab. 3.

1006 B.2 PROMPTING METHODS

1007 For prompting, we used the `apply_chat_template` method to convert conversations from a list of
1008 Python dictionaries to LMM-specific prompts. This helps in reusing the code. An example from
1009 LMC (regular) with one exemplar containing both video and question-answer pair in the conversation
1010 style of LLaVA-NeXT-Video is given below:

```

1015 [
1016   {
1017     "role": "system",
1018     "content": [{"type": "text",
1019       "text": "Understand the underlying physics from the following videos and
1020         choose only an option among A, B, C and D to answer the question. Do
1021         not provide reasoning."}]
1022   },
1023   {
1024     "role": "user",
1025     "content": [{"type": "video", "path": "path/to/exemplar_video.mp4"}, {
1026

```

⁵<https://huggingface.co/models>

Model	HF ID	#Params (B)	Vision encoder	Language model	MoE
InternVL3 (1B) (Zhu et al., 2025)	OpenGVLab/InternVL3-1B-hf	0.9	InternViT (Chen et al., 2024c)	Qwen2.5 (Yang et al., 2024b)	✗
InternVL3 (2B) (Zhu et al., 2025)	OpenGVLab/InternVL3-2B-hf	1.9	InternViT (Chen et al., 2024c)	Qwen2.5 (Yang et al., 2024b)	✗
VideoLaMA3 (2B) (Zhang et al., 2025)	DAMO-NLP-SG/VideoLaMA3-2B	2	SigLIP (Zhai et al., 2023)	Qwen2.5 (Yang et al., 2024b)	✗
Gemma 3 (4B) (Kamath et al., 2025)	google/gemma-3-4b-it	4	SigLIP (Zhai et al., 2023)	*	✗
LLaVA-NeXT-Video (Zhang et al., 2024)	llava-hf/LLaVA-NeXT-Video-7B-hf	7	CLIP-L (Radford et al., 2021)	Vicuna 1.5 (Zheng et al., 2023)	✗
LLaVA-OneVision (Li et al., 2024a)	llava-hf/llava-onevision-qwen-2b-si-hf	7	SigLIP (Zhai et al., 2023)	Qwen2 (Yang et al., 2024a)	✗
LLaVA-NeXT-Interleave (Li et al., 2024c)	llava-hf/llava-interleave-qwen-7b-hf	7	SigLIP (Zhai et al., 2023)	Qwen1.5 (Bai et al., 2023a)	✗
VideoLLaMA3 (7B) (Zhang et al., 2025)	DAMO-NLP-SG/VideoLaMA3-7B	7	SigLIP Zhai et al. (2023)	Qwen2.5 (Yang et al., 2024b)	✗
Qwen2-VL (Wang et al., 2024a)	Qwen/Qwen2-VL-7B-Instruct	7	Qwen-VL (Bai et al., 2023a)	Qwen2 (Yang et al., 2024a)	✗
Qwen2.5-Omni (Xu et al., 2025)	Qwen/Qwen2.5-0mni-7B	7	Qwen2.5-VL (Bai et al., 2025)	Qwen2.5 (Yang et al., 2024b)	✗
InternVL3 (8B) (Zhu et al., 2025)	OpenGVLab/InternVL3-8B-hf	8.1	InternViT (Chen et al., 2024c)	Qwen2.5 (Yang et al., 2024b)	✗
Gemma 3 (12B) (Kamath et al., 2025)	google/gemma-3-12b-it	12	SigLIP (Zhai et al., 2023)	*	✗
Aria (Li et al., 2024b)	rhymes-ai/Aria	24.9	SigLIP (Zhai et al., 2023)	*	✓

Table 3: We evaluate a diverse assortment of LMMs with varying architectural and data choices. * indicates that the language component was trained from scratch. “HF ID” is the identifier for the model weights on Huggingface.

```
{"type": "text", "text": "cyan cylinder and red cylinder have equal mass. How will the speed of cyan cylinder change after colliding with red cylinder? A: Speed does not change, B: cyan cylinder's speed decreases, C: cyan cylinder's speed will increase, D: Not enough data"}]  
  
assistant", [{"type": "text", "text": "B"}]  
  
user", [{"type": "video", "path": "path/to/evaluation_image.png"}, {"type": "text", "text": "yellow cube and purple sphere have equal mass. How will the speed of yellow cube change after colliding with purple sphere? A: Not enough data, B: Speed does not change, C: yellow cube's speed will decrease, D: yellow cube's speed will increase"}]
```

The exact style of the dictionary differs with the LMM. All prompts include a system prompt. When exemplars are provided, the system prompt is “Understand the underlying physics from the following videos and choose an option among A, B, C and D to answer the question. Do not provide reasoning.” When exemplars are absent, the system prompt is “Choose an option among A, B, C and D to answer the question based on your understanding of physical laws. Do not provide reasoning.”

However, these instructions are insufficient to restrict the model’s output to options. Since LLMs are first pre-trained for next-token prediction, they tend to complete the prompt instead of answering the question in it. Thus, the generated output tends to be descriptive, especially when there are no exemplars. For instance, suppose the model wants to choose option “D: Both objects move”. Instead of simply outputting “D”, the model may output “... Therefore, both objects may move.” Even instruction-tuned models sometimes fail to format their outputs, despite including the instruction “Do not provide reasoning” in the system prompt. Parsing the chosen option from such descriptive outputs is difficult.

Therefore, to avoid descriptive outputs, we provide demonstration samples in the expected output format since LLMs can understand output formatting from exemplars (Min et al., 2022). Even when exemplars do not contain question-answer pairs, we include randomly chosen options among {"A", "B", "C", "D"} to condition the model to output only the option index. An example of such a conversation for zero-shot evaluation is provided below:

```
[  
  {  
    "role": "system",  
    "content": [{"type": "text"}]
```

```

1080
1081         "text": "Choose an option among A, B, C and D to answer the question
1082             based on your understanding of physical laws. Do not provide
1083             reasoning."}]
1084     },
1085     {
1086         "role": "assistant",
1087         "content": [{"type": "text", "text": "A"}]
1088     },
1089     {
1090         "role": "assistant",
1091         "content": [{"type": "text", "text": "D"}]
1092     },
1093     {
1094         "role": "assistant",
1095         "content": [{"type": "text", "text": "C"}]
1096     },
1097     {
1098         "role": "user",
1099         "content": [{"type": "video", "path": "path/to/evaluation_image.png"},

1100             {"type": "text", "text": "yellow cube and purple sphere have equal mass.
1101                 How will the speed of yellow cube change after colliding with purple
1102                     sphere? A: Not enough data, B: Speed does not change, C: yellow
1103                         cube's speed will decrease, D: yellow cube's speed will increase"}]
1104     }
1105 ]

```

1102 Here, options in the assistant dictionaries do not have any relation to the video in the exemplar.
1103 Therefore, we still refer to this approach as “zero-shot evaluation” in the sense that no useful samples
1104 are provided as exemplars to the model.

1106 B.3 PARSING THE CHOSEN OPTION FROM GENERATED OUTPUT

1108 We ask the model to generate a maximum of 10 new tokens. The tokens generated by the model are
1109 decoded using its corresponding tokenizer. To obtain the chosen option from this decoded output, we
1110 “clean” the decoded string first until the first character is the option index. We remove the following
1111 substrings in our “cleaning” procedure:

- 1113 1. Placeholders for image and video tokens. E.g., <|im_start|>, <fim_suffix>.
- 1114 2. Partial placeholders for image and video tokens. E.g., only <|im_st from <|im_start|>.
- 1115 3. Strings such as “The correct answer is” prepending the chosen option. Such strings are first
1116 collected manually and then removed during the cleaning procedure.
- 1117 4. Strings that follow the chosen option. E.g., “Human: Which movie...”. Similar to the
1118 previous case, these strings can be collected for each model and then removed during the
1119 experimental evaluation.

1121 If multiple options are chosen, then the model’s output is marked to be incorrect. In some cases
1122 where not enough exemplars are available for the model, we allow the model to generate more tokens
1123 and attempt to find the chosen option based on textual overlap between the generated output and the
1124 given options.

1126 B.4 ABSOLUTE FEW-SHOT ACCURACY OF LMMs IN IRREGULAR SCENARIOS

1128 Tabs. 4 and 5 show the absolute accuracy values for the experiments in §§ 4.4 and 4.5.

1131 B.5 OTHER DETAILS

1133 **Compute:** Almost all experiments were run on individual A6000 GPUs on a server with 128 AMD
1134 EPYC 7502 (32-core) processors. Very few experiments were run on H200 and A100 GPUs.

1134	LMM	LMC	Wall	AMC	Red-LMC	Red-Pass	SB	CC
1135	InternVL3-1B (Zhu et al., 2025)	48.24 (-23.22)	18.49 (+9.20)	83.22 (+11.76)	58.45 (-13.01)	55.99 (-15.47)	10.45 (-76.97)	47.94 (-23.52)
1136	VideoLLaMA3-2B (Zhang et al., 2025)	37.14 (-25.83)	22.36 (-15.33)	59.35 (-3.62)	35.69 (-27.28)	49.47 (-13.49)	8.09 (-55.84)	46.03 (-16.93)
1137	InternVL3-2B (Zhu et al., 2025)	15.08 (-74.92)	0.25 (-91.36)	99.05 (+9.05)	25.06 (-64.94)	21.10 (-68.90)	0.10 (-76.81)	9.35 (-80.65)
1138	Gemma 3-4B (Kamath et al., 2025)	86.38 (+33.92)	56.13 (-21.56)	59.70 (+7.24)	80.65 (+28.19)	62.11 (+9.64)	24.62 (-44.88)	37.09 (-15.38)
1139	LLaVA-NeXT-Vid (Zhang et al., 2024)	16.68 (-39.50)	35.28 (+27.69)	45.58 (-10.60)	7.62 (-48.56)	11.78 (-44.40)	18.44 (-16.62)	31.61 (-24.57)
1140	InternVL3-8B (Zhu et al., 2025)	94.32 (-5.33)	98.54 (-0.20)	100.00 (+0.35)	71.78 (-27.87)	47.27 (-52.38)	45.98 (-53.87)	68.94 (-30.70)
1141	LLaVA-OneVision (Li et al., 2024a)	98.19 (-0.90)	97.19 (-2.56)	99.40 (+0.30)	74.94 (-24.16)	67.72 (-31.38)	31.41 (-67.88)	65.78 (-33.32)
1142	VideoLLaMA3-7B (Zhang et al., 2025)	83.62 (-14.42)	81.41 (+29.65)	97.74 (-0.30)	49.07 (-48.97)	54.04 (-44.01)	64.17 (-29.28)	76.28 (-21.76)
1143	LLaVA-NeXT-IL (Li et al., 2024c)	93.72 (-3.42)	94.17 (+15.33)	92.16 (-4.97)	62.51 (-34.63)	59.85 (-37.29)	43.72 (-21.48)	98.09 (+0.95)
1144	Qwen2-VL (Wang et al., 2024a)	96.03 (-2.11)	100.00 (+0.75)	95.33 (-2.81)	99.15 (+1.01)	96.69 (-1.45)	13.77 (-84.96)	90.35 (-7.79)
1145	Qwen2.5-Omni (Xu et al., 2025)	63.82 (+5.83)	39.30 (-4.97)	90.10 (+32.11)	53.63 (-4.36)	63.61 (+5.62)	56.23 (-38.29)	44.27 (-13.72)
1146	Gemma 3-12B (Kamath et al., 2025)	57.29 (-28.04)	92.36 (+23.52)	91.51 (+6.18)	27.67 (-57.66)	21.40 (-63.92)	18.09 (-68.62)	87.14 (+1.81)
1147	Aria (Li et al., 2024b)	27.24 (-25.88)	0.70 (-65.18)	80.35 (+27.24)	28.57 (-24.54)	19.95 (-33.17)	6.93 (-85.35)	7.49 (-45.63)

Table 4: 3-shot evaluation results of LMMs on irregular scenarios. The exemplars contain **both** videos and QA pairs.

1146	LMM	LMC	Wall	AMC	Red-LMC	Red-Pass	SB	CC
1147	InternVL3-1B (Zhu et al., 2025)	23.17 (-25.08)	7.74 (-10.75)	31.81 (-51.41)	26.12 (-32.33)	28.57 (-27.42)	16.98 (+6.53)	49.50 (+1.56)
1148	VideoLLaMA3-2B (Zhang et al., 2025)	13.17 (-23.97)	13.27 (-9.10)	33.22 (-26.13)	14.19 (-21.50)	18.20 (-31.28)	26.13 (+18.04)	13.17 (-32.86)
1149	InternVL3-2B (Zhu et al., 2025)	5.73 (-9.35)	0.00 (-0.25)	62.71 (-36.33)	8.32 (-16.74)	8.72 (-12.38)	7.94 (+7.84)	0.15 (-9.20)
1150	LLaVA-NeXT-Vid (Zhang et al., 2024)	15.68 (-1.01)	42.46 (+7.19)	43.22 (-2.36)	16.84 (+9.22)	16.14 (+4.36)	29.25 (+10.80)	41.46 (+9.85)
1151	InternVL3-8B (Zhu et al., 2025)	18.19 (-76.13)	57.44 (-41.11)	58.34 (-41.66)	16.69 (-55.09)	20.95 (-26.32)	14.12 (-31.86)	9.80 (-59.15)
1152	LLaVA-OneVision (Li et al., 2024a)	3.22 (-94.97)	25.63 (-71.56)	56.73 (-42.66)	2.81 (-72.13)	3.21 (-64.51)	13.77 (-17.64)	0.05 (-65.73)
1153	VideoLLaMA3-7B (Zhang et al., 2025)	4.12 (-79.50)	20.10 (-61.31)	45.08 (-52.66)	9.02 (-40.05)	10.43 (-43.61)	29.90 (-34.27)	9.05 (-67.24)
1154	LLaVA-NeXT-IL (Li et al., 2024c)	0.40 (-93.32)	16.53 (-77.64)	49.40 (-42.76)	0.40 (-62.11)	0.40 (-59.45)	20.00 (-23.72)	32.31 (-65.78)
1155	Qwen2-VL (Wang et al., 2024a)	3.82 (-92.21)	45.68 (-54.32)	66.83 (-28.49)	4.61 (-94.54)	3.21 (-93.48)	7.74 (-6.03)	45.53 (-44.82)
1156	Qwen2.5-Omni (Xu et al., 2025)	0.15 (-63.67)	22.01 (-17.29)	59.15 (-30.95)	1.80 (-51.83)	2.26 (-61.35)	18.39 (-37.84)	41.51 (-2.76)
1157	Gemma 3-12B (Kamath et al., 2025)	10.35 (-46.93)	0.45 (-91.91)	67.14 (-24.37)	5.16 (-22.51)	15.04 (-6.37)	5.03 (-13.07)	0.00 (-87.14)
1158	Aria (Li et al., 2024b)	0.90 (-26.33)	3.42 (+2.71)	29.35 (-51.01)	1.30 (-27.27)	1.30 (-18.65)	13.02 (+6.08)	0.20 (-7.29)

Table 5: 3-shot evaluation results of LMMs in irregular scenarios. The exemplars contain **only** videos.

Modifications to Huggingface: Some of the evaluated LMMs did not account for multiple videos in the prompt. Even the latest version of the Transformers library⁶ had this bug. So we made minor changes to the codebase of LLaVA-NeXT-Video, LLaVA-OneVision, and InternVL3 models. The modified “transformers” library is included in the codebase.

C OTHER RELATED WORKS

In this section, we include some recent works that evaluated various reasoning aspects of LLMs and LMMs. We will also clarify that our objective has never been explored in any of these works.

Intuitive Physics Understanding: Physically impossible scenarios have been employed to evaluate physical reasoning in learned models, following the “violation of expectation” principle from cognitive theory (Margoni et al., 2024). Here, the key hypothesis is that a model with excellent physical reasoning can also understand when the underlying physical laws in the given scenario violate the known physical laws. **However, violation of expectation in infants and children is often the initial step towards adaptation to a new physical environment** (Kotovsky & Baillargeon, 1998; Denison & Xu, 2010; Faßbender et al., 2025). For instance, (Faßbender et al., 2025) showed that infants and children adapted their force while opening and closing drawers, whose friction was temporally altered. **Violation of expectation in learned models in the context of physical laws** can be used as a proxy for physical reasoning. An early example of such work is the IntPhys (Riochet et al., 2021) benchmark that quantified the physical reasoning abilities of models trained on visual datasets that obeyed universal physical laws using their next-frame prediction errors on physically impossible scenarios. More works on intuitive physics understanding have emerged since (Epstein et al., 2020; Weihs et al., 2022; Jassim et al., 2024; Garrido et al., 2025).

Intuitive physics understanding is not inductive physical reasoning: Intuitive physics understanding differs from INPHYRE in the final objective, as the underlying assumption in intuitive physics understanding does not impact our setting. INPHYRE evaluates how well a large multimodal model can infer the underlying physical laws from the demonstration samples and apply them for physical reasoning when given a scenario the model has not seen during its training. This property, which we refer to as inductive physical reasoning in the main paper, is the key question we pose. The absolute physical reasoning ability (that we refer to as parametric knowledge) of this model on regular physical

⁶<https://github.com/huggingface/transformers>

1188 tasks that the model might have seen during training is not of interest to us. However, since we do
1189 not know which scenarios were observed during training and which were not, we rely on impossible
1190 scenarios to evaluate the inductive physical reasoning.
1191

1192 **Evaluation of physical reasoning in learned models:** Research interests in learning visual physical
1193 reasoning predate the era of large models. Early works generated synthetic vision datasets that
1194 depicted physical events such as collisions and falls, and trained models to predict future events (Lerer
1195 et al., 2016; Baradel et al., 2020; Bear et al., 2021), answer questions about cue events Mottaghi
1196 et al. (2016), or interact with the physical simulator to achieve an end goal (Bakhtin et al., 2019).
1197 Other tasks involved visually inferring latent physical properties, such as mass and friction, from the
1198 physical interactions (Chen et al., 2022; Tung et al., 2023) and causal physical reasoning (Yi et al.,
1199 2020; Ates et al., 2022).

1200 **Reasoning from demonstration samples:** Prior efforts have attempted to reason *how* LLMs utilize
1201 demonstration samples. These works consider both parametric knowledge (Min et al., 2022; Li et al.,
1202 2024d; Nafar et al., 2025) and inductive reasoning hypotheses (Garg et al., 2022; Bai et al., 2023b;
1203 Wang et al., 2024b; Vacareanu et al., 2024; Nafar et al., 2025). However, their findings are usually
1204 limited to synthetic regression tasks on LLMs (Garg et al., 2022; Bai et al., 2023b; Wang et al.,
1205 2024b), and they do not consider physical reasoning tasks on LMMs.
1206

1207 **Glitch detection using LMMs:** Another task similar to intuitive physics understanding is “glitch
1208 detection.” Here, the intuition is that a model that understands the underlying physics can also detect
1209 glitches in a given scenario. Some examples of glitch detection using LLMs are (Taesiri et al.,
1210 2022b;a; 2024; Cao et al., 2024).
1211

1212 **Use of synthetic data for physical reasoning:** Synthetically generated images and videos are
1213 commonly used for physical reasoning, as collecting visual data on real physical events is both
1214 taxing and time-consuming. Several of the works that we listed above and in § 2 also use synthetic
1215 data. In Tab. 6, we list some additional works that use synthetically generated collision events for
1216 physical reasoning. We also include CLEVR (Johnson et al., 2017) dataset in the table due to its
1217 visual resemblance with INPHYRE. Note: The tasks in ComPhy vary in terms of the underlying law
1218 required for reasoning (e.g., objects with the same charge repelling after a collision). All the events
1219 are still collision events.
1220

Benchmark	# of Tasks	Physics Engine	Renderer	Events other than collision events
CLEVR (Johnson et al., 2017)	-	No physics, only images	Blender	No events, only images
CLEVRER (Yi et al., 2020)	4 question types, 5 description types	Bullet	Blender	None
ComPhy (Chen et al., 2022)	4 (mass, charge, color, collision)	Bullet	Blender	None
CoPhy (Baradel et al., 2020)	3 (BlocktowerCF, BallsCF, CollisionCF)	PyBullet	PyBullet	Stability of stacked objects
INPHYRE (ours)	10 (spanning linear and angular momentum conservation, object permanence)	PyBullet	Blender	None

1221 Table 6: A tabular comparison of INPHYRE with other works that use synthetically generated
1222 collision events for physical reasoning.
1223

1224 **Different w.r.t. ContPhy and PhysBench:** ContPhy (Zheng et al., 2024) and PhysBench (Chow
1225 et al., 2025) are among the most comprehensive physical reasoning benchmarks that appeared recently.
1226 They include both real and synthetic videos that show physical events governed by a wide span
1227 of physical laws, such as Newton’s laws of motion, friction, fluid mechanics, etc. Therefore, they
1228 successfully evaluate the knowledge of LMMs on diverse topics required for physical reasoning. The
1229 key difference between INPHYRE and these works is the objective. INPHYRE evaluates the ability of
1230 the models to adapt to an unseen scenario, while these works evaluate the parametric knowledge about
1231 physics in these models. As a consequence, ContPhy and PhysBench arrive at conclusions different
1232 from ours. Zheng et al. (2024) find that these models “struggle to perform well on our benchmark,
1233 highlighting their limited physical commonsense for the continuum, especially soft bodies, and fluids.”
1234 Similarly, Chow et al. (2025) “identified significant gaps in physical world understanding, particularly
1235 in open-source models, due to inadequate training data” and postulated that these models “struggle
1236 with understanding the physical world – likely due to the absence of physical knowledge in their
1237 training data and the lack of embedded physical priors.” In contrast, we find that LMMs struggle to
1238

1242 adapt to an unseen scenario. It is also not clear if more training data can improve inductive physical
1243 reasoning from demonstration samples.
1244

1245
1246
1247 **D VARIOUS TYPES OF REASONING**
1248
1249
1250

1251 In this section, we will distinguish between general visual reasoning, inductive reasoning, and
1252 inductive physical reasoning (our work).

1253 **General visual reasoning** refers to the broad set of tasks that involve answering questions from
1254 visual signals (one or more images and/or videos). To address these tasks, the model must extract
1255 information from the visual signal and apply auxiliary information that the model already has about
1256 the content of the visual signal. This information is generally factual. For example, the input image
1257 may contain a knife and a fruit, and the auxiliary information corresponding to this content is that
1258 knives are sharp and can be used to cut fruits (Aroca-Ouellette et al., 2021; Bisk et al., 2020; Wang
1259 et al., 2023; Dong et al., 2024). The skills required for general visual reasoning include localization,
1260 understanding, and information retrieval.

1261 Visual reasoning is different from physical reasoning, although they share the input modalities and
1262 skill set partially. In physical reasoning, the task is to apply the physical knowledge possessed by the
1263 model. Unlike factual information, physical knowledge is a framework that is actionable only when
1264 applied to a specific context. For example, in the previous example of a knife next to a fruit, a relevant
1265 physical knowledge is that an object remains at rest unless acted upon by an external force (Newton’s
1266 first law of motion). To use this physical knowledge, the model must not only localize and understand
1267 the objects in the scene, but also realize that Newton’s first law of motion applies to the objects. In
1268 contrast, if one of the objects in the scene were a fluid, the model must realize that the laws of fluid
1269 dynamics also apply to that object. In summary, physical reasoning involves an additional application
1270 of mathematical frameworks over visual reasoning and is, therefore, more challenging.

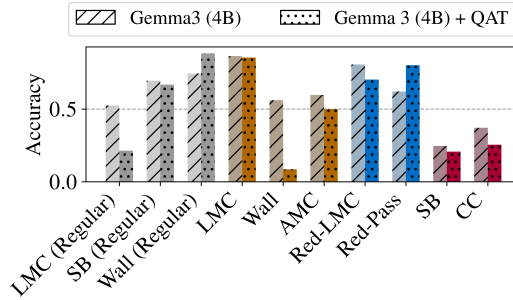
1271 **Inductive reasoning** is the ability of an agent to infer the underlying rules from a few samples and
1272 then apply these rules in a new evaluation scenario. Since the samples may not fully inform the agent
1273 about every underlying rule, inductive reasoning involves a degree of uncertainty. Existing works that
1274 evaluate inductive reasoning in LLMs follow this premise. As an example of inductive reasoning,
1275 consider the following sequence: A000, B001, C010, D011, E100. Which is the next element in
1276 this sequence? A possible (not necessarily unique) underlying rule of the sequence that we can infer
1277 from the premise is that the alphabets follow their canonical alphabetical order, while the remaining
1278 numbers encode the position of the alphabets in binary format. According to this rule, the next two
1279 elements in the sequence are F101 and G110.

1280 **Is evaluating inductive physical reasoning similar to evaluating inductive reasoning?** Unlike our
1281 work on inductive physical reasoning, evaluating inductive reasoning does not contradict any existing
1282 knowledge in the models. For instance, it is unlikely that an evaluated model has any knowledge
1283 regarding the above sequence example of inductive reasoning. It is also possible that the model has
1284 never seen any sequence like that during training. In contrast, we are evaluating the ability of the
1285 model to adapt any existing physical knowledge that it might have to the evaluation scenario. Thus,
1286 inductive physical reasoning is not only inferring the underlying physics from demonstration samples
1287 but also doing so when the inferred physics potentially contradicts the parametric knowledge of the
1288 model.

1289 **Evaluating inductive reasoning in LLMs:** There exists a long line of works that evaluate the
1290 abstract reasoning abilities of LLMs. Most of the other prior efforts to evaluate inductive reasoning
1291 are restricted to reasoning from textual inputs about abstract tasks (Mirchandani et al., 2023; Gendron
1292 et al., 2024; Wang et al., 2024c; Cheng et al., 2024; He et al., 2024; Bowen et al., 2024; Yan et al.,
1293 2025; Li et al., 2025). One notable work is Abstract and Reasoning Corpus (ARC) (Chollet, 2019),
1294 containing abstract tests similar to traditional IQ tests to evaluate “general artificial intelligence” in
1295 large models. It provides a training set that allows the candidate (human or machine learning agent)
1296 to understand the reasoning required to solve the tasks. Unlike our work, these tasks are largely
1297 symbolic and used to evaluate LLMs.

1296 E ADDITIONAL EXPERIMENTAL EVALUATION

1297 1298 E.1 EFFECT OF WEIGHT QUANTIZATION ON INDUCTIVE PHYSICAL REASONING



1312 Figure 18: Effect of weight quantization on inductive physical reasoning

1313
1314 LLMs and LMMs are billion-parameter models with expensive inference. Therefore, weight quantization
1315 is used to reduce their resource needs. An important concern with weight quantization is
1316 the drop in performance due to lower precision. In this subsection, we examine whether weight
1317 quantization adversely affects inductive physical reasoning in LMMs. We compare the prediction
1318 accuracy of Gemma 3 (4B) with its quantized version, obtained by fine-tuning using Quantization
1319 Aware Training (QAT) (Jacob et al., 2018). The models are evaluated in both regular and irregular
1320 scenarios with exemplars including both videos and question-answer pairs.

1321 Fig. 18 compares the accuracy of the quantized model against its non-quantized counterpart. Out
1322 of the ten evaluated scenarios, the quantized model performs worse than the full-precision model
1323 on all but two scenarios. In **LMC**, they perform comparably, while in **Wall** and **LMC** (regular), the
1324 quantized model shows a stark drop in accuracy. Notably, the quantized model outperforms the full
1325 precision model in **Wall** (regular) and **Red-Pass**. The results indicate that quantization indeed affects
1326 inductive physical reasoning, but its impact varies with the physical reasoning task.

1327 1328 E.2 EVALUATION OF PROPRIETARY MODELS

LMM	LMC	Wall	AMC	Red-LMC	Red-Pass	SB	CC
GPT 4.1 Mini	5.08 (-69.05)	31.61 (-61.26)	68.89 (-5.23)	6.97 (-67.15)	6.57 (-67.55)	90.25 (+31.40)	52.36 (-21.76)
GPT 4.1 Nano	37.54 (+1.16)	32.91 (-39.55)	53.77 (+17.39)	43.71 (+7.33)	30.28 (-6.11)	29.05 (-21.94)	18.34 (-18.04)
Gemini 2.5 Flash	16.93 (-20.55)	34.22 (-12.91)	59.75 (+22.26)	16.99 (-20.49)	16.19 (-21.30)	32.61 (-57.04)	68.24 (+30.75)
Gemini 2.5 Flash Lite	48.49 (-3.57)	54.82 (-28.39)	82.66 (+30.60)	30.13 (-21.93)	24.76 (-27.30)	50.75 (-34.69)	22.31 (-29.75)
Gemini 2 Flash	70.75 (-21.51)	98.19 (-0.50)	94.72 (+2.46)	15.59 (-76.67)	10.68 (-81.58)	87.14 (-9.36)	98.34 (+6.08)

1336 Table 7: Performance of some mainstream models in irregular scenarios. The numbers in parentheses
1337 show the difference between their performances in irregular scenarios and those in the corresponding
1338 regular scenarios.

1339
1340 In our main experiments in § 4, we evaluated open-source LMMs since they allowed more flexibility
1341 in prompting and output parsing. Proprietary LMMs generally only allow you to provide prompts
1342 and frames through their API and do not allow flexible output parsing. However, they are also
1343 more sophisticated and generally more accurate. In this section, we evaluate the inductive physical
1344 reasoning in these mainstream models. Specifically, we consider models from GPT (Achiam et al.,
1345 2023) and Gemini (Comanici et al., 2025) families. Due to the length limits of the prompts (since
1346 the API encodes images as string), we passed only 2 demonstration samples to the API. The results
1347 are shown in Tab. 7. The numbers show the accuracy in irregular scenarios, and the numbers in
1348 the parentheses show their difference with the accuracy in the corresponding regular scenario. We
1349 observe that mainstream models perform similarly to open-source models in inductive physical
1350 reasoning. The evaluated mainstream models fail in all scenarios except **AMC**.

E.3 CAN CHAIN-OF-THOUGHT PROMPTING IMPROVE INDUCTIVE PHYSICAL REASONING?

1352
1353
1354
1355
1356
1357

The experiments in § 4 show that LMMs struggle to infer the underlying physical laws from demonstration samples and apply them for physical reasoning. These experiments also revealed the underlying language bias of these models. In this section, we evaluate if chain-of-thought (CoT) prompting (Wei et al., 2022) can help with inductive physical reasoning. Intuitively, CoT can alleviate the burden of inferring the underlying physical laws from video frames and multiple-choice question-answer pairs by enunciating the physical laws required for reasoning in the prompt.

1358
1359
1360
1361
1362
1363
1364
1365

LMM	LMC (Reg.)	SB (Reg.)	Wall (Reg.)	LMC	Wall	AMC	Red-LMC	Red-Pass	SB	CC
InternVL3-1B	73.32 (+40.05)	97.82 (+50.28)	91.21 (+81.91)	90.20 (+41.96)	70.65 (+52.16)	97.69 (+14.47)	33.23 (+25.21)	69.42 (+13.43)	9.90 (-0.55)	36.48 (-11.46)
VideoLLaMA3-2B	98.89 (+35.93)	98.88 (+34.96)	97.84 (+60.15)	99.65 (+62.51)	69.55 (+47.19)	98.49 (+39.15)	3.16 (-32.53)	34.24 (-15.24)	27.34 (+19.25)	89.15 (+43.12)
InternVL3-2B	99.90 (+9.90)	99.80 (+22.88)	99.90 (+8.29)	99.95 (+84.87)	45.63 (+45.38)	95.38 (-3.67)	1.55 (-23.51)	12.08 (-9.02)	36.28 (+36.18)	83.17 (+73.82)
Gemma 3-4B	95.88 (+43.42)	98.53 (+29.02)	99.30 (+24.87)	99.30 (+12.91)	69.60 (+43.47)	96.98 (+37.29)	17.04 (-63.61)	62.76 (+0.65)	35.03 (+10.40)	72.21 (+35.13)
LLaVA-NeXT-Vid	68.29 (-12.11)	61.95 (+26.89)	82.86 (+75.28)	75.43 (+58.74)	89.60 (+54.32)	69.45 (+23.87)	10.98 (+3.36)	33.43 (+21.65)	29.30 (+10.85)	62.36 (+30.75)
InternVL3-8B	100.00 (+0.35)	100.00 (+0.15)	100.00 (+1.26)	100.00 (+5.68)	100.00 (+1.46)	100.00 (0.0)	2.66 (-69.12)	29.67 (-17.59)	49.05 (+3.07)	100.00 (+31.06)
LLaVA-OneVision	99.95 (+0.85)	99.85 (+0.56)	99.45 (-0.30)	98.89 (+0.70)	99.75 (+2.56)	98.29 (-1.11)	21.55 (-53.38)	48.52 (-19.20)	12.76 (-18.64)	99.45 (+33.67)
VideoLLaMA3-7B	99.80 (+1.76)	99.70 (+6.24)	94.72 (+42.96)	99.35 (+15.73)	99.45 (+18.04)	98.34 (+0.60)	2.46 (-46.62)	21.50 (-32.53)	52.41 (-11.76)	100.00 (+23.72)
LLaVA-NeXT-IL	100.00 (+2.86)	94.47 (+30.75)	95.68 (+16.83)	99.65 (+5.93)	96.48 (+2.31)	97.64 (+5.48)	8.77 (-53.73)	61.20 (+1.35)	52.86 (+9.15)	99.65 (+1.56)
Qwen2-VL	100.00 (+1.86)	100.00 (-1.27)	99.90 (+0.65)	100.00 (+3.97)	99.95 (-0.05)	96.18 (+0.85)	4.56 (-94.59)	30.88 (-65.81)	28.29 (+14.52)	99.95 (+9.60)
Qwen2.5-Omni	96.38 (-50.55)	99.49 (+12.84)	93.07 (+47.79)	99.05 (+55.23)	99.55 (+60.25)	99.50 (+9.40)	4.36 (-49.27)	31.38 (-32.23)	58.24 (+2.01)	93.67 (+49.40)
Gemma 3-12B	82.46 (-2.86)	95.84 (+19.33)	73.17 (+12.41)	87.59 (+30.30)	94.42 (+2.06)	97.59 (+6.08)	29.47 (+1.80)	68.32 (+46.92)	11.71 (-6.38)	98.99 (+11.86)

1366
1367
1368

Table 8: Performance of various LMMs in both regular and irregular scenarios when evaluated using chain-of-thought (CoT) prompting, where the underlying physical law is explicitly included along with the answers in demonstration samples.

1369
1370
1371
1372
1373
1374
1375
1376
1377
1378
1379

Tab. 8 shows the reasoning accuracies for various LMMs in both regular and irregular scenarios. The red and green numbers in the parentheses show the decrease and increase in the accuracy against the corresponding accuracy without CoT. We note a significant improvement in the performance across almost all model-scenario combinations, except Red-Pass and Red-LMC. CoT prompting fails to help multiple models in Red-Pass and Red-LMC scenarios, even worsening the performance of some models. In Red-Pass and Red-LMC, all except red colored objects follow the true physical laws. That is, unlike the remaining scenarios, Red-Pass and Red-LMC require the LMM to apply conditional reasoning depending on the color of the object. Although the demonstration samples include collisions with and without red colored objects, it appears that LMMs are unable to infer the conditional nature of the underlying reasoning.

1380
1381
1382

E.4 EFFECT OF FINE-TUNING ON INDUCTIVE PHYSICAL REASONING

1383
1384
1385
1386
1387
1388
1389
1390
1391
1392
1393

In this section, we explore the performance improvement on INPHYRE that we can obtain through fine-tuning. Fine-tuning through direct supervision and reinforcement learning has been shown to improve visual reasoning across diverse tasks (Zhai et al., 2024; Tan et al., 2025; Cai et al., 2025). Note that we cannot evaluate inductive physical reasoning by fine-tuning LMMs on INPHYRE samples, as it becomes unclear if the LMM’s output is due to the fine-tuning or due to the inductive physical reasoning. We conduct this experiment as a proxy way to obtain an “upper bound” on what an LMM can achieve on INPHYRE. Since fine-tuning is an expensive process, we limit our experiment to the smallest LMM in the evaluated cohort, InternVL3-1B. We use supervised fine-tuning without any low-rank adaptation techniques such as LoRA (Hu et al., 2022). Since no single hyperparameter combination worked consistently well for all scenarios, presumably due to the diversity between the tasks, we report the results for all hyperparameter combinations from a grid search.

1394
1395
1396
1397
1398
1399
1400
1401
1402
1403

Epochs	LR	LMC (Reg.)	SB (Reg.)	Wall (Reg.)	LMC	Wall	AMC	Red-LMC	Red-Pass	SB	CC
20	2×10^{-5}	12.01 (-21.26)	42.97 (-4.57)	18.29 (+8.99)	56.38 (+8.14)	23.72 (+5.23)	62.56 (-20.65)	68.57 (+10.13)	48.27 (-7.72)	25.38 (+14.92)	58.44 (+10.50)
50	2×10^{-5}	32.36 (-0.90)	35.16 (-12.38)	31.16 (+21.86)	54.27 (+6.03)	46.68 (+28.19)	66.48 (-16.73)	29.32 (-29.12)	35.79 (-20.20)	28.94 (+18.49)	70.40 (+22.46)
100	2×10^{-5}	38.09 (+4.82)	54.19 (+0.65)	42.21 (+32.91)	75.03 (+26.78)	93.47 (+74.97)	89.25 (+6.03)	42.76 (-15.69)	33.28 (-22.71)	56.48 (+46.03)	83.97 (+36.03)
120	2×10^{-5}	83.12 (+49.85)	92.85 (+43.31)	58.69 (+49.40)	56.83 (+8.59)	68.34 (+49.85)	75.63 (-7.59)	54.94 (-3.51)	50.08 (-5.91)	38.94 (+28.49)	90.10 (+42.16)
20	2×10^{-4}	37.64 (+4.37)	25.72 (-21.82)	24.37 (+15.08)	0.70 (-47.54)	0.00 (-18.49)	7.09 (-76.13)	23.91 (-34.54)	28.02 (-27.97)	0.00 (-10.45)	28.44 (-19.50)
50	2×10^{-4}	73.57 (+40.30)	95.08 (+47.54)	27.99 (+18.69)	43.22 (-5.03)	30.40 (+11.91)	81.86 (-1.36)	27.42 (-31.03)	28.92 (-27.07)	23.92 (+13.47)	70.60 (+22.66)
100	2×10^{-4}	94.07 (+60.80)	30.70 (-16.84)	39.30 (+30.00)	27.84 (-20.40)	31.11 (-12.61)	38.84 (-44.37)	31.68 (-26.77)	34.49 (-21.50)	35.58 (+25.13)	42.11 (-5.83)
120	2×10^{-4}	42.46 (+9.20)	71.08 (+23.54)	87.04 (+77.74)	30.80 (-17.44)	69.55 (+15.06)	59.90 (-33.22)	42.26 (-16.19)	24.91 (-31.08)	32.31 (+21.86)	35.43 (-12.51)
20	1×10^{-3}	0.00 (-33.27)	0.00 (-47.54)	14.42 (+5.13)	0.00 (-48.24)	0.00 (-18.49)	0.00 (-83.22)	0.00 (-58.45)	0.00 (-55.99)	0.00 (-10.45)	0.00 (-47.94)
50	1×10^{-3}	0.00 (-33.27)	1.78 (-45.76)	0.00 (-9.30)	0.00 (-48.24)	0.00 (-18.49)	0.00 (-83.22)	0.00 (-58.45)	25.56 (-30.43)	0.00 (-10.45)	0.00 (-47.94)
100	1×10^{-3}	18.39 (-14.87)	24.15 (-23.39)	19.70 (+10.40)	29.10 (-19.15)	11.51 (-6.98)	26.38 (-56.83)	6.37 (-52.08)	27.42 (-28.57)	15.78 (+5.33)	23.12 (-24.82)
120	1×10^{-3}	10.00 (-23.27)	8.73 (-38.81)	28.19 (+18.89)	29.95 (-18.29)	20.95 (+2.46)	23.27 (-59.95)	26.42 (-32.03)	0.05 (-55.94)	24.82 (+14.37)	21.36 (-26.58)
Best		94.07 (+60.80)	95.08 (+47.54)	87.04 (+77.74)	75.03 (+26.78)	93.47 (+74.97)	89.25 (+6.03)	68.57 (+10.13)	50.08 (-5.91)	56.48 (+46.03)	90.10 (+42.16)

Table 9: Results of fine-tuned InternVL3-1B on regular and irregular scenarios for different hyperparameter combinations. The best results for each scenario are given in the last row.

1404 Tab. 9 shows the accuracy of fine-tuned InternVL3-1B on both regular and irregular scenarios for
1405 different hyperparameter combinations. We observe that fine-tuning improves the performance in all
1406 scenarios with at least one hyperparameter combination, except for the **Red-Pass** scenario. These
1407 observations are similar to those from our experiments on CoT prompting. As we mentioned in the
1408 previous section, **Red-Pass** and **Red-LMC** require conditional reasoning, and it seems that fine-tuning
1409 cannot improve conditional physical reasoning in LMMs. The absolute accuracies are comparatively
1410 small for **Red-LMC** and **SB**.

1411

1412 E.5 DO THE RESULTS FROM CoT PROMPTING AND FINE-TUNING EXPERIMENTS INVALIDATE 1413 INDUCTIVE PHYSICAL REASONING?

1414

1415 In the previous sections, we evaluated the effects of CoT prompting and fine-tuning on the prediction
1416 accuracy for INPHYRE benchmark. Although both CoT prompting and fine-tuning improved the
1417 performance of multiple LMMs on most scenarios (except **Red-Pass** and **Red-LMC**), we emphasize
1418 that neither of these solutions is viable when the inductive physical reasoning ability is put to the test
1419 in practice. Specifically, both these techniques require prior access to the underlying physical laws or
1420 the inference samples themselves.

1421

1422 In CoT prompting, we included the underlying physical law in the impossible scenario as part of the
1423 prompt. This would not be possible in unseen scenarios where we do not possess any information
1424 about the physical laws involved. In contrast, throughout this paper, we had instead made a milder
1425 assumption that we only had access to prior visual samples and the right response in those samples.
1426 The more arduous and crucial task of inferring the underlying physical law was left to the model itself.
1427 Similarly, the models are trained on these samples in the fine-tuning experiments. Once these samples
1428 become part of the training data, it becomes nearly impossible to know if the model predictions
1429 are based on their inductive physical reasoning or because they remember their fine-tuning samples.
1430 Nonetheless, we included these experiments for the sake of completion, as they provide a surrogate
1431 for an upper bound on the performance achievable in INPHYRE.

1432

1433 E.6 QUALITATIVE INSPECTION OF GENERATED OUTPUTS

1434

1435 In § 4.2, we evaluated the parametric knowledge of LMMs in regular scenarios. We used the accuracy
1436 with which the model chose the correct option as our evaluation metric. Although this metric is
1437 useful for quantifying physical reasoning, it does not inform us how the model arrived at the option.
1438 This lack of clarity is outside the scope of a quantitative benchmark like INPHYRE. Nonetheless,
1439 we look at some of the open-ended generation output of these LMMs in regular scenarios to obtain
1440 insights into the underlying physical reasoning in these models. For this experiment, we provide the
1441 LMMs with only the input image and the question. Answer options are **not** included in the prompt
1442 so that the model will resort to open-ended generation to answer the question. We do not conduct
1443 this experiment on irregular scenarios as (1) video-only sub-setting did not show any competent
1444 performance, and (2) video-text sub-setting cannot be conducted without providing the options in
1445 exemplars, which would lead to the model predicting just the option alone.

1446

1447 The following subsubsections show the open-ended generation outputs for **LMC** (regular), **SB** (regular),
1448 and **Wall** (regular). Horizontal lines are used to demarcate the outputs of each LMM. In each
1449 output, incorrect physical reasoning is highlighted in **red**, correct physical reasoning relevant to the
1450 task is highlighted in **green**, and partially true physical reasoning in **yellow**. If any information from
1451 the prompt is ignored or if new assumptions are hallucinated, we highlight them in **blue**. After each
1452 generation output, we describe our observations. We do not list observations for the models that do
1453 not provide sufficient information about their reasoning. Note that the outputs of the same LMM
1454 could vary between individual samples. Therefore, the outputs of an LMM for this specific evaluation
1455 sample may not be similar to the model’s outputs on other evaluation samples from the same scenario.

1456

1457 E.6.1 OPEN-ENDED GENERATION OUTPUT FOR LMC (REGULAR)

1458



1460

1461

1462

1463 **System prompt:** Answer the question based on your understanding of physical laws.

1458 **Question:** yellow cube and purple sphere have equal mass. How will the speed of yellow cube
1459 change after colliding with purple sphere?

1460
1461 **InternVL3-1B** (Zhu et al., 2025): If the yellow cube and the purple sphere **have equal mass**, the
1462 **collision will result in both objects moving in opposite directions**. Since the collision is **elastic**, the
1463 **speed of the yellow cube will be halved**. This is because the **kinetic energy is conserved in an elastic**
1464 **collision**.

1465 **Observations:** InternVL3-1B hallucinated that the collision was elastic, instead of stating it as an
1466 assumption. Moreover, the speed will not be halved even if the collision is elastic.

1468 **VideoLLaMA3-2B** (Zhang et al., 2025): After the collision, the yellow cube will move at a slower
1469 speed than before.

1470
1471 **InternVL3-2B** (Zhu et al., 2025): When the yellow cube collides with the purple sphere, the speed
1472 of the yellow cube will decrease. This is because the collision will **transfer momentum** from the
1473 **yellow cube to the purple sphere**, causing the yellow cube to slow down. The exact change in speed
1474 depends on the masses and the nature of the collision (elastic or inelastic). **In an elastic collision**,
1475 **both momentum and kinetic energy are conserved**, while in an inelastic collision, kinetic energy is
1476 not conserved, and some energy is converted into other forms, such as heat or deformation.

1477 **Observations:** The reasoning is correct and derived from accurate physical laws.

1478
1479 **Gemma3-4B** (Kamath et al., 2025): Okay, let's analyze this collision based on physics principles.

1480 ****Here's the breakdown:****

1481
1482 1. ****Conservation of Momentum:**** In a closed system (like this one, assuming no external forces),
1483 **the total momentum *before* a collision equals the total momentum *after* the collision**. Momentum
1484 is calculated as mass (m) times velocity (v): $p = mv$.

1485
1486 2. ****Newton's Third Law (Action-Reaction):**** For every action, there is an equal and opposite
1487 reaction. This means that when the sphere hits the cube, the cube exerts an equal and opposite force
1488 back on the sphere.

1489
1490 3. ****Collision Dynamics:**** Because the cube and sphere have equal mass, and the collision is likely
1491 to be fairly brief, we can assume it's an ***elastic*** collision (or close to it – perfectly elastic collisions
1492 are rare in reality). **In an elastic collision, kinetic energy is also conserved**.

1493 ****Now, let's apply this:****

1494
1495 * ****Before the collision:**** Both the cube and sphere are at rest. Total momentum = 0. * ****During**
1496 **the collision:**** The sphere transfers its momentum to the cube. Since the masses are equal, the
1497 ***change* in momentum for each object will be the same, but the *velocity* will change differently.** *
1498 ****After the collision:**** The cube will move in one direction, and the sphere will move in the opposite
1499 direction. Because the masses are equal, the ***speeds*** of the cube and sphere will be equal, but in
1500 opposite directions.

1501
1502 ****Therefore, the speed of the yellow cube will change, and it will move with a speed equal in**
1503 **magnitude, but opposite in direction, to the speed the purple sphere had before the collision.****

1504
1505 ****Important Note:**** This assumes a ***perfect*** elastic collision. In a real-world scenario, some kinetic
1506 energy would be lost as heat or sound due to friction between the objects, so the speeds after the
1507 collision wouldn't be ***exactly*** equal. However, the principle of conservation of momentum and
1508 Newton's Third Law still apply.

1509
1510 Would you like me to explain any part of this in more detail or consider a slightly different collision
1511 scenario?

1512
1513 **Observations:** Gemma3-4B incorrectly assumed that objects would be at rest before the collision. It
1514 also contradicts itself later and states that the purple sphere was in motion before the collision.

1515
1516 **LLaVA-NeXT-Video** (Zhang et al., 2024): The speed of the yellow cube **will not change after**
1517 **colliding with the purple sphere because they have equal mass**. **The conservation of momentum is**

1512 a fundamental principle in physics that states that the total momentum of a closed system remains
1513 constant. When two objects collide, the total momentum of the system is the sum of the momenta of
1514 the individual objects. If the objects have equal mass, then the momentum of the system is the same
1515 before and after the collision.

1516
1517 **Observations:** The stated law of momentum conservation is accurate but is applied incorrectly.
1518 Additionally, momentum conservation is a universal law and does not depend on the masses of the
1519 individual objects.

1520 **InternVL3-8B** (Zhu et al., 2025): To determine how the speed of the yellow cube will change after
1521 colliding with the purple sphere, we need to consider the principles of conservation of momentum
1522 and kinetic energy, assuming an elastic collision.

1523 1. ****Conservation of Momentum**:** In an elastic collision, the total momentum before the collision
1524 is equal to the total momentum after the collision. If the masses of the yellow cube and the purple
1525 sphere are equal, and they are initially at rest, the momentum before the collision is zero. After
1526 the collision, the momentum of the cube and the sphere will be equal in magnitude but opposite in
1527 direction.

1528 2. ****Conservation of Kinetic Energy**:** In an elastic collision, the total kinetic energy before the
1529 collision is equal to the total kinetic energy after the collision. Since the masses are equal and initially
1530 at rest, the kinetic energy before the collision is zero. After the collision, the kinetic energy will be
1531 distributed between the cube and the sphere.

1532 Given these principles, let's analyze the situation:

1533 - ****Initial State**:** Both the yellow cube and the purple sphere are at rest. Therefore, the initial
1534 momentum and kinetic energy are zero.

1535 - ****Collision**:** When the yellow cube collides with the purple sphere, they will exchange velocities
1536 due to the conservation of momentum and kinetic energy. Since the masses are equal, the velocities
1537 will be equal in magnitude but opposite in direction.

1538 - ****Final State**:** After the collision, the yellow cube will move in the opposite direction of the
1539 purple sphere with the same speed it had before the collision, and the purple sphere will move in the
1540 opposite direction of the yellow cube with the same speed it had before the collision.

1541 Therefore, if the yellow cube and the purple sphere have equal mass and the collision is perfectly
1542 elastic, the speed of the yellow cube will remain the same after the collision, but its direction will be
1543 reversed.

1544 **Observations:** InternVL3-8B states the physical laws correctly. However, it incorrectly believes
1545 that the objects are at rest before collision. This hallucinated assumption led it to provide the wrong
1546 reasoning.

1547 **LLaVA-Onevision** (Li et al., 2024a): The speed of the yellow cube will decrease after colliding with
1548 the purple sphere. This is because the cube will transfer some of its kinetic energy to the sphere,
1549 causing it to slow down. The exact change in speed will depend on the masses and velocities of the
1550 cube and sphere before the collision, as well as the angle of the collision.

1551 **Observations:** The stated law of kinetic energy transfer is accurate. The model seems to have ignored
1552 the information about the mass of the objects stated in the prompt.

1553 **VideoLLaMA3-7B** (Zhang et al., 2025): decrease

1554 **LLaVA-NeXT-Interleave** (Li et al., 2024c): The speed of the yellow cube will change after colliding
1555 with the purple sphere. The exact change depends on the nature of the collision, which is not specified
1556 in the image. If the collision is elastic and the yellow cube and purple sphere have equal mass, the
1557 speed of the yellow cube will change to a value that depends on the angle of impact and the initial
1558 speeds of the two objects.

1559
1560
1561
1562
1563
1564
1565

1566 **Observations:** The reasoning is accurate, although the reasoning principle is not explicitly stated. It
1567 additionally states that the exact change in velocity will depend on factors that are unavailable from
1568 the prompt.

1569
1570 **Qwen2-VL** (Wang et al., 2024a): The speed of the yellow cube will decrease after colliding with the
1571 purple sphere.

1572 **Qwen2.5-Omni** (Xu et al., 2025): The speed of the yellow cube will decrease after colliding with the
1573 purple sphere. This is because, according to the law of conservation of momentum, the total
1574 momentum of a closed system remains constant. When the yellow cube collides with the purple
1575 sphere, they exert equal and opposite forces on each other. Since they have equal mass, the yellow
1576 cube will experience a force that will slow it down, while the purple sphere will experience a force
1577 that will accelerate it.

1578 **Observations:** Qwen2.5-Omni reasoned that the yellow cube will slow down due to the objects
1579 having equal mass. In reality, the mass of the objects do not decide whether the colliding object slows
1580 down or not, but only how much it slows down.

1581 **Gemma3-12B** (Kamath et al., 2025): Here's an analysis of what would happen, based on the laws of
1582 physics, assuming an elastic collision:

1583 ****Understanding the Principles****

1584 * ****Conservation of Momentum:**** In a closed system (meaning no external forces like friction), the
1585 total momentum before a collision is equal to the total momentum after the collision. Momentum is
1586 mass x velocity. * ****Elastic Collision:**** This is a collision where kinetic energy is conserved. In
1587 reality, collisions are rarely perfectly elastic (some energy is typically lost as heat or sound), but we'll
1588 assume it for simplicity.

1589 ****Analysis of the Scenario****

1590 1. ****Initial State:**** The cube is moving, and the sphere is stationary. Let's say the cube's velocity is
1591 $*v*$. The sphere's velocity is 0. 2. ****Collision:**** During the collision, the cube transfers some of its
1592 momentum to the sphere. 3. ****Final State (Ideal Elastic Collision):**** Since the masses are equal, the
1593 collision will result in the cube stopping and the sphere moving off with a velocity equal to the initial
1594 velocity of the cube ($*v*$).

1595 ****Therefore, the speed of the yellow cube will change and it will come to a complete stop.****

1596 ****Important Considerations:****

1597 * ****Perfect Elasticity:**** The assumption of a perfectly elastic collision is rarely true. In a real-world
1598 scenario, the cube would likely not stop completely. Some of the cube's kinetic energy would be
1599 converted to other forms (sound, heat due to deformation). * ****Direction:**** This analysis only
1600 considers speed (magnitude of velocity). The direction of motion after the collision would also
1601 change.

1602 **Observations:** Gemma3-12B states the physical principles accurately and provides the correct
1603 reasoning using these principles.

1604 **Aria** (Li et al., 2024b): In a collision between two objects of equal mass, assuming an elastic collision,
1605 the speed of each object will change such that the yellow cube will come to a stop, and the purple
1606 sphere will move forward at the initial speed of the yellow cube. This is due to the principle of
1607 conservation of momentum and kinetic energy. The yellow cube transfers all its momentum and
1608 kinetic energy to the purple sphere.

1609 **Observations:** The laws stated by Aria are correct, and the laws are applied accurately during
1610 physical reasoning.

1611
1612
1613
1614
1615
1616
1617
1618
1619

1620 E.6.2 OPEN-ENDED GENERATION OUTPUT FOR SB (REGULAR)
1621



1625 **System prompt:** Answer the question based on your understanding of physical laws.
1626

1627 **Question:** green cylinder has more mass than blue cube. What occurs when green cylinder and blue
1628 cube collide?

1629 **InternVL3-1B** (Zhu et al., 2025): When the green cylinder and the blue cube collide, the following
1630 physical law applies:

1631 The collision between the two objects will result in a change in their velocities. Specifically, the blue
1632 cube will move forward with a higher velocity than the green cylinder, and the green cylinder will
1633 move backward with a lower velocity. This is because the blue cube has more mass and thus a greater
1634 inertia, causing it to move faster than the green cylinder.
1635

1636 The direction of the velocities can be determined using the principle of conservation of momentum.
1637 The change in momentum of the blue cube will be equal to the change in momentum of the green
1638 cylinder. Mathematically, this can be expressed as:
1639

$$\Delta p_{\text{blue}} = \Delta p_{\text{green}}$$

1640 Where: - Δp_{blue} is the change in momentum of the blue cube. - Δp_{green} is the change in momentum
1641 of the green cylinder.
1642

1643 Since the blue cube has more mass, it will have a greater change in momentum, leading to a higher
1644 velocity for the blue cube. Conversely, the green cylinder will have a lower change in momentum and
1645 thus a lower velocity.
1646

1647 Thus, the blue cube will move forward with a higher velocity than the green cylinder.
1648

1649 **Observations:** InternVL3-1B confused the unequal mass relation between the objects from the
1650 prompt. The prompt said that the green cylinder has more mass than the blue cube, but the model
1651 inferred that the blue cube had more mass than the green cylinder. It additionally reasoned that
1652 an object with more mass will undergo a greater change in momentum. However, these mistakes
1653 canceled each other and accidentally led the model to the right answer.
1654

1655 **VideoLLaMA3-2B** (Zhang et al., 2025): green cylinder and blue cube collide
1656

1657 **InternVL3-2B** (Zhu et al., 2025): When the green cylinder and the blue cube collide, the green
1658 cylinder will likely deform or compress due to the force exerted by the blue cube. The blue cube
1659 will exert a force on the green cylinder, causing it to move or change shape. The exact outcome will
1660 depend on the masses, velocities, and other physical properties of the objects involved.
1661

1662 **Observations:** InternVL3-2B assumed about the material properties of the objects and reasoned that
1663 the green cylinder could potentially deform. It also incorrectly reasoned that the outcome would
1664 depend on the mass and the velocities. Since information was provided about the mass, the correct
1665 answer is that both objects would move in the same direction.
1666

1667 **Gemma3-4B** (Kamath et al., 2025): Here's what will likely happen when the green cylinder and blue
1668 cube collide, based on our understanding of physics:
1669

1670 ****1. Impulse and Momentum Conservation:****
1671

1672 * ****Impulse:**** When the objects collide, they exert forces on each other for a brief period. This
1673 exchange of forces is called impulse. * ****Momentum:**** The total momentum of the system (cylinder
1674 + cube) before the collision must equal the total momentum after the collision. Momentum is mass
1675 times velocity ($p = mv$).
1676

1677 ****2. The Outcome – The Cylinder Will Move Less****
1678

1674 * Since the green cylinder has more mass than the blue cube, it will have more momentum before the
1675 collision. * During the collision, the cylinder will decelerate (slow down) more quickly than the cube.
1676 * Because of its greater initial momentum, it will transfer more momentum to the cube. * As a result,
1677 the blue cube will experience a larger change in velocity, resulting in a greater deflection from its
1678 initial direction, while the green cylinder will experience a smaller change in velocity and will move
1679 less significantly.
1680

1681 **In simpler terms:** The heavier object (cylinder) will have a harder time changing its motion
1682 during the collision compared to the lighter object (cube).

1683 **Important Note:** This assumes an *elastic* collision (no energy loss due to heat, sound, or
1684 deformation). If the collision was inelastic (e.g., the objects deform significantly and some energy is
1685 lost), the outcome would be slightly different.

1686 If you would like, you can provide another scenario and I can analyze it using the same principles.
1687

1688 **Observations:** Gemma3-4B stated several physical laws accurately but applied them incorrectly. It
1689 also incorrectly stated that an object with a larger initial momentum will transfer more momentum.

1690 **LLaVA-NeXT-Video** (Zhang et al., 2024): When a green cylinder and a blue cube collide, the
1691 collision will result in a change in their motion and possibly a change in their position relative to each
1692 other. The exact outcome depends on the relative speed and direction of the cylinder and the cube at
1693 the time of collision. If the cylinder is moving faster or in the same direction as the cube, the cylinder
1694 will push the cube to one side, and if the cylinder is moving in the opposite direction, the cube will
1695 push the cylinder to the other side. If the cylinder is moving at a right angle to the cube, the cylinder
1696 will change direction and the cube will change direction. The collision will also result in a transfer of
1697 momentum from the cylinder to the cube or vice versa, depending on the direction of the collision.
1698

1699 If the cylinder is moving faster than the cube, the cylinder will push the cube to one side, and the
1700 cube will move in the opposite direction. If the cylinder is moving slower, the cube will push the
1701 cylinder to the other side. If the cylinder is moving at a right angle to the cube, the cylinder will
1702 change direction and the cube will change direction.

1703 **Observations:** Although the stated reasoning is true, the model does not use the information about
1704 the mass of the objects provided in the prompt. The reasoning is incomplete due to the model ignoring
1705 useful information from the prompt.

1706 **InternVL3-8B** (Zhu et al., 2025): When the green cylinder and the blue cube collide, several factors
1707 determine the outcome, primarily based on the principles of physics, specifically Newton's laws of
1708 motion and the concept of momentum.

1709 1. **Mass and Momentum**: The green cylinder has more mass than the blue cube. Momentum is
1710 the product of mass and velocity ($p = mv$). If both objects are moving with the same velocity before
1711 the collision, the green cylinder will have more momentum due to its greater mass.

1712 2. **Elastic vs. Inelastic Collision**: The nature of the collision (whether it is elastic or inelastic)
1713 also plays a role. In an elastic collision, both momentum and kinetic energy are conserved. In an
1714 inelastic collision, momentum is conserved, but kinetic energy is not. The objects may stick together
1715 or deform upon impact.

1716 3. **Resultant Motion**: - **Elastic Collision**: If the collision is perfectly elastic, the green
1717 cylinder will exert a greater force on the blue cube, potentially causing the blue cube to rebound
1718 with some velocity. The green cylinder might slow down slightly due to the transfer of momentum. -
1719 **Inelastic Collision**: If the collision is inelastic, the objects may stick together after the collision.
1720 The combined mass of the green cylinder and the blue cube will move with a velocity determined by
1721 the conservation of momentum.

1722 4. **Energy Considerations**: In an elastic collision, the kinetic energy before and after the collision
1723 remains the same. In an inelastic collision, some kinetic energy is converted into other forms of
1724 energy, such as heat or deformation energy.

1725
1726
1727

1728 In summary, when the green cylinder and the blue cube collide, the green cylinder, having more mass,
1729 will exert a greater force on the blue cube. Depending on whether the collision is elastic or inelastic,
1730 the blue cube **may rebound or stick to the green cylinder**, and the green cylinder may slow down. The
1731 exact outcome depends on the initial velocities and the nature of the collision.

1732 **Observations:** InternVL3-8B states the principles in physics correctly and applies them accurately.

1734 **LLaVA-Onevision** (Li et al., 2024a): The green cylinder will likely push the blue cube away from it
1735 due to its greater mass and momentum. The blue cube will also experience a force in the opposite
1736 direction of the green cylinder's motion. The exact outcome of the collision will depend on the speed
1737 and angle of the green cylinder's impact with the blue cube.

1738 **Observations:** LLaVA-Onevision states and applies the physical laws correctly.

1739 **VideoLLaMA3-7B** (Zhang et al., 2025): green cylinder will not move

1740 **LLaVA-NeXT-Interleave** (Li et al., 2024c): When the green cylinder and blue cube collide, **the blue**
1741 **cube will likely move and change its position** as a result of the interaction. The green cylinder **may**
1742 **also change its position or velocity** depending on the nature of the collision.

1743 **Observations:** LLaVA-NeXT-Interleave reasons that the green cylinder *may* change its position or
1744 velocity, while, in reality, it would always change its position due to its larger mass, irrespective of
1745 the nature of the collision.

1746 **Qwen2-VL** (Wang et al., 2024a): The green cylinder will push the blue cube.

1747 **Qwen2.5-Omni** (Xu et al., 2025): When the green cylinder collides with the blue cube, the cylinder
1748 will exert a force on the cube, **causing the cube to accelerate and move in the direction of the force**.
1749 The cylinder will also experience a reaction force, which will cause it to slow down slightly. The
1750 exact outcome of the collision depends on the masses and velocities of the objects, as well as the
1751 nature of the collision (e.g., elastic or inelastic).

1752 **Observation:** Qwen2.5-Omni correctly states and applies the relevant physical laws.

1753 **Gemma3-12B** (Kamath et al., 2025): Here's what would likely happen based on physical laws,
1754 considering the image and the premise that the green cylinder has more mass than the blue cube:

1755 ****The Collision****

1756 When the green cylinder and the blue cube collide, the following will generally occur:

1757 1. ****Momentum Transfer:**** Momentum is a measure of mass in motion (mass x velocity). Since the
1758 green cylinder has more mass, it will have more momentum. During the collision, **some of the green**
1759 **cylinder's momentum will be transferred to the blue cube.**

1760 2. ****Green Cylinder's Slowdown:**** **The green cylinder, having lost some momentum, will slow**
1761 **down after the collision.**

1762 3. ****Blue Cube's Speedup:**** **The blue cube, gaining momentum, will speed up after the collision. It**
1763 **will move in roughly the direction the green cylinder was traveling.**

1764 4. ****Elasticity Matters:**** The specifics will depend on how **elastic** the collision is: * ****Perfectly**
1765 **Elastic Collision:**** (Rare in the real world). Kinetic energy is conserved. The cylinder would slow
1766 down significantly, the cube would speed up significantly, and the total kinetic energy would remain
1767 the same. * ****Inelastic Collision:**** (More common). Some kinetic energy is lost as heat or sound
1768 during the impact. The cylinder will slow down more, and the cube will speed up less than in a
1769 perfectly elastic collision.

1770 ****In summary:**** The green cylinder will slow down, and the blue cube will speed up. The greater
1771 the mass difference, the more pronounced these effects will be.

1772 ****Important Note:**** This explanation assumes a simplified scenario. Factors like friction, the exact
1773 shapes of the objects, and how they bounce off each other would influence the outcome in a real-world
1774 situation.

1782 **Observations:** The reasoning is accurate, although the laws were not explicitly stated.
1783

1784 **Aria** (Li et al., 2024b): When the green cylinder and blue cube collide, the green cylinder, having
1785 more mass, will likely exert a greater force on the blue cube due to its greater momentum. This could
1786 cause the blue cube to move or change direction, depending on the angle and speed of the collision.
1787 The outcome will also depend on factors such as the material properties and the speed of the objects.
1788 If the collision is elastic, both objects might bounce off each other; if inelastic, some energy may be
1789 lost as heat or sound.

1790 **Observations:** Aria restates the information about the mass of the objects from the prompt, but
1791 reasons that the objects may bounce off each other, which cannot happen when one object has a
1792 higher mass than the other.

1794 E.6.3 OPEN-ENDED GENERATION OUTPUT FOR WALL (REGULAR) 1795

1796 **Frames:**



1799 **System prompt:** Answer the question based on your understanding of physical laws.
1800

1801 **Question:** black cylinder collides elastically with the wall. What is the outcome of black cylinder
1802 colliding with wall?

1803 **InternVL3-1B** (Zhu et al., 2025): When a black cylinder collides elastically with the wall, the
1804 outcome depends on the specific nature of the collision. Here are a few possible scenarios:
1805

- 1806 1. ****Inelastic Collision:**** - If the collision is inelastic, meaning the two objects stick together after
1807 the collision, the black cylinder will move with some velocity after the collision. The wall will exert
1808 a force on the moving cylinder, causing it to deform or change direction.
- 1809 2. ****Elastic Collision:**** - If the collision is elastic, meaning the two objects bounce off each other,
1810 the black cylinder will move with some velocity after the collision. The wall will exert a force on the
1811 moving cylinder, causing it to change direction and possibly deform.
- 1812 3. ****Perfectly Inelastic Collision:**** - If the collision is perfectly inelastic, meaning the two objects
1813 stick together, the black cylinder will move with some velocity after the collision. The wall will exert
1814 a force on the moving cylinder, causing it to change direction and possibly deform.

1816 Without additional information about the specific nature of the collision, it is not possible to determine
1817 the exact outcome. However, in general, the outcome will depend on whether the collision is inelastic
1818 or elastic.

1819 **Observations:** InternVL3-1B ignores the information in the prompt that the collision was elastic. It
1820 also generates a contradictory statement that the objects will move with some velocity after sticking
1821 to each other if the collision is inelastic.

1822 **VideoLLaMA3-2B** (Zhang et al., 2025): black cylinder bounces
1823

1824 **InternVL3-2B** (Zhu et al., 2025): When a black cylinder collides elastically with a wall, the outcome
1825 is that the cylinder will bounce back with the same speed and direction it initially had. This is because
1826 the collision is perfectly elastic, meaning there is no loss of kinetic energy. The wall exerts an equal
1827 and opposite force on the cylinder, causing it to reverse its motion.

1828 **Observation:** InternVL3-2B states and applies physical laws accurately.
1829

1830 **Gemma3-4B** (Kamath et al., 2025): Here's an analysis of what happens when a black cylinder
1831 collides elastically with a wall, based on the principles of physics:
1832

1833 ****Understanding Elastic Collisions****

1834 * ****Elastic Collision:**** In an elastic collision, both momentum and kinetic energy are conserved.
1835 This means the total momentum of the system before the collision equals the total momentum after
the collision, and the total kinetic energy before equals the total kinetic energy after. * ****Conservation**

1836 of Momentum:** The law of conservation of momentum states that the total momentum of a closed
1837 system remains constant. * **Conservation of Kinetic Energy:** The law of conservation of kinetic
1838 energy states that the total kinetic energy of a system remains constant.

1839 **What Happens in the Collision**

1841 1. **Momentum Transfer:** As the cylinder hits the wall, momentum is transferred from the cylinder
1842 to the wall. The cylinder initially has a certain velocity (let's call it v), and the wall is initially at
1843 rest. After the collision, the cylinder will likely have a velocity in the opposite direction (let's call it
1844 $-v$), and the wall will have a velocity (v). 2. **Angle of Reflection:** The cylinder won't bounce
1845 straight back. It will bounce at an angle. The angle of reflection depends on the relative velocities of
1846 the cylinder and the wall *before* the impact. A more detailed calculation would require knowing
1847 the initial velocity and angle, and the coefficient of restitution (which describes the "bounciness" of
1848 the collision). 3. **Kinetic Energy is Preserved:** Since it is an elastic collision, the kinetic energy
1849 of the system will remain the same, meaning no energy will be lost as heat or sound.

1850 **Outcome**

1851 The black cylinder will bounce off the wall at an angle, and the wall will move in the opposite
1852 direction with the same speed as the cylinder.

1853 **Important Note:** Without knowing the initial velocity and angle of the cylinder, it's impossible to
1854 predict the exact angle of reflection.

1855 Let me know if you'd like a more detailed explanation or want to explore scenarios with specific
1856 initial conditions!

1857 **Observations:** Although Gemma3-4B states and uses the appropriate physical laws, it treats the wall
1858 as an object that can move, leading to a wrong prediction.

1859 **LLaVA-NeXT-Video** (Zhang et al., 2024): The image you've provided is a simple illustration of
1860 a black cylinder colliding with a wall, but it doesn't provide enough information to determine the
1861 outcome of the collision. The outcome would depend on the properties of the cylinder and the wall,
1862 such as their mass, size, material, and the speed at which they collide.

1863 If the cylinder is a solid object and the collision is elastic, it would bounce off the wall without any
1864 permanent deformation or damage to either object. The cylinder would lose some of its kinetic energy
1865 during the collision, and the wall would also experience a deformation, but it would return to its
1866 original state after the collision.

1867 If the cylinder is a liquid or a gas, the collision would be more complex, and the outcome would
1868 depend on the properties of the liquid or gas, such as its viscosity and the pressure. The cylinder
1869 would likely spread out upon impact, and the wall would experience a deformation, but the cylinder
1870 would not bounce back.

1871 If the cylinder is a solid and the collision is inelastic, the cylinder would break or deform upon impact,
1872 and the wall would also experience a deformation.

1873 Without more information, it's impossible to provide a specific outcome.

1874 **Observations:** As one of the possibilities, LLaVA-NeXT-Video assumes the collision is elastic and
1875 correctly predicts that the colliding object would bounce off the wall. However, it then adds wrong
1876 physical reasoning that the object would lose its kinetic energy and the wall would be deformed,
1877 neither of which is possible during an elastic collision. It also hallucinates the extremely unlikely
1878 situation that the object could be a liquid or a gas as another possibility.

1879 **InternVL3-8B** (Zhu et al., 2025): When a black cylinder collides elastically with a wall, the outcome
1880 can be described using the principles of elastic collisions and conservation of momentum and kinetic
1881 energy.

1882 1. **Elastic Collision:** In an elastic collision, both momentum and kinetic energy are conserved.
1883 This means that the total momentum before the collision is equal to the total momentum after the
1884 collision, and the total kinetic energy before the collision is equal to the total kinetic energy after the
1885 collision.

1890 2. **Collision with a Wall**: When the black cylinder collides with the wall, the wall is considered
1891 to be stationary and much more massive than the cylinder. This simplifies the analysis because the
1892 wall does not move significantly.
1893 3. **Reversal of Velocity**: Since the wall is stationary and much more massive, the black cylinder
1894 will reverse its direction of motion upon collision. The velocity of the cylinder will change direction
1895 but not magnitude, assuming no other forces act on it (like friction or air resistance).
1896 4. **Conservation of Momentum**: The momentum of the cylinder before the collision ($p_{\text{initial}} =$
1897 $m * v_{\text{initial}}$) will be equal to the momentum after the collision ($p_{\text{final}} = m * v_{\text{final}}$). Since the
1898 wall is stationary, the momentum of the wall remains zero. Therefore, the momentum of the cylinder
1899 before the collision is equal to the momentum of the cylinder after the collision but in the opposite
1900 direction.
1901 5. **Conservation of Kinetic Energy**: The kinetic energy of the cylinder before the collision
1902 ($KE_{\text{initial}} = 0.5 * m * v_{\text{initial}}^2$) will be equal to the kinetic energy after the collision ($KE_{\text{final}} = 0.5 * m * v_{\text{final}}^2$). Since the
1903 magnitude of the velocity remains the same, the kinetic energy is
1904 conserved.
1905

1906 In summary, the outcome of the black cylinder colliding elastically with the wall is that the cylinder
1907 will rebound with the same speed but in the opposite direction. The wall remains stationary, and the
1908 collision conserves both momentum and kinetic energy.
1909

1910 **Observation:** InternVL3-8B states and applies the true physical laws to obtain the accurate output.

1911 **LLaVA-Onevision** (Li et al., 2024a): The black cylinder will bounce back and move away from the
1912 wall.
1913

1914 **VideoLLaMA3-7B** (Zhang et al., 2025): The black cylinder will bounce back with the same speed it
1915 had before colliding with the wall.
1916

1917 **LLaVA-NeXT-Interleave** (Li et al., 2024c): The black cylinder collides elastically with the wall,
1918 which means that the kinetic energy is converted into potential energy, and the cylinder rebounds in
1919 the opposite direction. The final velocity of the cylinder after the collision is zero, as it is moving at
1920 the same speed as the wall before the collision.
1921

1922 **Observations:** LLaVA-NeXT-Interleave incorrectly states that kinetic energy is converted to potential
1923 energy during an elastic collision. Then it generates contradictory statements that the cylinder would
1924 rebound while having zero final velocity. The model also hallucinates that the wall was at the same
1925 speed as the cylinder before the collision.
1926

1927 **Qwen2-VL** (Wang et al., 2024a): The black cylinder will bounce off the wall.
1928

1929 **Qwen2.5-Omni** (Xu et al., 2025): When a black cylinder collides elastically with a wall, the outcome
1930 depends on the initial velocity and direction of the cylinder. In an elastic collision, both momentum
1931 and kinetic energy are conserved. If the cylinder is moving towards the wall, it will bounce back with
1932 the same speed but in the opposite direction. If the cylinder is moving away from the wall, it will
1933 continue moving in the same direction with the same speed. The exact outcome can be calculated
1934 using the conservation of momentum and kinetic energy equations.
1935

1936 **Observations:** Qwen2.5-Omni claims that the outcome would depend on the initial velocity of the
1937 cylinder and its direction. While the exact outcome would depend on the initial velocity, the general
1938 outcome that the cylinder would bounce back is independent of the velocity when the collision is
1939 elastic. After making the correct prediction with the appropriate reasoning, it also considers the
1940 scenario where the object was initially moving away from the wall, without realizing that the collision
1941 would not have occurred in that scenario.
1942

1943 **Gemma3-12B** (Kamath et al., 2025): Here's an analysis of what happens when the black cylinder
1944 collides elastically with the wall, based on physical laws:

1945 **Understanding Elastic Collisions**
1946

1944 * **Elastic Collision:** In an elastic collision, both momentum and kinetic energy are conserved.
1945 This means: * The cylinder will bounce off the wall. * No energy is lost during the collision (no heat,
1946 sound, or deformation). * The wall is assumed to be rigid, meaning it doesn't move or deform.
1947

1948 **Outcome of the Collision**

1949 * **Reversal of Velocity:** The key outcome is that the cylinder will reverse its direction of motion.
1950 If it was traveling towards the wall, it will now travel away from the wall. * **Speed is the same:**
1951 Because kinetic energy is conserved, the cylinder's speed immediately *after* the collision will be
1952 the same as its speed *before* the collision. * **Angle:** The angle at which it bounces off will
1953 depend on the angle of incidence (the angle at which it hit the wall). The angle of incidence equals
1954 the angle of reflection.

1955 **Therefore, the black cylinder will bounce back away from the wall with the same speed it had
1956 before the collision, and with a trajectory determined by the laws of reflection.**

1957 * **Important Note:** True, perfectly elastic collisions are rare in the real world. However, for a solid,
1958 rigid object like a cylinder colliding with a solid wall, we often *approximate* the collision as elastic
1959 for simplicity in analysis.

1960 **Observations:** Gemma3-12B generates correct physical laws and uses them for accurate reasoning.

1961 **Aria** (Li et al., 2024b): In an elastic collision, the black cylinder would bounce off the wall with the
1962 same speed but in the opposite direction. This means if the cylinder was moving towards the wall, it
1963 would move away from the wall at the same speed after the collision. The direction of motion would
1964 be reversed, but the magnitude of the velocity would remain unchanged.

1965 **Observation:** Aria provides the correct reasoning, although it does not state the underlying physical
1966 laws.

1967 **Conclusion:** Most models can state the underlying physical laws, but often hallucinate assumptions
1968 such as the wall moving or the objects deforming (despite the collision described as “elastic” in
1969 the prompt). In some cases, such as Gemma3-4B and InternVL3-1B, the generated output has
1970 contradicting statements about the outcome of the collision.

1971 **Overall Conclusion about Parametric Knowledge:** Most evaluated LMMs can state the principles
1972 of momentum and energy conservation accurately. However, they struggle to apply these laws to
1973 reasoning. In some cases, their reasoning contradicts the earlier parts of their output. Sometimes,
1974 they also hallucinate new assumptions (*e.g.*, about the object material) that stray their output from
1975 the correct reasoning. We conjecture that the LMMs know these physical laws as they know factual
1976 information, and not as mathematical models that must be applied flexibly.

1977 E.7 EXPLAINING THE APPARENT INDUCTIVE PHYSICAL REASONING IN AMC

1978 In § 4.4, we observed that LMMs performed better in **AMC** compared to **LMC** (Reg.) when exemplars
1979 containing videos and question-answer pairs were provided. This is surprising since **LMC** (Reg.)
1980 followed universal physical laws and **AMC** did not. An LMM that can correctly infer custom physical
1981 laws from exemplars must also be able to do so when the scenarios follow the true physical laws. To
1982 explain this peculiar behavior of LMMs, we will manually inspect the open-ended generation outputs
1983 of LMMs on **AMC**. We follow the procedure from § E.6: the evaluation sample consists of the video
1984 and the question without any answer options. We also add “Will any object rotate?” at the prompt’s
1985 end to elicit an output about the angular momentum conservation from the LMMs. We follow the
1986 highlighting style in the previous section. The outputs of various LMMs are given below.

1987 E.7.1 OPEN-ENDED GENERATION OUTPUT FOR AMC (REGULAR)

1988 **Frames:** 

1989 **System prompt:** Answer the question based on your understanding of physical laws.

1998
1999
2000
Question: blue cube and green cube have equal mass. What is the outcome of green cube colliding with blue cube? Will any object rotate?

2001
2002
InternVL3-1B (Zhu et al., 2025): When two cubes collide, the outcome depends on the nature of the collision. In this case, the blue cube and the green cube have equal mass.

2003
2004
1. **Collision Outcome**: - If the collision is elastic, the two cubes will stick together after the collision. This means they will form a single larger cube. - If the collision is inelastic, the two cubes will separate and move apart.

2005
2006
2007
2. **Rotation of Objects**: - In an elastic collision, the two cubes will stick together, so they will not rotate. - In an inelastic collision, the two cubes will separate, and they will not rotate.

2008
2009
Given that the collision is elastic, the outcome is that the two cubes will stick together. Therefore, the outcome of the collision is that the two cubes will stick together.

2010
2011
2012
2013
2014
2015
2016
Observations: InternVL3-1B states illogical physical laws that objects stick together after an elastic collision and that objects stay separate after an inelastic collision. In reality, elastic collision ensures that the objects stay apart, while inelastic collision may result in objects sticking together. Interestingly, the output of the model is independent of this assumption as the model believes that neither elastic nor inelastic collision will result in the objects rotating.

2017
2018
2019
VideoLLaMA3-2B (Zhang et al., 2025): When the green cube collides with the blue cube, both objects will rotate around their respective axes of symmetry. The collision is perfectly elastic and frictionless, meaning no energy or momentum is lost during the interaction.

2020
2021
2022
Observation: VideoLLaMA3-2B incorrectly reasons that objects will rotate about the axes of symmetry due to the collision, but it does not provide any reasoning.

2023
2024
2025
2026
InternVL3-2B (Zhu et al., 2025): When the green cube collides with the blue cube, the outcome depends on the nature of the collision. If the collision is perfectly elastic, both cubes will continue to move after the collision, and no rotation will occur. If the collision is perfectly inelastic, the two cubes will stick together, and one of them will rotate while the other moves.

2027
2028
2029
Since the problem states that the green cube and the blue cube have equal mass, we can infer that the collision is likely to be perfectly elastic. In this case, both cubes will continue to move after the collision, and no rotation will occur.

2030
2031
2032
2033
Observations: InternVL3-2B reasons correctly that no rotation will happen if the collision is elastic. However, it reasons that one of the objects may rotate while the other moves in the case of an inelastic collision. This is not true. Angular momentum is not preserved in the model's reasoning.

2034
2035
2036
Gemma3-4B (Kamath et al., 2025): Okay, let's analyze this collision based on physical principles.

2037
2038
Here's a breakdown of what will likely happen:

2039
2040
1. **Conservation of Momentum**: The most important principle here is the conservation of momentum. In a closed system (assuming no external forces like friction or air resistance), the total momentum *before* the collision equals the total momentum *after* the collision. Momentum is calculated as mass x velocity.

2041
2042
2. **Equal Masses**: We are told that both cubes have the same mass. This simplifies the calculation considerably.

2043
2044
3. **Collision Dynamics**: Because both cubes have equal mass, when the green cube hits the blue cube, they will exert equal and opposite forces on each other. This means the green cube will recoil backward and the blue cube will move forward.

2045
2046
2047
4. **Rotation**: Here's the key: Because the cubes are colliding with equal and opposite forces and they have the same mass, the system will conserve angular momentum. This means the overall rotation of the two cubes will be *zero*. While *each individual cube might rotate slightly* during the impact (due to the unevenness of the collision surface), the *combined* rotation of the pair will cancel out.

2052 **Therefore, the outcome is:**
2053
2054 * **The green cube will recoil backward, and the blue cube will move forward.** * **Neither cube
2055 will rotate noticeably.** The rotation will be minimal and quickly damped out.
2056 **Important Note:** This analysis assumes an *elastic* collision, where kinetic energy is conserved.
2057 In reality, some energy will be lost as heat and sound due to the inelastic deformation of the cubes
2058 during the impact. However, the fundamental principle of angular momentum conservation still
2059 holds.
2060 Would you like me to delve deeper into a specific aspect of this, such as calculating the resulting
2061 velocities (if we knew the initial velocities)?
2062
2063 **Observations:** Gemma3-4B states the principle of angular momentum conservation and uses it
2064 correctly to predict that no rotation will happen.
2065 **LLaVA-NeXT-Video** (Zhang et al., 2024): The image you've provided shows two cubes, one blue
2066 and one green, with equal mass. If they were to collide, the outcome would depend on the direction
2067 of the collision and the relative orientation of the cubes. If they were to collide head-on, the collision
2068 would be perfectly elastic, and no rotation would occur. If they were to collide at an angle, the cubes
2069 could rotate due to the conservation of momentum and the transfer of momentum.
2070
2071 In an elastic collision, the total momentum of the system is conserved, so if the blue cube is moving
2072 faster than the green cube, it would transfer its momentum to the green cube, causing it to move in
2073 the opposite direction. If the green cube is moving faster, it would transfer its momentum to the blue
2074 cube, causing it to move in the same direction. If they are moving at the same speed, they would pass
2075 each other without any change in momentum.
2076 If the cubes were to collide at an angle, the collision would be inelastic, and the cubes would deform
2077 and possibly change shape. The cube that is struck would absorb the energy of the collision, and the
2078 other would rebound. The cube that absorbed the energy would rotate due to the conservation of
2079 angular momentum. The cube that rebound would have a change in its orientation, and the cube that
2080 struck it would have a change in its position.
2081 Without more information about the specifics of the collision, it's impossible to predict the exact
2082 outcome.
2083
2084 **Observations:** LLaVA-NeXT-Video correctly states that no rotation will happen during an elastic
2085 collision. However, it additionally outputs that rotation is possible due to the conservation of
2086 momentum. Later, the model states that an object that absorbs energy could rotate due to the
2087 conservation of angular momentum. Here, the model states the right principle that objects could
2088 rotate to preserve angular momentum. But its output is wrong as the principle does not affect the
2089 rotation in this particular example.
2090
2091 **InternVL3-8B** (Zhu et al., 2025): When two objects with equal mass collide, the outcome depends
2092 on the nature of the collision (elastic or inelastic) and the initial velocities of the objects.
2093
2094 In an elastic collision, both momentum and kinetic energy are conserved. If the green cube and the
2095 blue cube have equal mass and they collide head-on with equal and opposite velocities, they will
2096 exchange velocities after the collision. This means the green cube will stop and the blue cube will
2097 continue moving with the velocity of the green cube before the collision.
2098
2099 In an inelastic collision, some kinetic energy is converted into other forms of energy (like heat or
2100 deformation), and the objects may stick together after the collision. If the green cube and the blue
2101 cube stick together after the collision, they will move as a single combined mass with a velocity
2102 determined by the conservation of momentum.
2103
2104 In either case, if the collision is perfectly head-on and the objects are rigid, they will likely rotate if
2105 they are not perfectly smooth or if there is friction between them. The rotation will depend on the
2106 distribution of mass and the point of contact during the collision.
2107
2108 So, yes, both objects could rotate depending on the specifics of the collision and the properties of the
2109 cubes.

2106 **Observation:** The model outputs the true outcome of the collision first. To answer our specific
2107 question about the rotation, it outputs that the objects could rotate if there is friction between them.
2108 However, this is not possible if the collision is head-on as the model states.
2109

2110 **LLaVA-Onevision** (Li et al., 2024a): The outcome of the green cube colliding with the blue cube
2111 will depend on the angle and speed of the collision. If the collision is head-on and at a high speed,
2112 the cubes may not rotate at all. However, if the collision is at an angle, the cubes may rotate around
2113 their point of contact. The exact outcome would depend on the specific details of the collision, such
2114 as the mass and velocity of the cubes, as well as the surface they are colliding on.

2115 **Observation:** This is correct reasoning since the model is only stating, under proper assumptions,
2116 the possibility of objects rotating around their point of contact.
2117

2118 **VideoLLaMA3-7B** (Zhang et al., 2025): yes
2119

2120 **LLaVA-NeXT-Interleave** (Li et al., 2024c): The outcome of the green cube colliding with the blue
2121 cube would depend on the initial velocity and angle of impact. If the green cube is moving towards
2122 the blue cube, it could potentially cause the blue cube to rotate. However, without knowing the initial
2123 conditions, it's not possible to predict the exact outcome.
2124

2125 **Observation:** LLaVA-NeXT-Interleave is wrong in stating that rotation can happen if one object
2126 moves towards (and collides) with another object.
2127

2128 **Qwen2-VL** (Wang et al., 2024a): Yes, the green cube will collide with the blue cube. When the green
2129 cube collides with the blue cube, the cubes will rotate around their center of mass. The exact amount
2130 of rotation will depend on the initial velocities and masses of the cubes.
2131

2132 **Observations:** Qwen2-VL provides the wrong output that the objects would rotate around their
2133 center of mass. It also supports this wrong reasoning with factually incorrect physical laws.
2134

2135 **Qwen2.5-Omni** (Xu et al., 2025): When the green cube collides with the blue cube, both cubes will
2136 experience a force that causes them to move in opposite directions. Since they have equal mass, the
2137 force exerted on each cube will be equal in magnitude but opposite in direction. This means that both
2138 cubes will rotate after the collision. The rotation will be due to the force of impact, which causes the
2139 cubes to change their orientation in space.
2140

2141 **Observations:** Qwen2.5-Omni generates the correct outcome first (linear motion) and then incorrectly
2142 outputs that both objects will rotate after the collision. It also provides invalid reasoning for this
2143 output.
2144

2145 **Gemma3-12B** (Kamath et al., 2025): Here's an analysis of what would likely happen when the green
2146 cube collides with the blue cube, based on physical laws:
2147

2148 ****Outcome of the Collision:****
2149

2150 Given that the cubes have equal mass and assuming an elastic collision (meaning no energy is lost
2151 due to friction or deformation), here's what would happen:
2152

2153 1. ****Momentum Exchange:**** Momentum is conserved in the collision. The green cube is initially
2154 moving, and the blue cube is stationary. During the collision, the green cube will transfer some of its
2155 momentum to the blue cube. 2. ****Equal and Opposite Velocities:**** Because the masses are equal,
2156 ideally the green cube will come to a stop and the blue cube will move away with approximately the
2157 same velocity that the green cube originally had. 3. ****Equal Velocity:**** As a result of the above,
2158 both cubes would move in a similar direction with equal velocity.
2159

2156 ****Will the Objects Rotate?****
2157

2158 It's **highly unlikely** that either cube will rotate significantly during the collision. Here's why:
2159

2160 * ****Impulse Applied:**** The force during the collision is applied along a line. For rotation to occur,
2161 there would need to be an off-center force (a torque). Unless the collision isn't head-on, it's unlikely
2162 to generate such a torque. * ****Shape:**** Cubes are not ideal shapes for rotating due to collisions.
2163 Spheres would rotate the most.
2164

2160 **Important Considerations/Simplifications:**
2161

2162 * **Elasticity:** We've assumed an elastic collision. In reality, some energy would likely be lost as
2163 heat or sound, making the outcome slightly different. * **Perfect Alignment:** A perfectly head-on
2164 collision is assumed. If the cubes collide at an angle, the situation becomes more complex, and there
2165 could be some rotation, but it would still likely be minimal. * **Friction:** Any friction with the
2166 surface would also influence the outcome, slowing the cubes down.

2167 Let me know if you'd like a deeper dive into any of these aspects!

2168 **Observations:** Gemma3-12B provides both correct and incorrect reasoning about the outcome
2169 regarding the motion of the objects after the collision. It also provides accurate reasoning about the
2170 possibility of rotation, although it adds a partially true statement that cubes are less likely to rotate.

2172 **Aria** (Li et al., 2024b): When the green cube collides with the blue cube, assuming they have equal
2173 mass and the collision is head-on, the outcome will depend on the nature of the collision. If it is an
2174 elastic collision, both cubes will bounce off each other with the same speed they approached with. If
2175 it is an inelastic collision, they might stick together and move as one object.

2176 In either case, since the cubes are symmetrical and have no initial angular momentum, they will not
2177 rotate as a result of the collision. The collision will primarily affect their linear momentum.

2178 **Observations:** Aria states and applies the principles of linear and angular momentum conservation.

2180 **Conclusion:** Some LMMs accurately predict the change in linear velocity, and then incorrectly add
2181 that the objects may rotate after the collision. Moreover, the laws stated to support their rotation
2182 argument are irrelevant to rotation. Comparing these outputs with those in § E.6.1, we conjecture that
2183 these models generated incorrect reasoning since they were explicitly prompted to make predictions
2184 about the rotation of the objects. However, we also note that some models accurately predicted that
2185 the colliding objects could rotate if certain conditions, such as colliding at an angle or frictional
2186 surfaces, were met. We believe that the apparent inductive physical reasoning in § 4.4 was due to
2187 these inaccurate beliefs that objects could rotate after a collision.

2188 E.8 DO THE FINDINGS HOLD FOR MORE COMPLEX SCENES?

2190 In this section, we increase the scene complexity of INPHYRE by including background objects and
2191 randomly positioning illumination sources and cameras during the rendering stage. Our intuition is
2192 that, since LMMs failed to demonstrate inductive physical reasoning in a simple environment such
2193 as INPHYRE, they should fail worse as scene complexities increase. However, since the nature of
2194 object attributes in the complex version of INPHYRE (which we refer to as INPHYRE_{com}) is similar
2195 to INPHYRE, we may also expect the LMMs to at least partially overcome the scene complexities.

2196 Similar to our main experiments in § 4, we will evaluate the LMMs on (1) regular scenarios without
2197 any demonstration samples, (2) regular scenarios with demonstration samples, and (3) irregular
2198 scenarios with demonstration samples. As before, inductive physical reasoning will be measured as
2199 the difference in performance between irregular and regular scenarios when demonstration samples
2200 were available. Our findings are discussed below.

2202 **Findings:** Fig. 19a shows the zero-shot performance of LMMs in the regular scenarios of
2203 INPHYRE_{com}. Similar to our results on INPHYRE in Tab. 2, the LMMs perform fairly well in
2204 LMC (Reg.) and SB (Reg.), and poorly in Wall (Reg.). When demonstration samples comprising
2205 video frames and question-answer pairs are provided, the results improve significantly, and multiple
2206 LMMs achieve >90% accuracy in many scenarios (Fig. 19b). We measure inductive physical rea-
2207 soning in Fig. 19c by comparing the 3-shot performance of LMMs in irregular scenarios against the
2208 LMMs' best corresponding performance in regular scenarios under zero-shot and few-shot settings.
2209 The results appear similar to those in Fig. 4 with many LMMs struggling in Red-LMC, Red-Pass, SB,
2210 and CC. Like in Fig. 4, the largest average drop in performance was observed for InternVL3-2B. One
2211 notable difference between the results on INPHYRE and INPHYRE_{com} is that Gemma3-4B showed
2212 a larger drop in performance in Fig. 19c compared to Fig. 4. Also, although Qwen2.5-Omni has a
2213 smaller drop in Fig. 19c compared to Fig. 4, we also point out that Qwen2.5-Omni's performance in
the regular scenarios was proportionately worse on INPHYRE_{com}. Fig. 19d shows the further drop in
accuracy when the demonstration samples include only the video frames, and not the question-answer

	LMC (Regular)				SB (Regular)				Wall (Regular)				Average over scenarios				LMC (Regular)				SB (Regular)				Wall (Regular)				Average over scenarios							
2214	InternVL3-1B	71.66	86.81	5.18	54.55	38.17	52.04	52.04	InternVL3-1B	-34.52	-44.80	7.64	-23.89				InternVL3-1B	-34.52	-44.80	7.64	-23.89				InternVL3-1B	-34.52	-44.80	7.64	-23.89							
2215	VideoLLaMA3-2B	57.99	52.11	4.42	58.09	58.09	52.04	52.04	VideoLLaMA3-2B	6.08	10.30	25.53	13.97				VideoLLaMA3-2B	6.08	10.30	25.53	13.97				VideoLLaMA3-2B	6.08	10.30	25.53	13.97							
2216	InternVL3-2B	77.59	67.07	29.60	58.09	58.09	52.04	52.04	InternVL3-2B	8.64	18.26	61.11	29.34				Gemma 3-4B	61.51	17.15	-6.48	24.06				Gemma 3-4B	61.51	17.15	-6.48	24.06							
2217	Gemma 3-4B	20.10	58.04	77.99	52.04	52.04	52.04	52.04	Gemma 3-4B	1.26	18.16	3.57	7.66				LLaVA-NeXT-Vid	23.22	18.16	3.57	7.66				LLaVA-NeXT-Vid	23.22	18.16	3.57	7.66							
2218	LLaVA-NeXT-Vid	50.35	16.59	2.71	51.68	51.68	49.79	49.79	LLaVA-NeXT-Vid	14.42	14.36	92.96	40.58				InternVL3-8B	38.29	5.78	41.46	28.51				InternVL3-8B	38.29	5.78	41.46	28.51							
2219	InternVL3-8B	61.46	93.96	56.58	70.67	70.67	54.79	54.79	InternVL3-8B	22.71	15.07	94.97	44.25				LLaVA-OneVision	22.71	15.07	94.97	44.25				LLaVA-OneVision	22.71	15.07	94.97	44.25							
2220	LLaVA-OneVision	75.83	83.82	4.72	51.68	51.68	49.79	49.79	LLaVA-OneVision	20.55	28.01	57.69	35.42				VideoLLaMA3-7B	20.55	28.01	57.69	35.42				VideoLLaMA3-7B	20.55	28.01	57.69	35.42							
2221	VideoLLaMA3-7B	78.79	69.46	6.78	51.68	51.68	49.79	49.79	VideoLLaMA3-7B	14.42	14.36	92.96	40.58				LLaVA-NeXT-IL	14.42	14.36	92.96	40.58				LLaVA-NeXT-IL	14.42	14.36	92.96	40.58							
2222	LLaVA-NeXT-IL	83.92	64.64	0.80	48.77	48.77	48.77	48.77	Qwen2-VL	31.76	27.30	92.01	50.35				Qwen2-VL	31.76	27.30	92.01	50.35				Qwen2-VL	31.76	27.30	92.01	50.35							
2223	Qwen2-VL	67.04	72.60	6.68	51.02	51.02	51.02	51.02	Qwen2-VL	-28.19	-13.29	36.28	-1.73				Gemma 3-12B	45.03	-5.53	10.65	16.72				Gemma 3-12B	45.03	-5.53	10.65	16.72							
2224	Qwen2.5-Omni	54.42	94.72	3.92	51.02	51.02	51.02	51.02	Gemma 3-12B	36.63	85.90	69.05	63.86				Average over LMMs	61.31	70.48	22.37					Average over LMMs	15.63	7.56	43.12								
2225	Gemma 3-12B	36.63	85.90	69.05	63.86																															
2226	Average over LMMs	61.31	70.48	22.37					Average over LMMs	15.63	7.56	43.12																								
2227	(a) Zero-shot performance in regular scenarios												(b) Change in performance in regular scenarios under 3-shot setting																							
2228																																				
2229																																				
2230	LMC				Wall				AMC				Red-LMC				Red-Pass				SB				CC				Average over scenarios							
2231	InternVL3-1B	-22.41	3.62	4.67	-20.18	-20.73	-78.27	-26.35	InternVL3-1B	-23.27	-5.03	-49.50	-27.22	-24.11	7.24	3.78	InternVL3-1B	-23.27	-5.03	-49.50	-27.22	-24.11	7.24	3.78	InternVL3-1B	-23.27	-5.03	-49.50	-27.22	-24.11	7.24	3.78	Average over scenarios	-16.87		
2232	VideoLLaMA3-2B	-23.47	-3.82	-11.91	-25.52	-16.55	-55.47	-16.59	VideoLLaMA3-2B	-28.59	-11.66	-16.73	-24.66	-30.88	18.29	-34.66	VideoLLaMA3-2B	-28.59	-11.66	-16.73	-24.66	-30.88	18.29	-34.66	VideoLLaMA3-2B	-28.59	-11.66	-16.73	-24.66	-30.88	18.29	-34.66	Average over scenarios	-18.41		
2233	InternVL3-2B	64.57	-90.10	12.11	-74.65	66.88	-85.29	-69.18	InternVL3-2B	-16.13	-0.50	-36.23	2.81	-12.28	7.29	-16.70	InternVL3-2B	-16.13	-0.50	-36.23	2.81	-12.28	7.29	-16.70	InternVL3-2B	-16.13	-0.50	-36.23	2.81	-12.28	7.29	-16.70	Average over scenarios	-11.05		
2234	Gemma 3-4B	2.06	-24.42	-17.29	-6.67	-18.80	-47.40	-52.19	Gemma 3-4B	-61.21	-36.98	-9.40	-53.43	-39.15	2.86	-24.67	Gemma 3-4B	-61.21	-36.98	-9.40	-53.43	-39.15	2.86	-24.67	Gemma 3-4B	-61.21	-36.98	-9.40	-53.43	-39.15	2.86	-24.67	Average over scenarios	-31.71		
2235	LLaVA-NeXT-Vid	-33.77	42.41	-2.51	-39.68	-41.43	-17.12	-18.16	LLaVA-NeXT-Vid	-1.51	-6.63	-5.13	4.51	6.37	11.36	10.85	LLaVA-NeXT-Vid	-1.51	-6.63	-5.13	4.51	6.37	11.36	10.85	LLaVA-NeXT-Vid	-1.51	-6.63	-5.13	4.51	6.37	11.36	10.85	Average over scenarios	2.83		
2236	InternVL3-8B	-5.33	1.81	0.25	-40.65	-34.74	-48.44	-22.71	InternVL3-8B	-75.48	-44.72	-40.40	-41.70	-44.66	-37.14	-55.85	InternVL3-8B	-75.48	-44.72	-40.40	-41.70	-44.66	-37.14	-55.85	InternVL3-8B	-75.48	-44.72	-40.40	-41.70	-44.66	-37.14	-55.85	Average over scenarios	-48.57		
2237	LLaVA-OneVision	-2.21	-3.22	0.90	-24.81	-37.79	-68.73	-28.87	LLaVA-OneVision	-93.57	-71.81	-44.92	-70.88	-57.64	-15.93	-68.21	LLaVA-OneVision	-93.57	-71.81	-44.92	-70.88	-57.64	-15.93	-68.21	LLaVA-OneVision	-93.57	-71.81	-44.92	-70.88	-57.64	-15.93	-68.21	Average over scenarios	-60.42		
2238	VideoLLaMA3-7B	-15.23	17.49	-3.37	-55.29	-58.19	-40.38	-29.37	VideoLLaMA3-7B	-79.70	-60.90	-52.26	-34.54	-30.08	-28.04	-45.31	VideoLLaMA3-7B	-79.70	-60.90	-52.26	-34.54	-30.08	-28.04	-45.31	VideoLLaMA3-7B	-79.70	-60.90	-52.26	-34.54	-30.08	-28.04	-45.31	Average over scenarios	-47.26		
2239	LLaVA-NeXT-IL	-3.12	0.65	-9.05	-36.99	-42.00	-37.39	-1.07	Qwen2-VL	-91.66	-53.52	-30.50	-97.39	-91.53	-5.88	-46.37	Qwen2-VL	-91.66	-53.52	-30.50	-97.39	-91.53	-5.88	-46.37	Qwen2-VL	-91.66	-53.52	-30.50	-97.39	-91.53	-5.88	-46.37	Average over scenarios	-57.58		
2240	Qwen2-VL	-3.37	1.11	-2.01	0.55	-3.81	-85.88	-2.53	Qwen2-VL	-91.66	-29.65	-35.18	-52.93	-70.13	-40.25	1.01	Qwen2-VL	-91.66	-29.65	-35.18	-52.93	-70.13	-40.25	1.01	Qwen2-VL	-91.66	-29.65	-35.18	-52.93	-70.13	-40.25	1.01	Average over scenarios	-59.55		
2241	Qwen2.5-Omni	-2.81	13.02	39.30	0.57	17.66	-34.92	10.01	Qwen2.5-Omni	-51.46	-29.65	-35.18	-52.93	-70.13	-40.25	1.01	Qwen2.5-Omni	-51.46	-29.65	-35.18	-52.93	-70.13	-40.25	1.01	Qwen2.5-Omni	-51.46	-29.65	-35.18	-52.93	-70.13	-40.25	1.01	Average over scenarios	-39.80		
2242	Gemma 3-12B	-18.64	8.39	13.12	-58.90	-61.56	-67.55	5.48	Gemma 3-12B	-53.92	-87.99	-27.04	-17.04	-5.56	-12.71	-86.78	Gemma 3-12B	-53.92	-87.99	-27.04	-17.04	-5.56	-12.71	-86.78	Gemma 3-12B	-53.92	-87.99	-27.04	-17.04	-5.56	-12.71	-86.78	Average over scenarios	-41.58		
2243	(c) Change in performance in irregular scenarios under 3-shot setting												(d) Change in performance in irregular scenarios under 3-shot and video-only setting																							
2244																																				
2245																																				
2246																																				
2247																																				
2248																																				
2249																																				

complete their task. They were provided with the same information about the tasks as the LMMs. The only additional assistance provided during the test was regarding the meaning of certain questions.

	LMC (Reg)	SB (Reg)	Wall (Reg)	LMC	Wall	AMC	Red-LMC	Red-Pass	SB	CC
Subject 1	0	1	1	0	1	1	1	1	1	1
Subject 2	1	1	1	1	1	1	0	0	1	0
Subject 3	1	1	1	1	1	1	0	0	1	0
Subject 4	1	1	1	1	1	1	0	0	1	0
Subject 5	1	1	1	0	1	1	1	0	1	1
Subject 6	1	1	1	1	1	1	1	1	1	1
Subject 7	1	1	1	1	1	1	1	0	1	1
Subject 8	1	1	0	1	1	1	0	0	0	0
Subject 9	1	1	1	0	1	1	1	0	1	1
Subject 10	1	1	1	1	1	1	1	0	1	1
Mean	0.9	1.0	0.9	0.7	1.0	1.0	0.6	0.2	0.9	0.6

Figure 20: Accuracy of human subjects in various scenarios. “1” indicates correct prediction, and “0” indicates otherwise.

The results are shown in Fig. 20. We observe that most subjects had little trouble in both regular and irregular scenarios, despite being provided only one visual demonstration without any textual description. Here, the human subjects inferred laws from demonstration samples (e.g., “the speed remained constant after collision”) and applied them to the evaluation sample, irrespective of any contradictions between the inferred law and the premise given with the evaluation sample (e.g., “the objects have equal mass and undergo elastic collision”). However, the subjects did struggle with **Red-LMC** and **Red-Pass**, where the required reasoning depended on the color of the objects. For these scenarios, we provided four demonstration samples: two scenarios with red-colored objects that violate the true physics, and two scenarios without any red-colored objects and that do not violate any true physics. Since we did not inform them specifically to use color information for reasoning in these scenarios, many subjects answered that there was not enough information to predict the answer.

E.10 DOES USING ALL EVALUATION FRAMES IMPROVE PERFORMANCE?

	LMC	Wall	AMC	Red-LMC	Red-Pass	SB	CC	Average over scenarios
InternVL3-1B	-6.43	-6.93	2.21	-25.16	-27.77	2.86	10.65	-7.22
VideoLLaMA3-2B	6.48	-6.53	10.30	4.16	9.67	-0.45	5.68	4.19
InternVL3-2B	-8.19	-1.81	1.36	-19.20	-20.85	1.91	-2.21	-7.00
Gemma 3-4B	-20.30	-1.11	0.65	-18.65	-13.98	1.86	-25.93	-11.07
LLaVA-NeXT-Vid	0.90	-13.87	-4.67	-6.47	0.75	-0.15	-1.71	-3.60
InternVL3-8B	-28.84	-5.93	0.00	-35.79	-17.99	-14.27	-23.27	-18.01
LLaVA-OneVision	-3.62	-3.32	0.15	-9.77	-2.51	5.18	-6.98	-2.98
VideoLLaMA3-7B	8.99	-17.24	2.36	-6.17	-11.18	-0.35	-3.82	-3.91
LLaVA-NeXT-IL	-40.45	-10.40	-4.57	-43.61	-45.16	-10.60	-17.34	-24.59
Qwen2-VL	-38.44	0.05	4.97	-13.63	-18.75	-1.21	11.31	-7.96
Qwen2.5-Omni	-18.04	22.21	4.92	-14.74	-30.18	13.57	10.65	-1.66
Gemma 3-12B	-16.88	19.20	-3.57	-7.22	-14.34	-4.67	-37.49	-14.77
Average over LMMs	-13.74	-5.34	1.18	-16.35	-16.02	-0.53	-6.70	

Figure 21: Difference in 2-shot performance when all evaluation frames are provided instead of just the first frame. The results indicate that despite having access to all the frames, the LMMs generally struggle to infer the dynamics from visual inputs, further asserting language bias.

In our main experiments, we provided only the initial frame from each evaluation sample to the LMMs, following the standard procedure for predictive physical reasoning. Thus, we posed physical

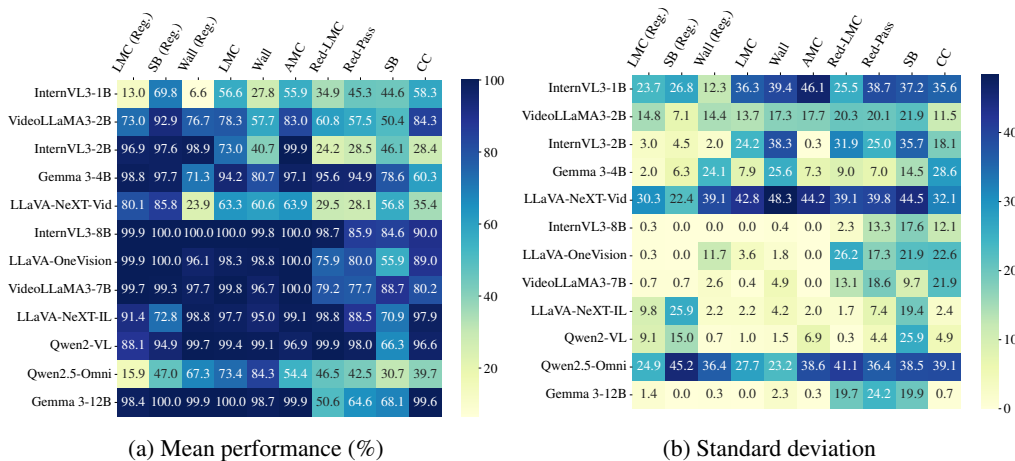
2322 reasoning as a normative task that requires LMMs to apply some rule to make their predictions.
 2323 Intuitively, if all the frames from the evaluation sample were provided to the LMM, then any inferred
 2324 physical rule becomes redundant. Interestingly, through the following experiments, we find that even
 2325 when provided with all the frames in the evaluation sample, LMMs fail to perceive object dynamics
 2326 from the visual inputs.

2327 In our current experiment using all evaluation frames, we provide only two demonstration samples
 2328 since using more frames (hence, more tokens) results in nearly approaching the LMMs' token limit.
 2329 We compare the performance in the current experiment with that from a similar setup, but with only
 2330 one evaluation frame. The differences in accuracy are shown in Fig. 21. Compared to the main
 2331 experiments where only the initial frame was provided, we notice that across scenarios and LMMs,
 2332 performance either remained roughly the same or decreased significantly. Our results convey two
 2333 important findings:

- 2335 1. LMMs struggle to perceive object dynamics from visual samples when the underlying
 2336 physics contradict the existing parametric knowledge.
- 2337 2. This behavior is further evidence of language bias, as LMMs were largely able to apply the
 2338 underlying physical laws in Tab. 8 when these laws were provided as explicit reasoning
 2339 in the demonstration samples. In § F, we will show that Gemma3-12B spent an order of
 2340 magnitude less attention on image tokens compared to the text tokens, echoing similar
 2341 findings in prior works. We believe that the phenomenon we observed in § F, along with the
 2342 general *attention dilution* due to more tokens, is the primary reason for the accuracy drop
 2343 observed in Fig. 21.

2345 E.11 EFFECT OF STRUCTURAL PERTURBATIONS TO PROMPTS

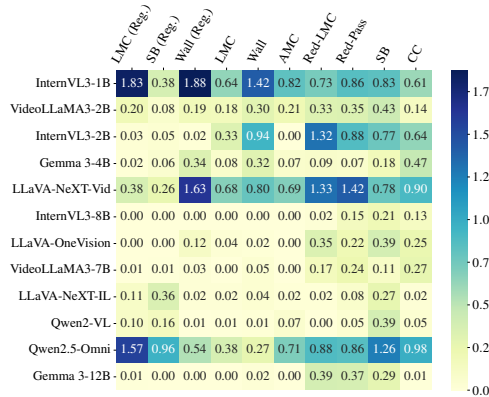
2347 This section evaluates the effect of minor prompt changes on the accuracy of LMMs. These minor
 2348 changes, which we refer to as “structural perturbations,” do not affect the semantic meaning of the
 2349 demonstration samples. We ablate the effects of the following types of structural perturbations:
 2350 (1) changing object attributes in the demonstration samples, (2) changing order of demonstration
 2351 samples, (3) minor text rewrites in the question and the options (e.g., “the speed will increase” or
 2352 “the speed increases”), and (4) option ordering in the evaluation and demonstration queries.



2369 Figure 22: Mean performances of various LMM-scenario combinations and their standard deviations
 2370 when there are structural perturbations in the prompt.

2372 For this experiment, we create multiple smaller versions of **INPHYRE** with only the first 100 samples
 2373 from each scenario. In each version, the structural perturbations are randomly chosen. The results
 2374 over 10 such versions are shown in Fig. 22. For each LMM and each scenario, we compute the
 2375 mean performance (Fig. 22a), the standard deviation in performance (Fig. 22b), and the coefficient of
 2376 variation (CoV) in the performance (Fig. 23). The CoV is measured as the ratio between the mean

2376 performance and its standard deviation. Our primary metric will be the CoV, as it captures the relative
 2377 variation due to the chosen structural perturbations.
 2378



2392
 2393 Figure 23: The coefficients of variation (CoV) for LMM-scenario combinations. CoV is computed as
 2394 the ratio between the corresponding mean (Fig. 22a) and standard deviation (Fig. 22b) values.
 2395

2396 The CoV for each LMM-scenario combination is shown in Fig. 23. Most LMM-scenario combinations
 2397 have very low CoV values, indicating the robustness of the evaluation to structural perturbations.
 2398 Some LMM-scenario combinations have unacceptable levels of CoV⁷. However, these values could
 2399 either be due to the LMMs or the scenario setups. The higher CoV values concentrate around
 2400 smaller LMMs (< 7B parameters), and there is no noticeable pattern where a specific scenario has
 2401 consistently high CoV. This suggests that higher CoV values are due to the sensitivity of the smaller
 2402 LMMs, and not due to the benchmark design.
 2403

F WHY DO LMMs PERFORM POORLY IN IRREGULAR SCENARIOS

2404 We observed that LMMs generally struggled in irregular scenarios, although they performed well
 2405 in regular scenarios. To develop methods to improve inductive physical reasoning in LMMs, we
 2406 must first understand its causes. However, there are several practical challenges in investigating the
 2407 causes of poor inductive physical reasoning in LMMs. The foremost challenge is the difficulty in
 2408 interpreting the outputs of an LMM. Common approaches inspect the hidden states and the attention
 2409 maps between tokens. In this section, we will use attention maps and linear probes on hidden states
 2410 to gain insights into why LMMs fail in irregular scenarios. Specifically, we will (1) evaluate the
 2411 attention values over image tokens and text tokens in Gemma3-12B, and (2) compare the hidden
 2412 states of a pre-trained InternVL3-1B with those of a fine-tuned InternVL3-1B that demonstrated
 2413 considerable inductive physical reasoning in § E.4 on regular and irregular scenarios. Although our
 2414 findings do not fundamentally explain the lack of inductive physical reasoning in LMMs, we believe
 2415 this discussion will foster future efforts.
 2416

F.1 ANALYSIS OF ATTENTION MAPS IN GEMMA3-12B

2417 We plot the normalized attention values over the tokens in the final layer of Gemma3-12B in Fig. 24.
 2418 To obtain these plots, we first choose three corresponding regular-irregular scenario pairs – **LMC**
 2419 and **LMC (Reg.)**, **SB** and **SB (Reg.)**, and **Wall** and **Wall (Reg.)**. In each pair, the scenarios only
 2420 vary in the underlying physical law. Note that the exact visual attributes may vary in the selected
 2421 samples. The plots are obtained by summing the attention values from 20 different samples from
 2422 these regular-irregular scenario pairs. Since each sample may have a different number of text tokens,
 2423 we use the image tokens as the “hinge” around which we arrange the pre-image and the post-image
 2424 text tokens. The x-axis shows the position of these tokens w.r.t. the image tokens. Orange- and
 2425 blue-colored regions denote text and image tokens, respectively. The black dashed lines show the
 2426 average attention values for each colored segment.
 2427

2428 ⁷Following standard practice, an acceptable CoV is less than 0.3.
 2429

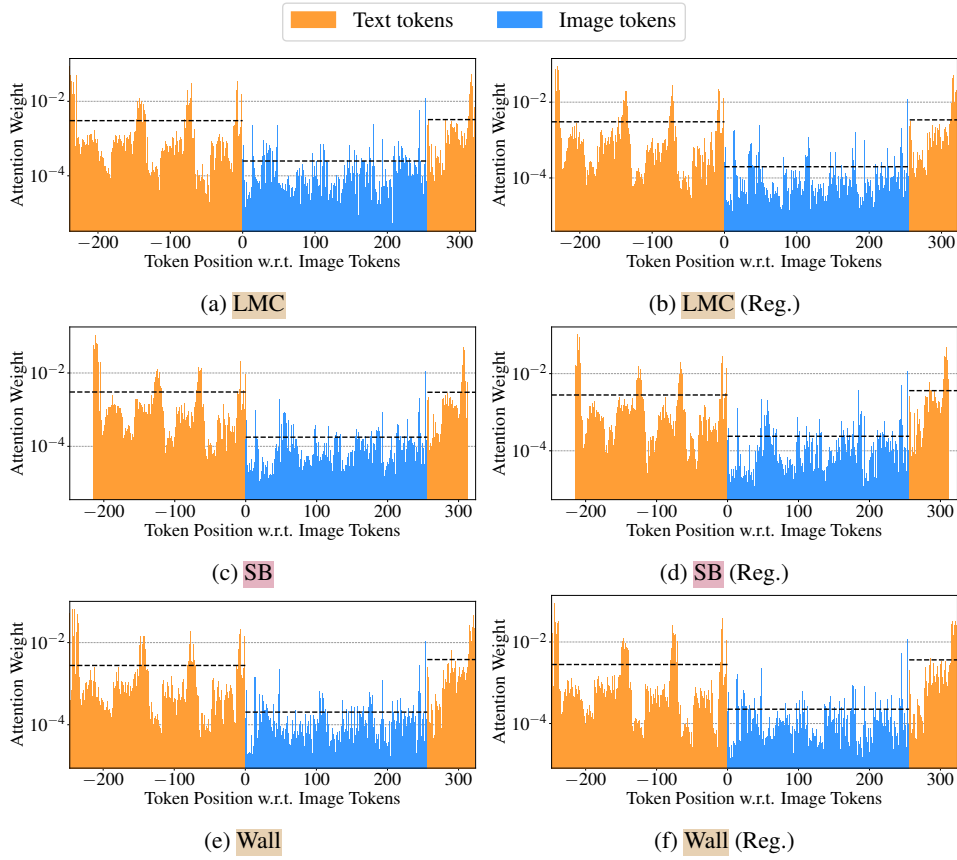


Figure 24: Attention values over image tokens are around an order of magnitude less compared to those over text tokens.

Gemma3-12B spent an order of magnitude less attention on image tokens, compared to text tokens. The lower attention values over image tokens are a possible reason for the observed language bias. It may also explain why LMMs failed to perceive the underlying physical laws even when all frames (including those that show the outcome of the collision event) from the evaluation sample were provided. Similar findings were reported in (Chen et al., 2024a), albeit in the context of natural images.

F.2 ANALYSIS OF HIDDEN STATES IN INTERNVL3-1B

To understand why an LMM showed poor performance in irregular scenarios, we compare its hidden states to a similar LMM that performed well in irregular scenarios. To that end, we compare a pre-trained (PT) InternVL3-1B with a fine-tuned (FT) InternVL3-1B. The results for the FT model were shown in § E.4. We compare the hidden states of the two models by training linear probes on them. We consider two target tasks for the linear probes: (T1) predict whether the given scenario is regular or irregular, and (T2) predict the attributes (color and shape) of the objects in demonstration and evaluation samples. Through (T1), we understand whether the LMMs learn different hidden states for regular and irregular scenarios. Through (T2), we check for any discrepancy in the amount of information carried by the hidden states from demonstration and evaluation samples.

(T1) Can we predict the underlying scenario from the hidden states? The task here is to predict whether the hidden states correspond to samples from a regular scenario or an irregular scenario. We evaluate PT and FT LMMs on this task using the three corresponding pairs of regular-irregular scenarios that we used in our previous experiment – **LMC**, **SB**, and **Wall**. We also vary the number of demonstration samples from one to three. To train the linear probe, we collect hidden states from all samples in each of the scenarios. The results are shown in Fig. 25.

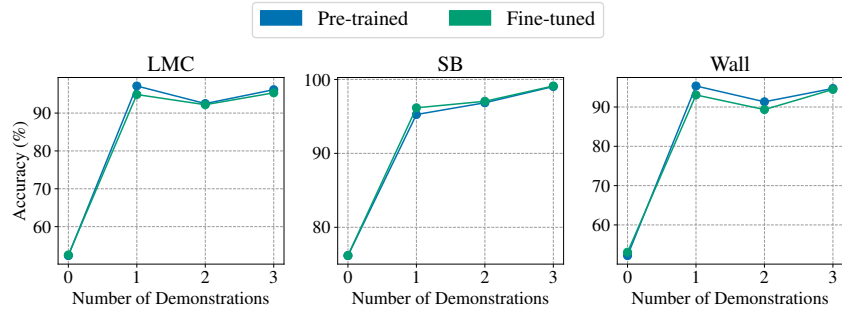


Figure 25: Accuracy of linear probes in predicting the underlying scenario from hidden states of pre-trained and fine-tuned models.

We find that the hidden states from both PT and FT LMMs have sufficient information to classify the underlying scenario with over 90% accuracy. The classification accuracy is not affected by the number of demonstration samples. We also compare these classification results against the case where no demonstration samples are provided. Note that without demonstration samples, the evaluation frame and the accompanying question-answer pair do not provide any discriminative information to suggest whether the underlying scenario is regular or not. Therefore, the classification accuracy in the case with no demonstration samples only acts as a baseline that validates our observations with ≥ 1 demonstration samples. In all scenario pairs, the linear probes achieve significantly less classification accuracy without demonstration samples. In LMC and Wall, they only match random chance performance. In the next task, we will understand how PT and FT LMMs understand the object attributes from the prompt differently.

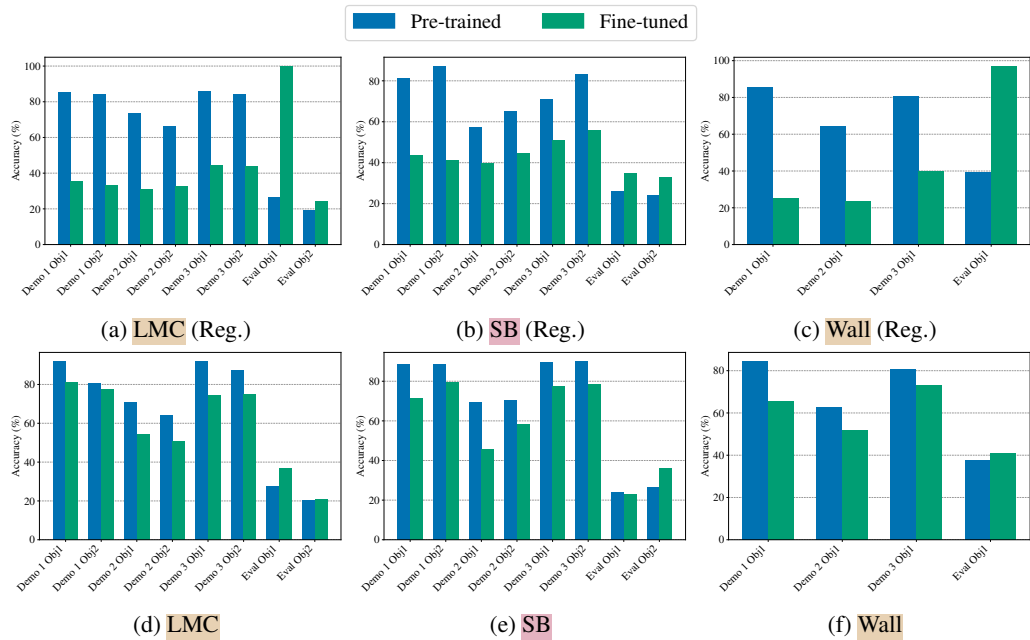


Figure 26: Accuracy of linear probes on hidden states from pre-trained and fine-tuned InternVL3-1B models in classifying the colors of the objects in demonstration and evaluation samples.

(T2) Do PT and FT LMMs perceive object attributes differently? Through task (T1), we saw that the hidden states from both PT and FT InternVL3-1B models carried sufficient information from the demonstration samples to classify the underlying scenario. It is not possible to semantically evaluate these scenario-specific differences in the hidden states exhaustively. Therefore, as a first step, in this task, we will quantify the object attribute information in the hidden states. Similar to task (T1),

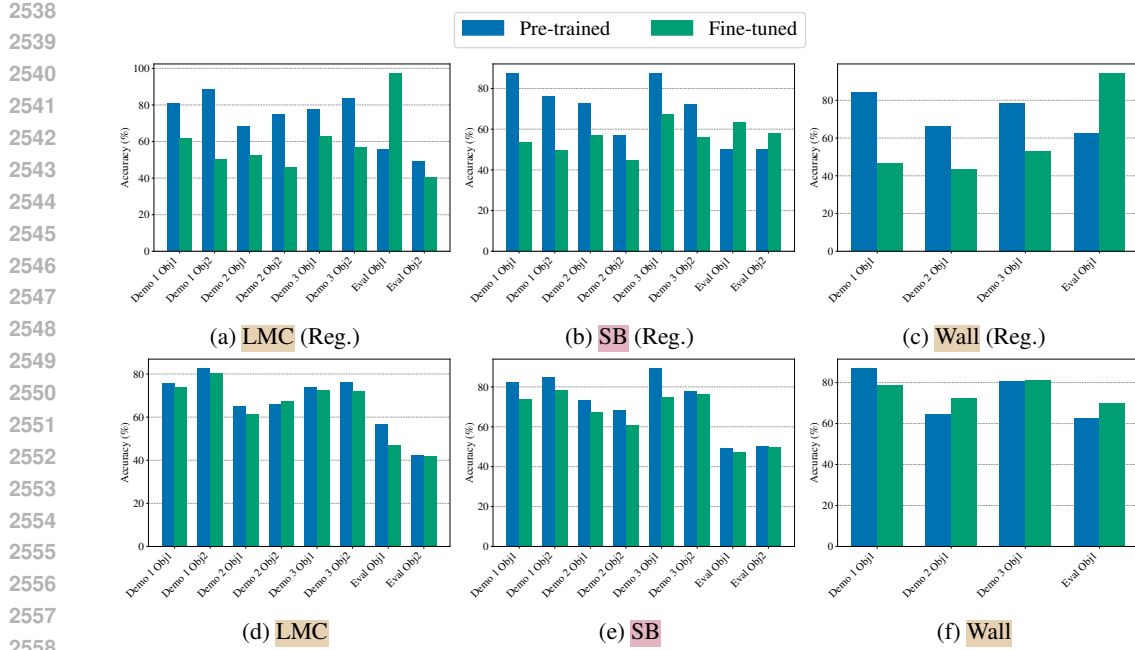


Figure 27: Accuracy of linear probes on hidden states from pre-trained and fine-tuned InternVL3-1B models in classifying the shapes of the objects in demonstration and evaluation samples.

we will use linear probes on the hidden states to classify the shapes and the colors of the objects in demonstration and evaluation samples. In total, the objects in INPHYRE were composed from three shapes and ten colors. The frames in LMC and SB showed two objects, while those in Wall showed only one. We will compare the attribute classification accuracy across scenarios and between PT and FT InternVL3-1B models.

Figs. 26 and 27 show the attribute classification accuracies on color and shape, respectively, of linear probes on the hidden states from PT and FT models in various scenarios. In each figure, the top row shows regular scenarios, while the bottom row shows irregular scenarios. By using accuracy as a proxy for the amount of information in the hidden states about the predicted attributes, we make the following observations:

- (O1) PT models contain more attribute-specific information about the objects in the demonstration samples than the objects in the evaluation sample. This pattern is evident across various scenarios and on both color and shape attributes.
- (O2) **FT models adapt their hidden states to the underlying scenario.** In irregular scenarios, their hidden states contain more information from the demonstration samples, and in regular scenarios, their hidden states contain more information from the evaluation sample. Indeed, in regular scenarios, the demonstration samples are not required since the parametric knowledge is sufficient. However, in irregular scenarios, demonstration samples are key in physical reasoning. Thus, this adaptation aligns with the expected behavior of an LMM in irregular scenarios.

(O1) is a surprising result, since we expect PT models to have less information about the demonstration samples due to their poor performance in irregular scenarios. Moreover, it is not clear from the linear probe whether this information came from the frames or the question-answer pairs in the prompt. (O2) suggests that fine-tuning introduces adaptive behavior when the fine-tuning dataset potentially contradicts parametric knowledge. While (O2) is an interesting finding, it does not explain whether information in the hidden states of PT and FT models are of different natures.

Conclusion of our analysis: Although our results indicate that LMMs indeed understand regular and irregular scenarios differently, they do not shed light on what causes them to be different. Understanding the cause of this difference is a prerequisite for building solutions to improve inductive

2592 physical reasoning. Our findings through task (T2) – that LMMs adapted their visual attribute
2593 reasoning after fine-tuning – are encouraging as the first steps in understanding inductive physical
2594 reasoning. Our analysis was also limited by the lack of reliable tools to interpret the outputs and
2595 the hidden states of LMMs. Therefore, future analysis would require better interpretability tools for
2596 LMMs, specifically regarding the visual inputs.
2597

2598 G USE OF LLMs AND GENERATIVE AI 2599

2600 Grammarly⁸ and Writefull⁹ (embedded in Overleaf) were used in correcting grammatical errors
2601 and spellcheck. LLMs were used to obtain feedback on the writing style. They were not used in
2602 generating sentences or summarizing paragraphs. Some figures in the paper used clip-art style images
2603 generated using Gemini¹⁰ – the cartoon image of a man holding a torch in the title, robot head, electric
2604 bulb, and book in Fig. 1, and palette in Fig. 3. Generative AI was not used in dataset creation.
2605
2606
2607
2608
2609
2610
2611
2612
2613
2614
2615
2616
2617
2618
2619
2620
2621
2622
2623
2624
2625
2626
2627
2628
2629
2630
2631
2632
2633
2634
2635
2636
2637
2638
2639
2640
2641
2642
2643

2644 ⁸<https://app.grammarly.com/>
2645 ⁹<https://www.writefull.com/>

¹⁰<https://gemini.google.com/app>